Effects of Perfluoroalkyl Acids on *In Ovo* Toxicity and Gene Expression in the Domestic Chicken (*Gallus gallus domesticus*)

Cristina Cassone

Thesis submitted to the
Faculty of Graduate and Postdoctoral Studies
in partial fulfilment of the requirements for the
M.Sc. degree in Chemical and Environmental Toxicology

Department of Biology
Faculty of Science
University of Ottawa

Abstract

Perfluoroalkyl acids (PFAAs) are a family of synthetic substances used in a wide variety of consumer and industrial applications, including non-stick and stain-resistant products. PFAAs, specifically perfluorinated sulfonates and carboxylates, are chemically stable and virtually non-biodegradable in the environment. In recent years, PFAAs have been detected in tissues and blood of humans and wildlife. Furthermore, PFAAs have a tendency to bioaccumulate and biomagnify in biota. Perfluorooctane sulfonate and perfluorooctanoate are known to be toxic when animals are exposed to environmentally-relevant levels, but scientists and regulators are challenged with determining and predicting their modes of action. There is some evidence to suggest that PFAAs can impact the thyroid hormone (TH) pathway and neurodevelopment.

The studies presented in this thesis investigated the developmental effects and potential modes of action of newer PFAAs that are being introduced into the global market place. Egg injection experiments were performed in domestic chicken (*Gallus gallus domesticus*) embryos to assess the *in ovo* toxicity of perfluorohexane sulfonate (PFHxS) and perfluorohexanoate (PFHxA) during development. Real-time RT-PCR was used to measure the transcription of candidate genes in the liver and cerebral hemisphere of day 21-22 embryos. Candidate genes were selected based on their responsiveness to PFAA exposure in an *in vitro* screening assay conducted previously. *In ovo* exposure to PFHxS decreased embryo pipping success and overall growth at 38,000 ng/g; several orders of magnitude higher than concentrations reported in wild bird eggs. The expression of TH-responsive genes, including type II and III 5'-deiodinase, neurogranin, and octamer motif binding factor 1, were induced. In addition, PFHxS diminished free thyroxine (T4) levels in plasma.

PFHxA had no affect on pipping success, gene expression or T4 levels in chicken embryos at the doses assessed.

The transcriptional profiles in the cerebral hemisphere of chicken embryos exposed to 890 and 38,000 ng/g PFHxS were compared to a solvent control using microarray technology. The expression of 78 different genes were significantly altered (fold change > 1.5, $p < 0.001$) by PFHxS. Functional analysis showed that PFHxS affected genes involved in tissue development and morphology and cellular assembly and organization. Pathway and interactome analysis suggested that gene expression may be affected through integrin receptors and signaling pathways via TH–dependent and –independent modes of action. It is expected that the findings presented in this thesis will be of general relevance and importance to regulatory agencies and of interest to research scientists and risk assessors.

Résumé

Les acides perfluoroalkyliques font partie de la famille de substances synthétiques utilisées dans une grande variété d'applications industrielles et de consommation, y compris les produits antiadhésifs et ceux résistants aux taches. Les acides perfluoroalkyliques, plus précisément les sulfonates perfluorés et les acides perfluorocarboxyliques, sont chimiquement stables et pratiquement non biodégradables dans l'environnement. Au cours des dernières années, les acides perfluoroalkyliques ont été décelés dans les tissus et le sang des humains et des animaux. En outre, les acides perfluoroalkyliques ont tendance à se bioaccumuler et à se bioamplifier dans le biote. Le sulfonate de perfluorooctane et le perfluorooctanoate sont connus pour être toxiques lorsque les animaux sont exposés à des niveaux environnementalement pertinents, mais les scientifiques et les organismes de réglementation doivent trouver un moyen de déterminer et de prévoir leurs modes d'action. Certaines données laissent croire que les acides perfluoroalkyliques peuvent avoir une incidence sur le mécanisme d'hormones thyroïdiennes ainsi que sur le développement neurologique.

Les études présentées dans cette thèse ont permis d'analyser les effets sur le développement et les modes d'action potentiels des plus récents acides perfluoroalkyliques qui sont introduits sur le marché mondial. Des expériences d'injection dans des œufs ont été réalisées dans des embryons de poulets domestiques (*Gallus gallus domesticus*) afin d'évaluer la toxicité *in ovo* du sulfonate de perfluorooctane (PFHxS) et du perfluorohexanoate (PFHxA) au cours du développement. Des méthodes PCR-CDNA en temps réel ont été utilisées pour mesurer la transcription des gènes candidats dans le foie et l'hémisphère cérébral des embryons aux jours 21 et 22. Les gènes candidats ont été choisis en fonction de leur réactivité à l'exposition des acides perfluoroalkyliques dans un essai de

dépistage *in vitro* réalisé par le passé. Une exposition *in ovo* au PFHxS a donné lieu à une diminution du bêchage des embryons et à une croissance globale à 38 000 ng/g; des concentrations supérieures de plusieurs ordres de grandeur par rapport aux concentrations déclarées dans les œufs d'oiseaux sauvages. L'expression des gènes sensibles aux hormones thyroïdiennes, y compris les 5'-déiodinases de types II et III, la neurogranine et le facteur de liaison 1 du motif octamérique, a été induite. De plus, on a constaté que le PFHxS avait réduit les niveaux de thyroxine libre (T4) dans le plasma. Le perfluorohexanoate (PFHxA) n'a eu aucune incidence sur le bêchage des embryons, l'expression génétique ou les concentrations de T4 des embryons de poulet aux doses évaluées.

Les profils transcriptionnels de l'hémisphère cérébral des embryons de poulet exposés à 890 et à 38 000 ng/g de PFHxS ont été comparés à des témoins traités avec solvant au moyen d'une technologie de microréseaux. On a constaté une modification importante des profils d'expression de 78 différents gènes (changement > 1,5, $p < 0{,}001$) par le PFHxS. Une analyse fonctionnelle a démontré que le PFHxS affecte les gènes qui interviennent dans le développement de tissu ainsi que la morphologie, l'assemblage et l'organisation des cellules. L'analyse des voies et interactome a révélé que l'expression génétique peut être influencée par les récepteurs intégrines et par les voies d'exposition au moyen de modes d'action dépendants et indépendants des hormones thyroïdiennes. On s'attend à ce que les conclusions énoncées dans la présente thèse soient d'une importance générale et pertinentes aux organismes de réglementation et sachent intéresser les chercheurs scientifiques et les évaluateurs de risques.

Table of Contents

List of Tables

List of Figures

List of Abbreviations

ACh	acetylcholine
ANOVA	analysis of variance
AOP	adverse outcome pathway
BBB	blood-brain barrier
BW	body weight
C/EBPβ	CCAAT/enhancer binding protein beta
CAREG	center for advanced research in environmental genomics
cDNA	complementary deoxyribonucleic acid
CEH	chicken embryonic hepatocytes
CEN	chicken embryonic neuronal
CLDN11	claudin 11
CMP	chemicals management plan
CNS	central nervous system
Ct	cycle threshold
CTP	cytidine triphosphate
Cy3	Cyanine 3
Cy5	Cyanine 5
CYP3A37	cytochrome P450 3A37
D2	type II 5'-deiodinase
D3	type III 5'-deiodinase
DA	dopamine
DE	differentially expressed
DEPC	diehtylpyrocarbonate
DMSO	dimethyl sulfoxide
DSP	desmoplakin
FC	fold change
FGGY	FGGY carbohydrate kinase domain containing
FN1	fibronectin 1
FTOH	fluorotelomer alcohol
GD	gestational day
GEO	gene expression omnibus
GGT1	gamma-glutamyltransferase 1
GH	growth hormone
GJIC	gap junction intercellular communication
HD	high dose
HGEN	herring gull embryonic neuronal
HIF1α	hypoxia inducible factor 1 alpha
HPLC	high performance liquid chromatography
HS6ST2	heparan sulfate 6-O-sulfotransferase 2

ILK	integrin-linked kinase
IPA	Ingenuity Pathway Analysis
ITGβ1	integrin beta 1
ITGβ5	integrin beta 5
LD	low dose
LOD	limit of detection
LOWESS	locally weighted scatterplot smoothing
LSMeans	least-squares means
MA	microarray
MAANOVA	microarray analysis of variance
MBP	myelin basic protein
MDL	method detection limit
$MgCl_2$	magnesium chloride
mRNA	messenger ribonucleic acid
MS/MS	tandem mass spectrometry
MYC	myelocytomatosis viral oncogene
NCBI	national centre for biotechnology information
NOV	nephroblastoma overexpressed gene
NTC	no template control
NTP	nucleoside triphosphate
OCT1	octamer motif binding factor 1
PD	postnatal day
PFAA	perfluoroalkyl acid
PFBS	perfluorobutane sulfonate
PFCA	perfluorinated carboxylate
PFDA	perfluorodecanoate
PFDS	perfluorodecane sulfonate
PFHxA	perfluorohexanoate
PFHxS	perfluorohexane sulfonate
PFOA	perfluorooctanoate
PFOS	perfluorooctane sulfonate
PFOSA	perfluorooctane sulfonamide
PFSA	perfluorinated sulfonate
PFUdA	perfluoroundecanoic acid
PGBD5	piggyBac transposable element derived 5
PGF	placental growth factor
PI3K	phosphatidylinositol 3-kinase
PIK3R1	phosphoinositide-3-kinase, regulatory subunit 1
PKC	protein kinase C
PTBP1	polypyrimidine tract binding protein 1
qPCR	quantitative polymerase chain reaction

RC3	neurogranin
RIN	RNA integrity number
RT-PCR	reverse transcription-polymerase chain reaction
SD	Standard deviation
SEM	standard error of the mean
SFRP2	secreted frizzled-related protein 2
SLUG	snail homolog 2
SPE	solid phase extraction
STAGE	strategic technology applications of genomics for the environment
T3	triiodothyronine
T4	thyroxine
TH	thyroid hormone
TJ	tight junction
TRE	thyroid hormone response element
TRβ1	thyroid receptor beta 1
TSPO	translocator protein
TSS	transcription start site
TTR	transthyretin
VIM	vimentin
WAX	weak anion exchange
WNT5A	wingless-type MMTV integration site family, member 5A
ww	wet weight

Statement of Contributions

Chapter Two	**Performed by:**
Experimental design, results analysis and manuscript preparation	Cristina Cassone Doug Crump Sean Kennedy Robert Letcher
Egg injections, dissections and real-time RT-PCR	Cristina Cassone Viengtha Vongphachan Suzanne Chiu
HPLC-MS/MS preparation and analysis	Rob Letcher Eric Pelletier
Free T4 determination	Cristina Cassone Kim Williams

Chapter Three	**Performed by:**
Experimental design, results analysis and manuscript preparation	Cristina Cassone Jason O'Brien Carole Yauk Doug Crump Sean Kennedy
Egg injections and dissections	Cristina Cassone Viengtha Vongphachan
RNA preparation and microarray hybridizations	Cristina Cassone
Microarray data processing	Cristina Cassone Andrew Williams Jason O'Brien
Primer and probe design and real-time RT-PCR	Cristina Cassone Jessica Taylor

Acknowledgements

Firstly, I would like to thank Dr. Sean Kennedy for giving me the opportunity to complete my M.Sc. thesis under his supervision at the National Wildlife Research Centre (NWRC) at Environment Canada. Thank you for all the support throughout the years and for helping me greatly with my recent employment opportunity. It was a pleasure working with you and I am sure that we will stay in touch over the years. My time at the NWRC was very pleasant, especially with the help and support from past and present members of the Kennedy lab. I would especially like to acknowledge Viengtha Vongphachan and Suzanne Chiu for their contributions to the egg injection experiments, Jessica Taylor for her assistance with RT-PCR assay optimizations, Kim Williams for his help with the thyroxine assays, Dr. Jason O'Brien for helping me with the microarray experiment and manuscript preparation, and Doug Crump for always making the time to answer my questions and review my work. Furthermore, a special thank you goes to the Letcher lab for their assistance with perfluoroalkyl acid detection in solutions and tissues as well as manuscript revisions.

I am also very grateful to the Yauk lab at the Environmental Health Centre at Health Canada for training me and allowing me to use their microarray facility and expertise. Furthermore, I would like to thank my committee members, Dr. Carole Yauk and Dr. Vance Trudeau, for their constructive ideas and helpful critique on my thesis research.

I would like to express my appreciation to my family and friends for all of their love and support throughout the years. My parents, Natale and Antonia Cassone, and siblings made me the person I am today. They encouraged my passion for science and always believed in me. A special thank you goes to Vivian Nguyen, who was has always been there for me, to talk to and share with for many years. Last but not least, I would like to thank Dave Inglis for all of his love and support over the last two years. You were always willing and able to help me and were great moral support during this experience. Thank you for keeping me sane and grounded during the stressful times. Thank you all very much; your help is greatly appreciated!

CHAPTER ONE

GENERAL INTRODUCTION

1.1. PERFLUOROALKYL ACIDS

Perfluoroalkyl acids (PFAAs) are a family of ubiquitous synthetic substances used in numerous commercial and industrial applications as surfactants, adhesives, fire retardants and in food packaging (Buck *et al.* 2011). PFAAs have been manufactured since the 1950s and production has steadily increased over the last two decades (Lau *et al.* 2004; Lau *et al.* 2007). Extensive use of PFAAs has led to increased detection in the environment and biota, while their toxicological effects remain unclear. A considerable amount of research has been conducted on PFAAs in attempt to determine their environmental fate and the adverse effects in response to exposure.

1.1.1. Structure and properties of perfluoroalkyl acids

PFAAs are composed of a completely fluorinated carbon backbone of varying chain length (typically four to 14 carbon atoms long) attached to a charged or highly polar functional group. Perfluorinated sulfonates (PFSAs) and carboxylates (PFCAs) are two classes of PFAAs that are attached to a sulfonate or a carboxylate moiety, respectively. The stability of the fluorine-carbon tail renders PFAAs persistent, resistant to metabolic and environmental degradation and gives lipophilic characteristics to the compounds (Jensen and Leffers 2008). The polar end imparts hydrophilic properties rendering PFAAs amphiphilic. It is this unique molecular structure that gives PFAAs the low surface tension and water-, oil- and soil-resistant properties desired by industry and commerce (Lau *et al.* 2004). Given the high production volumes, widespread use, and non-biodegradable nature, it is not surprising that PFAA contamination has been detected on a global scale.

PFAAs are generally highly acidic and exist in aqueous environments as their conjugate bases. In biota, the polar end of PFAAs preferentially binds with proteins, specifically fatty acid binding proteins, lipoproteins and albumin (Jones *et al.* 2003; Luebker *et al.* 2002). PFAAs are sequestered into protein-rich tissues, such as liver and blood. Complex mixtures of PFAAs and their precursor compounds have been detected in various tissues of numerous species of birds, mammals and fish worldwide (Giesy and Kannan 2001); however, their toxicological and biological effects are not well characterized.

1.1.2. Replacement perfluoroalkyl acids

PFSAs and PFCAs with a chain length of eight carbons (i.e. perfluorooctane sulfonate [PFOS] and perfluorooctanoate [PFOA]) have optimal surfactant properties. Consequently, PFOS and PFOA were used as primary components in most PFAA-containing products. Historically, estimated global production and use of PFOS in the U.S. reached 3,500 metric tons in 2000 (Lau *et al.* 2007). Due largely to the detection of high levels of PFOS in environmental media, wildlife samples and even human tissue, the leading manufacturer of PFOS phased-out production in 2002. As a result, the global production of PFOS dropped, while that of PFOA escalated to 1,200 metric tons per year by 2004 (Lau *et al.* 2007). The PFOA Stewardship Program was initiated in 2006 by the U.S. Environmental Protection Agency, where eight major PFAA manufacturers committed to eliminate global emissions and product contents of PFOA by 2015. Global output of PFOS and PFOA has since declined, although several international suppliers continue to manufacture and use these substances (OECD 2002).

In order to fill the commercial void following the phase-out of PFOS and PFOA, PFAA manufacturers have turned to shorter-chained PFAAs as replacements (Lau 2009). For example, perfluorohexane sulfonate (PFHxS) and perfluorohexanoate (PFHxA) (Figure

1.1) consist of a carbon chain-length of six and are candidate substances for use as PFOS and PFOA replacements. The work presented in this thesis focuses on the effects of these two substances in developing chicken embryos.

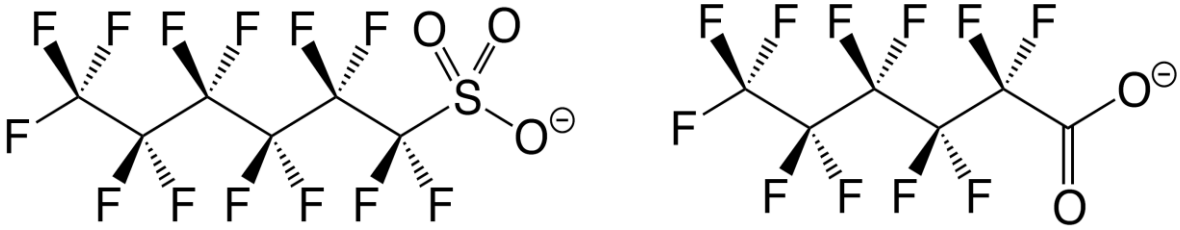

(A) PFHxS ($C_6F_{13}SO_3^-$) (B) PFHxA ($C_6F_{11}O_2^-$)

Figure 1.1. The chemical structure and molecular formula of (A) perfluorohexane sulfonate (PFHxS) and (B) perfluorohexanoate (PFHxA).

1.2. CONCERNS WITH PERFLUOROALKYL ACIDS

1.2.1. Sources of contamination and transport

PFAAs can be released into the environment via direct and indirect pathways. Direct sources include PFAA manufacture, fluoropolymer manufacture and dispersions, aqueous fire-fighting foams and use as additives in consumer and industrial products. For PFCAs alone, estimated total global historical emission from direct sources was 3,200 to 6,900 tonnes from 1951-2004. Fluoropolymer manufacturing contributes to 57% of PFCA emissions, of which 65%, 23% and 12% was discharged into the water, air and land, respectively (Prevedouros *et al.* 2006). Indirect sources include impurities and degradation of fluorotelomer alcohol (FTOH)- and perfluorooctyl sulfonyl-based products. Estimated total global historical PFCA indirect emission from 1951-2004 was 30-350 tonnes (Prevedouros *et al.* 2006). Furthermore, 3M estimated that 85% of indirect PFAA emissions were a result of losses from consumer products during use and disposal (Paul *et al.* 2009).

Once released, PFAAs can be moved to remote regions via two environmental pathways: aquatic and atmospheric transport. Aquatic transport via oceanic currents is considered to be the main means by which PFAAs are transported, based on their physical-chemical properties and the large quantities released into surface waters. PFOS and PFOA concentrations (pg/L) have been detected in surface waters of the Atlantic and Pacific Oceans, South China Sea, Sulu Sea, and the Labrador Sea (Yamashita *et al.* 2005). PFAAs are then transported to the Arctic via northern hemisphere ocean currents. It is estimated that 2-12 tonnes of PFOA are transported to the Arctic by oceanic transport per year (Prevedouros *et al.* 2006). Atmospheric transport of volatile precursors is the second method by which PFAAs can be transported. Perfluorinated sulfonamides and FTOHs are volatile precursors to PFSAs and PFCAs, respectively, and may undergo long-range transport before degradation in the atmosphere (Young *et al.* 2007). FTOH concentrations (pg/m^3) have been observed in the North American atmosphere and have an atmospheric lifetime of 10-20 days (Wallington *et al.* 2006). The many global sources of PFAAs and their tendency to broadly distribute within the hemisphere pose increasing concern over the widespread use of this family of substances.

1.2.2. Global distribution

PFAAs have a tendency to bioaccumulate in biota and have a poor elimination rate in most species. There are numerous biomonitoring studies that have measured PFAA levels, specifically PFOS and PFOA, in a variety of environmental media (i.e. water, air and soil), wildlife, and humans worldwide (Houde *et al.* 2006; Houde *et al.* 2011; Lau *et al.* 2007). PFHxS and PFHxA have also been detected in the environment and biota. In wild bird species, the highest reported mean PFHxS concentration was 50 ng/g wet weight (ww) in grey heron livers (Meyer *et al.* 2009) (see Table 1.1 for a summary of avian biomonitoring

data). PFHxA concentrations are often at or below detection limits in many samples (Karrman *et al.* 2010; Verreault *et al.* 2005); therefore few PFHxA biomonitoring data exist. Several PFSAs and PFCAs have also been reported in the eggs of wild avian species (Holmstrom *et al.* 2005; Kannan *et al.* 2001a; Verreault *et al.* 2005), suggesting oviparous transfer of these substances to offspring. Specifically, PFHxS and PFHxA have been detected in waterbird eggs from the Mississippi River (up to 3.0 ng/g ww; Custer *et al.* 2010) River and Hong Kong (<0.01-0.071 ng/g ww; Wang *et al.* 2008), respectively. The detection of PFHxS and PFHxA in bird eggs highlights the need to study their effects in developing embryos.

1.2.3. Bioaccumulation potential in the brain

While mixtures of PFAAs have mainly been found in blood and liver tissues of various wild species, they have also been detected in the brain tissues of wildlife (Van de Vijver *et al.* 2007; Verreault *et al.* 2005). This suggests that PFAAs are able to cross the blood-brain barrier (BBB), where they have the potential to elicit harmful effects (Van de Vijver *et al.* 2007; Verreault *et al.* 2005). Recent biomonitoring studies have reported PFOS to be located in the brains of sea otters from the west coast of the United States (< 35 ng/g ww) and in glaucous gulls from the Norwegian Arctic (Kannan *et al.* 2001b; Verreault *et al.* 2005). Similarly, PFOS was detected in the brains of harbor porpoises from the Black Sea at concentrations ranging from 3.5-100 ng/g ww (Van de Vijver *et al.* 2007).

An important *in vivo* laboratory study demonstrated that PFAAs accumulate in the brain after peripheral administration (Austin *et al.* 2003). For 2 weeks, adult female rats were intraperitoneally injected with PFOS at both low (1 mg/kg/day) and high (10 mg/kg/day) doses. PFOS was found to accumulate, in a dose-dependent manner, in multiple compartments of the brain. In the cortex alone, low and high doses of PFOS accumulated to

Table 1.1. Mean or range levels of PFHxS (ng/g ww in tissue and ng/mL in blood) in birds by geographical locations, adapted from Houde *et al.* (2011).

Antarctica/Southern Ocean	**Location**	**N**	**Year**	**Sample**	**[PFHxS]**	**Reference**
black-browed albatross	South Atlantic Ocean		1992-96	liver	<0.5	(Tao *et al.* 2006)
gray-headed albatross	South Atlantic Ocean		1992-96	liver	<0.5	(Tao *et al.* 2006)
light-mantled sooty albatross	South Atlantic Ocean		1992-96	liver	<0.5	(Tao *et al.* 2006)
royal albatross	South Atlantic Ocean		1992-96	liver	<0.5	(Tao *et al.* 2006)
shy albatross	South Atlantic Ocean		1992-96	liver	<0.5	(Tao *et al.* 2006)
wandering albatross	South Atlantic Ocean		1992-96	liver	<0.5	(Tao *et al.* 2006)
black-browed albatross	South Atlantic Ocean		1992-96	liver	<0.5	(Tao *et al.* 2006)
adélie penguin	Antarctica	13	2004-05	egg	Nd	(Schiavone *et al.* 2009)
gentoo penguin	Antarctica	13	2004-05	egg	Nd	(Schiavone *et al.* 2009)
Asia	**Location**	**N**	**Year**	**Sample**	**[PFHxS]**	**Reference**
mallard	Ariake Sea, Japan	11	2000-01		<1.5	(Nakata *et al.* 2006)
blackheaded gull	Ariake Sea, Japan	2	2001		<1.5	(Nakata *et al.* 2006)
black-browed albatross	Indian Ocean		1992-96	liver	<0.5	(Tao *et al.* 2006)
gray-headed albatross	Indian Ocean		1992-96	liver	<0.5	(Tao *et al.* 2006)
laysan albatross	Indian Ocean		1992-96	liver	<0.5	(Tao *et al.* 2006)
light-mantled sooty albatross	Indian Ocean		1992-96	liver	<0.5	(Tao *et al.* 2006)
royal albatross	Indian Ocean		1992-96	liver	<0.5	(Tao *et al.* 2006)
shy albatross	Indian Ocean		1992-96	liver	<0.5	(Tao *et al.* 2006)
wandering albatross	Indian Ocean		1992-96	liver	<0.5	(Tao *et al.* 2006)
yellow-nosed albatross	Indian Ocean		1992-96	liver	<0.5	(Tao *et al.* 2006)
cormorant	Japan	5		liver	<0.06-1.5	(Senthilkumar *et al.* 2007)
common cormorant	Lake Biwa, Japan	12	2001-02	liver	<1	(Nakayama *et al.* 2008)
little egret	South China	4	2004	egg	<0.01-0.33	(Wang *et al.* 2008)
night heron	South China	14	2004-06	egg	<0.01-0.37	(Wang *et al.* 2008)
great egret	South China	10	2006	egg	0.07	(Wang *et al.* 2008)
little egret	Lake Shihwa, Korea	20	2006	egg	2.3	(Yoo *et al.* 2008)
little ringed plover	Lake Shihwa, Korea	17	2006	egg	2.3	(Yoo *et al.* 2008)
parrot bill	Lake Shihwa, Korea	7	2006	egg	1.3	(Yoo *et al.* 2008)
sea gull	Rishiri Island, Hokkaido	14	1998	liver	<7.5-34	(Kannan *et al.* 2002a)

sea gull	Rishiri Island, Hokkaido	7	1998	liver	<7.5	(Kannan *et al.* 2002a)
sea gull	Haneda Airport, Tokyo	1	1998	liver	<7.5	(Kannan *et al.* 2002a)
spot-billed duck	Gyotoku bird observatory	1	1998	liver	<7.5	(Kannan *et al.* 2002a)
black-headed gull	Gyotoku bird observatory	1	1998	liver	<7.5	(Kannan *et al.* 2002a)
black-eared kite	Atsugi city, Kanagawa	1	1999	liver	34	(Kannan *et al.* 2002a)
black-eared kite	Haneda Airport, Tokyo	1	1999	liver	<7.5	(Kannan *et al.* 2002a)
gray heron	Gyotoku bird observatory	2	1997	liver	<7.5	(Kannan *et al.* 2002a)
common cormorant	Sagami River, Kanagawa	2	1999	liver	<7.5	(Kannan *et al.* 2002a)
common cormorant	Sagami River, Kanagawa	8	1999	liver	<7.5-10	(Kannan *et al.* 2002a)
little egret	South China	2	2004-06	egg	0.136-0.329	(Wang *et al.* 2008)
little egret	South China	2	2004-06	egg	<0.01-0.09	(Wang *et al.* 2008)
night heron	South China	2	2004-06	egg	0.291-0.293	(Wang *et al.* 2008)
night heron	South China	3	2004-06	egg	0.300-0.317	(Wang *et al.* 2008)
night heron	South China	9	2004-06	egg	<0.01-0.365	(Wang *et al.* 2008)
great egret	South China	10	2004-06	egg	0.0510-0.0920	(Wang *et al.* 2008)
Europe	**Location**	**N**	**Year**	**Sample**	**[PFHxS]**	**Reference**
velvet scoter	Baltic Sean, Poland	5	2003	blood	2.6	(Falandysz *et al.* 2007)
Eider duck	Baltic Sean, Poland	16	2003	blood	1.1	(Falandysz *et al.* 2007)
long-tailed duck	Baltic Sean, Poland	10	2003	blood	2.1	(Falandysz *et al.* 2007)
razorbill	Baltic Sean, Poland	10	2003	blood	0.71	(Falandysz *et al.* 2007)
red-throated diver	Baltic Sean, Poland	7	2003	blood	0.27	(Falandysz *et al.* 2007)
black-backed gull	N. Norway	80	2005	blood	0.78	(Bustnes *et al.* 2008)
common eider	Munkholmen, Norway	5	2004	egg	2.88	(Herzke *et al.* 2009)
common eider	Ekne, Norway	5	2004	egg	0.92	(Herzke *et al.* 2009)
common eider	Sklinna, Norway	10	2004	egg	1.7	(Herzke *et al.* 2009)
european shag	Sklinna, Norway	8	2004	egg	0.92	(Herzke *et al.* 2009)
european shag	Sklinna, Norway	11	2004	plasma	0.22	(Herzke *et al.* 2009)
european shag	Sklinna, Norway	6	2004	liver	1.42	(Herzke *et al.* 2009)
grey heron	Belgium	8		liver	<3.2–120.7	(Meyer *et al.* 2009)
herring gull	Belgium	5		liver	<3.2–9.0	(Meyer *et al.* 2009)
eurasian sparrowhawk	Belgium	8		liver	<3.2–40.6	(Meyer *et al.* 2009)
eurasian magpie	Belgium	5		liver	<3.2–6.7	(Meyer *et al.* 2009)

eurasian collared dove	Belgium	5		liver	<3.2–6.1	(Meyer *et al.* 2009)
common cormorant	Italy			liver	<7	(Kannan *et al.* 2002b)
North America	**Location**	**N**	**Year**	**Sample**	**[PFHxS]**	**Reference**
common merganser	New York, NY	20	1994-2000	liver	<7.5	(Sinclair *et al.* 2006)
hooded merganser	New York, NY	2	1994-2000	liver	<7.5	(Sinclair *et al.* 2006)
bufflehead	New York, NY	3	1994-2000	liver	<7.5	(Sinclair *et al.* 2006)
mallard	New York, NY	31	1994-2000	liver	<7.5	(Sinclair *et al.* 2006)
surf scoter	New York, NY	1	1994-2000	liver	<7.5	(Sinclair *et al.* 2006)
black duck	New York, NY	1	1994-2000	liver	<7.5	(Sinclair *et al.* 2006)
common goldeneye	New York, NY	20	1994-2000	liver	<7.5	(Sinclair *et al.* 2006)
greater scaup	New York, NY	2	1994-2000	liver	<7.5	(Sinclair *et al.* 2006)
lesser scaup	New York, NY	6	1994-2000	liver	<7.5	(Sinclair *et al.* 2006)
ring-neck duck	New York, NY	1	1994-2000	liver	<7.5	(Sinclair *et al.* 2006)
laysan albatross	Northern Ocean/Midway Atoll	10	1994	liver	<0.5	(Tao *et al.* 2006)
laysan albatross	Northern Ocean/Midway Atoll	10	1994	serum	0.27	(Tao *et al.* 2006)
laysan albatross	Northern Ocean/Midway Atoll	10	1994	egg	<1	(Tao *et al.* 2006)
black-fotted albatross	Northern Ocean		1994	egg	<1	(Tao *et al.* 2006)
great blue heron	Mississippi River, MN	10	1993	egg	nd-3.0	(Custer *et al.* 2010)
herring gull	Great Lakes	195	2007	egg	<1	(Gebbink and Letcher 2010)
bald eagle	USA			liver	<38	(Kannan *et al.* 2005)

concentrations of 294 ng/g and 4,487 ng/g, respectively. Once in the brain, PFOS is thought to affect neuroendocrine systems and disrupt critical endocrine functions, such as food intake, stress response and reproduction (Austin *et al.* 2003).

In pregnant rats, PFOS was administered orally from gestational day (GD) 0 to postnatal day (PD) 20 at 0.1, 0.3, and 1.0 mg/kg/day doses (Butenhoff *et al.* 2009b). A dose-dependent increase of PFOS concentrations was observed in the brain of both dam and fetus at GD 20 and PFOS concentrations in the fetal brain were 10 times higher than in the maternal brain (Butenhoff *et al.* 2009b). Therefore, indirect PFOS exposure via *in utero* placental transfer can lead to PFOS accumulation in the brain. This accumulation may be attributed to the BBB not yet being established by GD 20 in the rat fetus. Human biomonitoring studies have also demonstrated neonatal exposure to PFOS through gestational and lactational exposure (Chang *et al.* 2009). PFOS concentrations in the brain were found to decrease with age at different postnatal developmental stages, likely due to volume expansion (i.e., brain growth), even with continued lactational PFOS exposure (Chang *et al.* 2009; Wang *et al.* 2010a).

1.2.4. Toxicity

PFAA exposure has been associated with many toxic effects in developing and adult mammalian species, some of which include higher incidences of mortality, reduced body weight, hepatotoxicity and neurotoxicity (Lau *et al.* 2004; Lau *et al.* 2007). Single generation, sub-chronic toxicity studies in rats dosed with PFHxS did not produce any treatment-related mortality in adults or offspring at doses up to 10 mg/kg/day PFHxS (Butenhoff *et al.* 2009a). In addition, parental male rats treated with 10 mg/kg/day PFHxS by oral gavage demonstrated statistically significant decreases in body-weight gains and increases in liver somatic index (Butenhoff *et al.* 2009a). Developmental endpoints were also

assessed by Butenhoff *et al.* (2009a); PFHxS did not elicit any developmental effects in pups.

PFHxA did not produce any treatment-related mortality in adult rats or offspring at doses up to 500 mg/kg/day PFHxA; however, a single dose (acute study) of 1750 mg/kg or 5000 mg/kg PFHxA to fasted female rats killed 25% and 100% of individuals, respectively, on the day of dosing or the day following dosing (Loveless *et al.* 2009). Adult rats exposed to 500 mg/kg/day PFHxA for 90 days demonstrated decreased body weights and decreased weight gains (Chengelis *et al.* 2009; Loveless *et al.* 2009). No developmental, reproductive, neurobehavioural or genotoxic effects were observed (Loveless *et al.* 2009).

In avian studies, reduced hatching success has been observed following *in ovo* exposures to PFOS and PFOA (Molina *et al.* 2006; O'Brien *et al.* 2009a; Pinkas *et al.* 2010; Yanai *et al.* 2008). Two separate studies determined that PFOS exposure in white leghorn chicken embryos significantly reduced hatchability in a dose-dependent manner, where the median lethal dose was calculated to be 4.9 μg PFOS/g egg (Molina *et al.* 2006) and 93 μg PFOS/g egg (O'Brien *et al.* 2009a).

1.2.5. Effects on neurodevelopment

Recent studies have determined that PFAAs, particularly PFOS and PFOA, can act as neurotoxins by altering neuronal development, targeting specific events in neural cell differentiation, and influencing pre- and postnatal development (Slotkin *et al.* 2008; Yanai *et al.* 2008). The neurotoxic effects of PFOS, PFOA, perfluorooctane sulfonamide (PFOSA) and perfluorobutane sulfonate (PFBS) were assessed in undifferentiated and differentiated PC12 cell lines, a standard *in vitro* model for neuronal development (Slotkin *et al.* 2008). Various endpoints were studied: DNA synthesis, cell numbers and growth, oxidative stress, cell viability, and shifts in differentiation toward or away from the dopamine (DA) and

acetylcholine (ACh) neurotransmitter phenotypes. PFOS was found to promote differentiation into the ACh phenotype at the expense of the DA phenotype, PFBS suppressed differentiation of both phenotypes, PFOSA enhanced differentiation of both, and PFOA had little or no effect on phenotypic specification. These findings revealed that PFAAs caused developmental neurotoxicity through direct actions on replicating and differentiating neurons by shifting their differentiation fate. This study also determined that individual PFAAs exhibit different mechanisms of action and do not share one simple, common mechanism (Slotkin *et al.* 2008).

Wang *et al.* (2010) evaluated the developmental neurotoxicity of prenatal and postnatal exposure to PFOS in the developing rat brain (Wang *et al.* 2010a). Dams were given 3.2 mg/kg PFOS in their feed from GD 1 to PD 21 and the transcriptional effects of PFOS were assessed in pups by studying genes representative of neural functions in the cerebral cortex using RT-PCR on PD 1, 7, 14 and 21. Transcriptional effects of PFOS exposure on neurodevelopment occurred primarily by disrupting the interaction between the neuroendocrine system and the central nervous system (CNS) and that prenatal exposure was more effective in altering expression of several genes (Wang *et al.* 2010a).

Pinkas *et al.* (2009) studied fertilized chicken eggs injected with 5 or 10 mg/kg of PFOS or PFOA on incubation day 0 for neurobehavioral teratogenicity (Pinkas *et al.* 2010). On the day of hatching, both compounds impaired imprinting behaviour, which describes learning that occurs at a particular age or a particular life stage. It was postulated that PFOS and PFOA caused these behavioural changes by affecting protein kinase C (PKC) levels in the brain nucleus most closely associated with imprinting. PFOA evoked an increase in all PKC isoform (α, β, γ) protein levels, while PFOS demonstrated the opposite effect. This study demonstrates that PFOS and PFOA are developmental neurotoxicants that affect post-

hatch cognitive performance but that can also differ substantially in the underlying synaptic mechanisms (Pinkas *et al.* 2010).

The embryotoxicity and teratogenicity of PFAAs has also been considered by means of chicken egg injection studies with PFOS and PFOA. Chicken eggs injected with various doses of PFOS (0.1, 1, 10, or 20 μg PFOS/g egg) before incubation showed a dose-dependent reduction in hatching success (Molina *et al.* 2006). Chicken eggs injected with various doses of PFOA (5, 20, and 40 mg/kg) revealed teratogenic defects in hatching, including increased incidence of splayed legs, and interference with the appropriate development of yellow plumage (Yanai *et al.* 2008). It is postulated that these deficiencies may be associated with poor brain development because hatching success is influenced by motor function and splayed legs may reflect an interference with calcium metabolism (Yanai *et al.* 2008). Furthermore, higher incidences of brain asymmetry, physical deformities and behavioral effects have also been observed in PFAA-treated avian and mammalian species, suggesting poor brain development in response to these substances (Butenhoff *et al.* 2009b; Fuentes *et al.* 2007; Peden-Adams *et al.* 2009; Pinkas *et al.* 2010; Yanai *et al.* 2008).

1.2.6. Effects on the thyroid hormone pathway

PFAAs may indirectly affect the CNS by disrupting neuroendocrine systems. During embryonic development, the CNS is highly dependent on thyroid hormones (THs), triiodothyronine (T3) and thyroxine (T4). Developmental events in the CNS are initiated by the binding of T3 to its receptor and the subsequent transcription of specific genes encoding structural or enzymatic proteins (Zoeller *et al.* 2007). THs are critical for the establishment of brain architecture during CNS development and are required for the development of cellular branching processes that lead to the elaborate synaptic interconnections between brain neurons and the architecture of each brain region (McNabb 2007). Consequently,

altered thyroid states during development are likely to result in serious, permanent effects on CNS function.

Several aquatic, avian and mammalian studies demonstrated perturbation of the TH pathway as a result of PFAA exposure (Chang *et al.* 2007; Chang *et al.* 2008; Lau *et al.* 2004; Shi *et al.* 2008; Thibodeaux *et al.* 2003; Verreault *et al.* 2004; Weiss *et al.* 2009). THs play an essential role in avian development (i.e. metabolism, growth, and differentiation/maturation) and the possible disruption of the TH neuroendocrine system via PFAA exposure during development may result in irreversible effects that are harmful to avian species (McNabb 2007). The reported effects on the TH axis led our laboratory to utilize an *in vitro* screening method to determine the effects of exposure to 11 short- and long-chained PFAAs on mRNA levels of TH-responsive genes in primary cultures of chicken embryonic neuronal (CEN) and herring gull embryonic neuronal (HGEN) cells (Vongphachan *et al.* 2011). It was reported that short-chained PFAAs (< eight carbons) altered the expression of TH-responsive genes, including type II and III 5'-deiodinases (D2 and D3), transthyretin (TTR) and neurogranin (RC3), in CEN cells to a greater extent than long-chained PFAAs (≥ eight carbons) and that CEN cells were more sensitive to treatment than HGEN cells. In order to follow up on the effects of short-chained PFAAs, this M.Sc. thesis investigates the *in ovo* effects of PFHxS and PFHxA (six carbons) in developing chicken embryos.

1.3. THESIS OVERVIEW

1.3.1. Rationale

Despite the current levels of some PFAAs reported in wild birds and their eggs, few studies characterize the toxicity of *in ovo* exposure in an avian model. Recent evidence

suggests that PFAAs can impact endocrine systems and neurodevelopment in birds and mammals, although their mechanisms are not well understood. Furthermore, there is limited information on the effects of short-chained PFAAs, which are expected to fill the commercial void left by the PFOS and PFOA production phase-out. It is important to assess the effects of these replacement PFAAs in order to make well-informed regulatory decisions and to get a better understanding of their toxicity and modes of action in species that are at high risk of exposure. This M.Sc. thesis focuses on the *in ovo* effects of the six-carbon PFSA and PFCA (i.e. PFHxS and PFHxA, respectively) in developing chicken embryos.

1.3.2. Research objectives

Experiments were designed to investigate the effects of PFHxS and PFHxA in an avian model species, the white leghorn chicken (*Gallus gallus domesticus*). The specific hypotheses and objectives for Chapters 2 and 3 were as follows:

Chapter 2

Hypothesis: PFHxS and PFHxA will reduce the pipping success of developing chicken embryos exposed, *in ovo*, to environmentally-relevant concentrations. Since the TH pathway is essential to avian growth and development and is a proposed target for PFAA action, perturbation of the TH system and/or TH-responsive genes are predicted in developing chicken embryos exposed *in ovo* to PFHxS and PFHxA.

Objectives: 1) Investigate the embryotoxicity and adverse effects implicated by *in ovo* exposure to PFHxS and PFHxA in developing chicken embryos via egg injection experiments. 2) Determine the accumulation of PFHxS and PFHxA in yolk sac, liver and cerebral hemisphere with mass spectrometry. 3) Measure the plasma concentrations of TH and the transcriptional activity of TH-regulated genes in liver and cerebral hemisphere using various molecular assays.

Chapter 3

Hypothesis: PFHxS interferes with TH homeostasis in developing chicken embryos exposed *in ovo*. Since THs regulate brain development, disruption of the TH pathway will affect genes associated with neurodevelopmental pathways in developing chicken embryos exposed *in ovo* to PFHxS.

Objectives: 1) Investigate global gene expression profiles in the cerebral hemisphere of developing chicken embryos that demonstrated an adverse effect in response to *in ovo* exposure to PFHxS via microarray analysis. 2) Determine the TH-dependent impacts of PFHxS exposure on gene expression in the brain using Ingenuity Pathway Analysis. 3) Identify novel neurodevelopmental modes of PFHxS action.

CHAPTER TWO

IN OVO EFFECTS OF PERFLUOROHEXANE SULFONATE AND PERFLUOROHEXANOATE ON PIPPING SUCCESS, DEVELOPMENT, MRNA LEVELS AND THYROID HORMONE LEVELS IN CHICKEN EMBRYOS

Modified from Cassone, C.G., Vongphachan, V., Chiu, S., Williams, K.L., Letcher, R.J., Pelletier, E., Crump, D., and Kennedy, S.W. (2012). *In ovo* effects of perfluorohexane sulfonate and perfluorohexanoate on pipping success, development, mRNA expression and thyroid hormone levels in chicken embryos. *Toxicol. Sci.* 127(1): 216-224.

2.1. ABSTRACT

Perfluoroalkyl acids (PFAAs), specifically perfluorinated sulfonates (PFSAs) and carboxylates (PFCAs), are synthetic substances known for their chemical stability, resistance to degradation and potential to biomagnify in food chains. The toxicological and biological effects of PFAAs in avian species are not well characterized, although there is some evidence to suggest that they can impact neurodevelopment and hatching success. Our laboratory recently reported significant effects of perfluorohexane sulfonate (PFHxS) and perfluorohexanoate (PFHxA) on mRNA levels of thyroid hormone (TH)-responsive genes in chicken embryonic neuronal cells. In this study, I determined *in ovo* effects of PFHxS and PFHxA exposure (maximum dose = 38,000 and 9,700 ng/g egg, respectively) on embryonic death, developmental endpoints, tissue accumulation, mRNA levels in liver and cerebral hemisphere and plasma TH levels. Pipping success was reduced to 63% at the highest dose of PFHxS; no effects were observed for PFHxA. PFHxS exposure (38,000 ng/g) decreased tarsus length and embryo mass. PFHxS and PFHxA accumulated in the three tissue compartments analyzed as follows: yolk sac > liver > cerebral hemisphere. Type II and type III 5'-deiodinases (D2 and D3) and cytochrome P450 3A37 (CYP3A37) mRNA levels were induced in liver tissue of chicken embryos exposed to PFHxS, while D2, neurogranin (RC3)

and octamer motif binding factor 1 (OCT1) mRNA levels were up-regulated in cerebral hemisphere. Plasma TH levels were reduced in a concentration-dependent manner following PFHxS exposure; PFHxA had no effect. This *in ovo* study successfully validated previous *in vitro* results concerning the modulation of TH-responsive genes and identified adverse effects associated with TH homeostasis in response to PFHxS treatment.

2.2. INTRODUCTION

Perfluoroalkyl acids (PFAAs), specifically perfluorinated sulfonates (PFSAs) and carboxylates (PFCAs), are a family of man-made, fluorinated organic compounds used as surfactants and water and stain repellents in carpets, paper and textiles (National Toxicology Program 2011). PFAAs are resistant to biodegradation and persistent in the environment (Lau *et al.* 2004). Trophodynamic studies have demonstrated that PFSAs and PFCAs have the potential to bioaccumulate and biomagnify in the food chain, ultimately leading to their detection in wildlife occupying high trophic positions and humans worldwide (Giesy and Kannan 2001; Houde *et al.* 2011; Tomy *et al.* 2009; Yeung *et al.* 2009). In wild avian populations, PFAAs have been detected in protein-rich compartments, including blood serum, liver and egg samples (Gebbink *et al.* 2009; Gebbink and Letcher 2012; Houde *et al.* 2011). The two commonly detected and most studied PFAAs are perfluorooctane sulfonate (PFOS) and perfluorooctanoate (PFOA); however, PFOS, PFOA and their precursors have been voluntarily phased out of production by major manufacturers due to concerns about their potential toxicity to wildlife and humans (Martin *et al.* 2010). Short-chain PFAAs are currently being manufactured and used as PFOS and PFOA substitutes due to their similar water-, oil-, and stain-resistant properties (Buck *et al.* 2011).

Perfluorohexane sulfonate (PFHxS) and perfluorohexanoate (PFHxA) are two short-chain PFAAs for which avian biomonitoring and toxicological data are limited. PFHxS was detected in the blood of female herring gulls collected from Chantry Island, Lake Huron, with the highest proportion observed in plasma (Gebbink and Letcher 2012). PFHxS was also detected in liver of numerous avian species worldwide including grey herons, herring gulls, Eurasian sparrowhawks, magpies and collared doves; concentrations ranged from < 3.2 to 120.7 ng PFHxS/g wet weight (ww) (Houde *et al.* 2011; Kannan *et al.* 2002a; Meyer *et al.* 2009). In herring gull colonies from the Great Lakes, PFHxS concentrations ranged from below detection limits to 3.8 ng/g ww in whole eggs (Gebbink *et al.* 2011). PFHxA concentrations in avian samples are typically at or below the detection limit (Karrman *et al.* 2010; Verreault *et al.* 2005); however, it has been detected in waterbird eggs from Hong Kong (<0.01-0.071 ng/g ww) and herring gulls from Lake Huron (Gebbink and Letcher 2012; Wang *et al.* 2008).

There is some evidence to suggest that PFAAs can impact essential endocrine pathways and neurodevelopment in birds and other animals. In a study by Vongphachan *et al.* (2011), PFHxS and PFHxA altered the mRNA levels of thyroid hormone (TH)-responsive transcripts in chicken embryonic neuronal (CEN) cells. PFHxS induced the expression of type III 5'-deiodinase (D3) and neurogranin (RC3), and reduced the expression of transthyretin (TTR). PFHxA induced type II 5'-deiodinase (D2), D3, and myelin basic protein (MBP) mRNA levels. TH disruption effects were also observed in response to PFOS and PFOA treatment in mammalian models; PFOS and PFOA altered TH levels and hampered brain development in rodents (Johansson *et al.* 2008; Johansson *et al.* 2009; Lau *et al.* 2003; Thibodeaux *et al.* 2003; Yu *et al.* 2009). Central nervous system development is TH-dependent and altered thyroid status during development could result in serious,

permanent effects on central nervous system function. Chicken egg injection studies reported reduced hatching success in response to PFOS and PFOA, which may be a consequence of poor motor skills associated with altered brain development, as well as higher incidences of physical deformities (Molina *et al.* 2006; O'Brien *et al.* 2009a; O'Brien *et al.* 2009b; Yanai *et al.* 2008). Post-hatch cognitive behaviour (i.e. imprinting behaviour), immune alterations and brain asymmetry changes have also been observed following *in ovo* PFOS and PFOA exposure (Peden-Adams *et al.* 2009; Pinkas *et al.* 2010). The importance of studying the effects of PFAAs on avian endocrine systems and neurodevelopment is evident.

The present study determined the effects of *in ovo* PFHxS and PFHxA exposure on developing chicken embryos. The main objectives of this study were to: (1) determine pipping success over a large range of doses; (2) assess the impacts on growth and development; (3) measure the tissue-specific accumulation in yolk sac, liver and cerebral hemisphere; (4) determine the mRNA levels of TH-dependent transcripts and compare these findings with *in vitro* studies (hepatocytes and neuronal cells); and (5) evaluate the effects on circulating free thyroxine (T4) levels. THs play an essential role in avian development (i.e. metabolism, growth, and differentiation/maturation) (McNabb 2007) and the possible disruption of the TH neuroendocrine system via PFAA exposure during development may result in irreversible effects that are harmful to avian species.

2.3. MATERIALS AND METHODS

2.3.1. Chemicals

Linear sodium perfluorohexane sulfonate (PFHxS) and linear sodium perfluorohexanoate (PFHxA) were purchased from Wellington Laboratories (Guelph, ON; >98% pure). All stock solutions and serial dilutions were prepared in dimethyl sulfoxide

(DMSO; Fisher Scientific, Ottawa, ON) to yield actual, final injection concentrations ranging from 8.9-38,000 ng PFHxS/g egg and 9.7-9,700 ng PFHxA/g egg. The maximal dose assessed in the PFHxA egg injection experiment is lower than that of PFHxS due to insufficient quantities of the compound. The concentrations of the solutions injected into the eggs were determined by high performance liquid chromatography-tandem mass spectrometry (HPLC-MS/MS) in negative electrospray mode, as described below.

PFHxS and PFHxA standard solutions (50 µg/mL in methanol) for HPLC-MS/MS analysis and the appropriate internal standards, sodium perfluoro-1-hexane[$^{18}O_2$]sulfonate (MPFHxS) and perfluoro-n-[1,2,3,4-^{13}C]hexanoate (MPFHxA) (50 µg/mL in methanol), were purchased from Wellington Laboratories. Working solutions of the analytes and internal standards were prepared from stock solutions by several dilutions with methanol. Ammonium hydroxide (28-30%) and formic acid (98-100%) were American Chemical Society reagent grade and purchased from VWR (Mississauga, ON). Ammonium acetate (99.9%) was purchased from Sigma-Aldrich (Oakville, ON). HPLC-grade methanol and acetonitrile were purchased from Fisher Scientific.

2.3.2. Egg injection and tissue collection

Two separate egg injection experiments were performed to assess the effects of PFHxS and PFHxA on pipping success, embryonic development, tissue accumulation, hepatic and neuronal mRNA levels and plasma free T4 concentrations. A total of 220 unincubated, fertilized White Leghorn chicken (*Gallus gallus domesticus*) eggs were obtained from the Canadian Food Inspection Agency (Ottawa, ON). All procedures involving the handling of animals were conducted according to protocols approved by the Animal Care Committee at the National Wildlife Research Centre.

One hundred and twenty eggs were randomly distributed into a control group and five treatment groups for the PFHxS egg injection study. The groups were: DMSO control (n=20), 8.9 ng PFHxS/g egg (n=20), 93 ng PFHxS/g egg (n=20), 890 ng PFHxS/g egg (n=20), 9,300 ng PFHxS/g egg (n=20), and 38,000 ng PFHxS/g egg (n=20). One hundred eggs were randomly distributed into a control group and four treatment groups for the PFHxA study as follows: DMSO control (n=20), 9.7 ng PFHxA/g egg (n=20), 94 ng PFHxA/g egg (n=20), 1,000 ng PFHxA/g egg (n=20), and 9,700 ng PFHxA/g egg (n=20).

Egg injections were performed as previously described (Crump *et al.* 2010). In brief, a small hole was drilled through the egg shell at the centre of the air cell, and based on the average mass of the eggs (~50 g per egg), the same volume of DMSO or PFAA (~1 µl/g egg) was injected into the air cell to attain the desired concentrations described above. After injection, the hole was sealed with AirPore^{TM} Tape (Qiagen, Mississauga, ON) and eggs were then placed horizontally into an incubator (Petersime, Model XI) set at 37.5°C and 58% humidity. During incubation, embryos were monitored frequently by candling and brought to pipping (day 21-22, stage 46) (Hamilton and Hamburger 1951). Infertile and dead embryos were removed and the developmental stage was determined for dead embryos (data not shown). Pipping success was determined by dividing the number of embryos that pipped by day 22 by the number of total fertile eggs per treatment group. Embryos that did not make a pipping star by day 22 were considered unfit to hatch.

Embryos that pipped successfully were euthanized by decapitation and embryo, yolk sac, liver and cerebral hemisphere weights, tarsus length and time to pip were recorded. Significant differences in tarsus length, embryo/tissue weight and time to pip among dose groups were determined using a one-way ANOVA followed by a Bonferroni's t-test for

multiple comparisons versus the vehicle control (SigmaStat v2.03; SPSS). Changes were considered statistically significant if $p<0.05$.

The entire yolk sac and portions of the left lobe of the liver and left cerebral hemisphere were collected from 6-8 embryos/treatment group and stored at -20°C. Yolk sacs and sub-samples of liver and cerebral hemispheres were pooled (6-8 per treatment group) for subsequent chemical analysis of PFHxS and PFHxA concentrations. The right lobe of the liver and the right cerebral hemisphere were immediately frozen in liquid nitrogen and stored at -80°C for subsequent RNA isolation. Blood samples (~0.1-0.2 mL) were collected from each embryo and mixed with 10 µL of a heparin solution (0.2 mg/mL in sterile water) to prevent coagulation. Blood samples were kept on ice and then spun at 20,800 x *g* for 5 min to separate plasma and red blood cells. Plasma was stored at -80°C for subsequent free T4 concentration determination.

2.3.3. Determination of PFHxS and PFHxA

PFHxS and PFHxA analysis was performed using a previously described method (Gebbink and Letcher 2012) with modifications. In brief, tissue samples (0.1-0.2 g) were cleaned on Oasis weak anion exchange solid phase extraction (WAX SPE) cartridges (3 mL, 60 mg) purchased from Waters (Mississauga, ON) and spiked with 100 µl of an internal standard solution containing 1000 ng/mL of MPFHxS or MPFHxA prior to extraction. For PFHxS and PFHxA detection, a Waters Alliance 2695 HPLC system coupled to a Micromass Quattro Ultima triple quadrupole mass spectrometer equipped with an electrospray ionization interface was used. Analytes were separated chromatographically on an ACE 3 C_{18} column (50 mm L × 2.1 mm i.d., 3 µm particle size). The mobile phases were water (A) and methanol (B), both containing equal concentrations of 2 mM ammonium acetate. The elution

gradient was as follows: initial mix of 95% mobile phase A and 5% mobile phase B, increasing to 100% mobile phase B within 6 min and held for 4 min, then decreasing to 5 % mobile phase B within 1 min and held for 4 min. The MS/MS was operated in negative ion mode with multiple reaction monitoring.

Quantitative analysis was performed by the isotope dilution method. MPFHxS and MPFHxA were used as internal standards for PFHxS and PFHxA, respectively. A weighted (1/concentration) linear regression mode was selected on Masslynx (v 4.0) instrument software for fitting of the calibration curve. The method detection limit (MDL) value was measured by performing replicate analyses (n=8) of 1 g pork liver samples, which were spiked with analytes at a concentration 3-5 times the estimated detection limit and calculating the standard deviation. The limit of detection (LOD) was estimated based on a ratio, peak to peak, of 3 between the signal of the analyte and the baseline noise. The MDL was 0.1 ng/g for PFHxS and PFHxA, while the LOD was 0.2 ng/g and 0.1 ng/g for PFHxS and PFHxA, respectively. Linear regression analyses were performed to compare PFHxS and PFHxA concentrations in yolk sac, liver and cerebral hemisphere with the actual injection concentrations (based on the pool of 6-8 samples/treatment group).

2.3.4. RNA isolation and cDNA synthesis

Total RNA was isolated from a 20-30 mg portion of the right liver lobe and the right cerebral hemisphere (n=6-8 per treatment group) using the RNeasy mini kit according to the manufacturer's instructions (Qiagen). The concentration and purity of extracted RNA was quantified by determining the A260/A280 absorbance ratio on a NanoDrop 2000 spectrophotometer (Thermo Scientific, Wilmington, DE). All samples used for real-time RT-PCR analysis had an A260/A280 ratio between 1.9 and 2.1. Approximately 500 ng of total RNA was DNase treated using DNA-free kits according to the manufacturer (Ambion,

Austin, TX) and used for cDNA synthesis. RNA was reverse transcribed to cDNA using SuperScript II and random hexamer primers as described by the manufacturer (Invitrogen, Burlington, ON). Reactions containing an RNA template but lacking reverse transcriptase were run in parallel to verify the absence of contaminating genomic DNA (no-RT control). A 1:10 dilution of cDNA with diethylpyrocarbonate (DEPC)-treated water was prepared and stored at -80°C for subsequent real-time RT-PCR.

2.3.5. Real-time RT-PCR

Changes in mRNA levels were assessed by real-time RT-PCR using the Brilliant Q-PCR Core Reagent kit and MX3000P or MX3005P PCR systems (Stratagene, La Jolla, CA). Primer pairs (Invitrogen) and TaqMan fluorogenic probes (Biosearch, Novato, CA) for the transcripts listed in Table 2.1 were designed and optimized for real-time RT-PCR, as previously described.

Table 2.1. List of transcripts assessed in liver tissue and cerebral hemisphere of developing chicken embryos exposed to perfluorohexane sulfonate (PFHxS) and perfluorohexanoate (PFHxA) using real-time RT-PCR. Accession numbers and original references (for primer and probe nucleotide sequences and final concentrations) are also included.

Gene	Accession Number	Reference
β-actin (BA)	X00182	(Hickey *et al.* 2009)
Type II iodothyronine 5'-deiodinase (D2)	NM_204114	(Crump *et al.* 2008)
Type III iodothyronine 5'-deiodinase (D3)	NM_001122648	(Vongphachan *et al.* 2011)
Neurogranin (RC3)	XM_001232109	(Vongphachan *et al.* 2011)
Octamer motif binding factor 1 (OCT1)	NM_205472	(Vongphachan *et al.* 2011)
Cytochrome P450 3A37 (CYP3A37)	NM_001001751	(Crump *et al.* 2008)

Each 25 µL reaction contained 1X Core PCR buffer, 5 mM $MgCl_2$, 0.8 mM dNTP mix, 8% glycerol, 75 nM ROX reference dye, forward and reverse primers at concentrations previously optimized, 200 nM fluorogenic probe, 5 µL diluted cDNA (1:10), and 1.25 U SureStart Taq Polymerase. The thermocycle program included an enzyme activation step at 95°C (10 min) and 40 cycles of 95°C (30 sec) and 60°C (1 min). All reactions were

performed using cDNA from 4-8 individual embryos per treatment group run in duplicate for each assay. All gene targets were normalized to β-actin, as its expression was invariable across treatment groups (internal control). An identical reaction was conducted, in parallel, for each assay by replacing cDNA template with DEPC water (no template control, NTC) to monitor for contamination. Cycle threshold (Ct) data were normalized to β-actin and the fold change in target gene mRNA abundance in PFAA treatment groups compared to the vehicle control was calculated using the $2^{-\Delta Ct}$ equation (Schmittgen and Livak 2008). Statistically significant differences in mRNA levels were identified by performing a one-way ANOVA to $2^{-\Delta Ct}$-transformed data followed by a Bonferroni's t-test for multiple comparisons versus the vehicle control (SigmaStat v2.03; SPSS). Changes were considered statistically significant if $p<0.05$.

2.3.6. Free T4 determination

Free T4 levels were determined in plasma collected from chicken embryos following PFHxS- and PFHxA-exposure using the AccuBind free T4 kit (Monobind Inc., Lake Forest, CA) as per the manufacturer's instructions. The dose groups assessed were as follows: DMSO control (n=22 selected randomly from the two studies), 8.9 (n=6), 890 (n=12) and 38,000 ng PFHxS/g (n=11); and 9.7 (n=10), 1,000 (n=11) and 9,700 ng PFHxA/g (n=8). The kit is based on the competition between an immobilized antibody, an enzyme-antigen conjugate and free T4 in a 96-well microplate. In brief, standards, controls (human serum references 0.4 and 1.25 ng/dl, Randox Laboratories Ltd., Antrim, UK) and samples were added to the microplate and when equilibration was reached, the unbound antigen fraction was removed and the enzyme activity in the bound fraction was measured at 450 nm on a SpectraMax 190 UV-VIS microplate reader (Molecular Devices, Sunnyvale, CA). Enzyme

activity is inversely proportional to the concentration of free T4 in the sample. Concentration values (ng/dl) were determined from the standard curve, which was fitted using a variable slope (four parameter) method in Prism software (GraphPad, La Jolla, CA). The limit of detection was 0.05 ng/dl; values equal or less than this were assigned a value of half the detection limit (i.e. 0.025 ng/dl). A one-way ANOVA followed by Tukey's post-hoc test was used to determine significant differences in free T4 concentrations among the dose groups ($p<0.05$).

2.4. RESULTS

2.4.1. Pipping success

PFHxS decreased pipping success of the domestic chicken to 63% in embryos exposed to the highest dose group of 38,000 ng/g (Table 2.2). In the PFHxA egg injection

Table 2.2. Concentrations of perfluorohexane sulfonate (PFHxS) and perfluorohexanoate (PFHxA) in yolk sac, liver and cerebral hemisphere (ng/g wet weight) obtained from developing chicken embryos following 21-22 days of *in ovo* exposure. Tissues were harvested, pooled (n=6-8) and perfluoroalkyl acid (PFAA) concentrations were measured by HPLC-MS/MS. Stock concentrations (mg/mL) and injection concentrations (ng/g) are also included. Pipping success is reported as a ratio (# of embryos that pipped/# of total fertile embryos) and a percentage (%).

	Stock solution [PFAA]	Injected [PFAA]	Yolk Sac [PFAA]	Liver [PFAA]	Cerebral hemisphere [PFAA]	Pipping success	
	(mg/mL)	(ng/g)	(ng/g ww)	(ng/g ww)	(ng/g ww)	(ratio)	(%)
PFHxS	0	0	0	1.6	5.2	16/17	94
	0.0089	8.9	34	44	13	15/19	79
	0.093	93	180	160	26	18/20	90
	0.89	890	5,500	5,100	490	16/19	84
	9.3	9,300	63,000	36,000	3,800	17/19	89
	38	38,000	300,000	170,000	23,000	10/16	63
PFHxA	0	0	18	5.0	2.6	16/18	89
	0.0097	9.7	25	14	3.0	19/20	95
	0.094	94	180	160	16	17/19	89
	1.0	1,000	3200	2,900	70	17/20	85
	9.7	9,700	43000	30,000	800	15/19	79

study, pipping success was 80% in embryos exposed to the highest dose group of 9,700 ng/g (Table 2.2). The percent pipping success for all PFHxA-exposed embryos fell within the range observed in previous studies for DMSO-injected eggs (80-100%) (Crump *et al.* 2011; O'Brien *et al.* 2009a; O'Brien *et al.* 2009b); however, the highest dose group for PFHxS did not. Average time to pip did not significantly change (p>0.05) in either of the egg injection studies (data not shown).

2.4.2. Embryonic development

Of the morphometric parameters assessed in this study, tarsus length and embryo mass were affected by PFHxS exposure. Relative to the DMSO control, average tarsus length (27.1 mm vs. 25.2 mm) and embryo mass (30.4 g vs. 27.1 g) were significantly (p<0.05) decreased at the highest dose of PFHxS (38,000 ng/g; Figure 2.1). Liver weight was not significantly different among groups (p>0.05; data not shown). None of the morphometric parameters were significantly (p>0.05) affected in PFHxA-exposed embryos (data not shown).

2.4.3. PFHxS and PFHxA concentrations in yolk sac, liver and cerebral hemisphere

Significant linear correlations (r^2=0.99; p<0.0001 for all correlations) were observed between PFHxS dose group and concentration in yolk sac (y=7.8x-1997), liver (y=4.5x-742) and cerebral hemisphere (y=0.59x-275). These relationships demonstrate dose-dependent accumulation; however the extent of uptake was variable between yolk sac, liver and cerebral hemisphere. PFHxS preferentially accumulated in the yolk sac > liver > cerebral hemisphere, with the exception of the 9 ng/g dose group, where liver > yolk sac > cerebral hemisphere. Enrichment of PFHxS in yolk sac and liver was evident as the measured concentrations exceeded their respective actual whole-egg injection concentrations. For example, in the

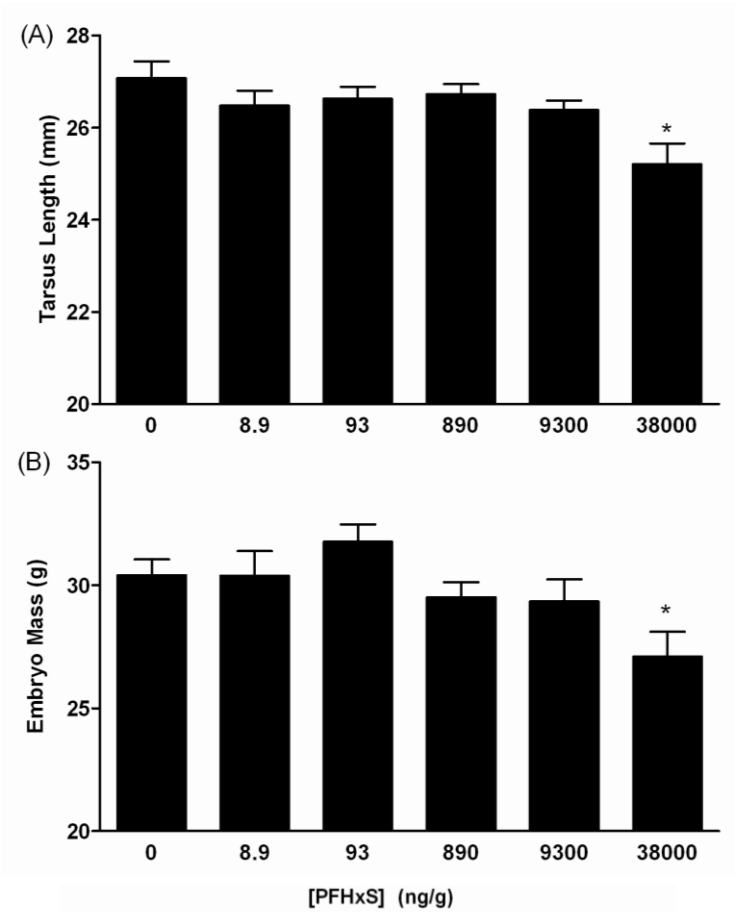

Figure 2.1. Morphometric effects of *in ovo* perfluorohexane sulfonate (PFHxS) exposure were observed for the following embryonic developmental parameters in chickens: (A) tarsus length (mm); and (B) embryo mass (g). Measurements were taken for all viable embryos at pipping and error bars represent the SEM (n=16-20; *p<0.05).

38,000 ng/g dose group, concentrations of 300,000, and 170,000 ng/g were reported in yolk sac and liver, respectively (Table 2.2).

Likewise, significant linear correlations (r^2=0.99; p<0.0001 for all correlations) were observed between PFHxA dose group and concentration in yolk sac (y=4.5x-404), liver (y=3.1x-107) and cerebral hemisphere (y=0.83x-0.69). Concentrations of PFHxA increased in a dose-dependent manner in yolk sac, liver and cerebral hemisphere to a maximum of 43,000, 30,000 and 800 ng/g, in the 9,700 ng/g dose group, respectively (Table 2.2). Similar to PFHxS, PFHxA preferentially accumulated in the yolk sac > liver > cerebral hemisphere

and enrichment was observed in yolk sac and liver as levels exceeded the actual whole-egg injection concentrations.

2.4.4. Hepatic and neuronal mRNA levels

Hepatic mRNA levels of two TH-responsive genes, D2 and D3, was up-regulated in liver tissue of embryos exposed to PFHxS. D2 mRNA increased 5-fold at doses of 9,300 ng/g and 38,000 ng/g (p<0.001), while D3 mRNA levels increased 6-fold or greater at doses ≥ 890 ng/g (p<0.05 for 890 ng/g dose group; Figure 2.2A). The mRNA of

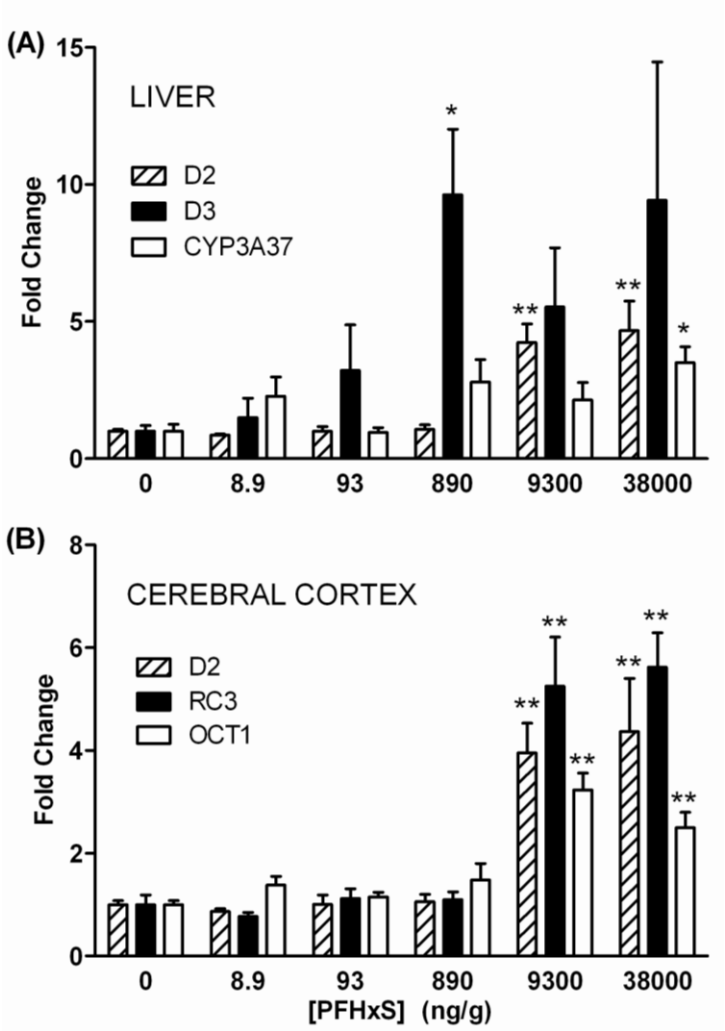

Figure 2.2. The relative mRNA levels of hepatic and neuronal genes following *in ovo* exposure of chicken embryos to perfluorohexane sulfonate (PFHxS). Messenger RNA levels of (A) D2, D3 and CYP3A37 in liver tissue and (B) D2, RC3 and OCT1 in cerebral hemisphere in response to PFHxS were determined by real-time RT-PCR (n=4-8; error bars represent SEM; *p<0.05; **p<0.001).

the phase I metabolizing enzyme, CYP3A37, was also induced 4-fold following exposure to 38,000 ng/g PFHxS in the liver (p<0.05; Figure 2.2A). Neuronal mRNA levels of D2 and two other TH-responsive genes, RC3 and octamer motif binding factor 1 (OCT1), were induced by PFHxS in chicken embryos. The D2, RC3 and OCT1 mRNA levels were significantly up-regulated by 4-, 6-, and 3-fold, respectively, at concentrations ≥ 9,300 ng/g (p<0.001; Figure 2.2B). None of the mRNA transcripts assessed were significantly affected in PFHxA-exposed chicken embryos (p>0.05; data not shown).

2.4.5. Free T4 determination

Free T4 concentrations were significantly reduced in plasma collected from chicken embryos exposed to 890 (p<0.05) and 38,000 ng PFHxS/g (p<0.001) compared to the DMSO control, whereas the lowest dose of 8.9 ng/g did not have a significant effect on free T4 levels (p>0.05; Figure 2.3A). No significant effects on free T4 levels were observed following exposure to any of the PFHxA concentrations assessed (p>0.05; Figure 2.3B).

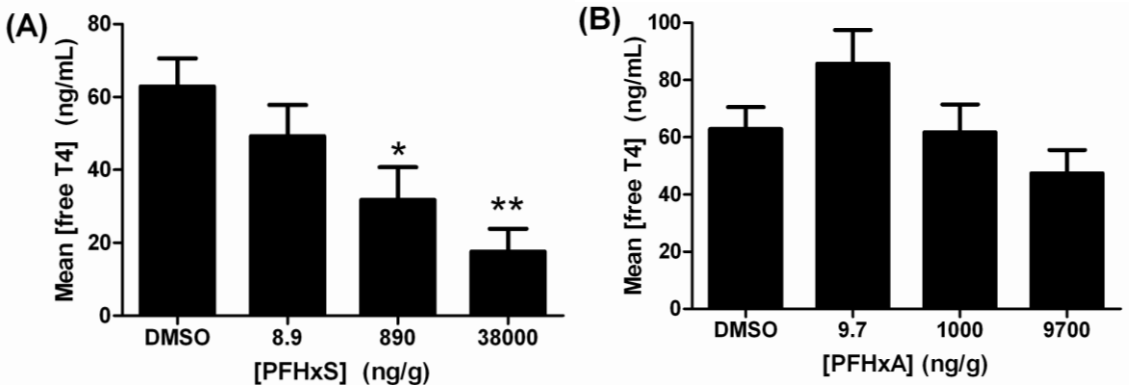

Figure 2.3. Free thyroxine (T4) levels (ng/mL) determined in plasma of embryos exposed to (A) perfluorohexane sulfonate (PFHxS) and (B) perfluorohexanoate (PFHxA), relative to the DMSO control using the AccuBind free T4 kit. Error bars represent the SEM (n=8-22; * p<0.05; **p<0.001).

2.5. DISCUSSION

This study determined the effects of PFHxS and PFHxA on embryonic lethality, developmental endpoints, tissue-specific accumulation, hepatic and neuronal mRNA levels and free T4 levels in chicken embryos. Given the chemical stability and persistence of PFAAs in the environment, their accumulation in blood serum, liver tissue and eggs of wild avian species, and the potential of this class of compounds to disrupt the thyroid hormone pathway, the importance of determining the effects of PFHxS and PFHxA in an avian species is apparent.

Limited toxicity data exist for PFHxS and PFHxA and those that are available are from chronic, sub-chronic and acute mammalian studies (Butenhoff *et al.* 2009a; Chengelis *et al.* 2009; Loveless *et al.* 2009); none are based on avian studies. In this study, embryo pipping success was decreased to 63% in the 38,000 ng PFHxS/g dose group (compared to 94% in the DMSO control). In the highest PFHxA dose group, 9,700 ng/g, pipping success was 80% (compared to 89% in the DMSO control). Variability in pipping success among DMSO and untreated control groups (80-100%) was observed in previous chicken egg injection studies (Crump *et al.* 2011; O'Brien *et al.* 2009a; O'Brien *et al.* 2009b). Therefore, PFHxA was not considered lethal to embryos at the doses assessed because the lowest value fell within the range expected for control groups. PFHxS, on the other hand, caused a decrease in pipping success below this range and was lethal to embryos at an injected concentration of 38,000 ng/g. This injected concentration yielded hepatic levels of 170,000 ng/g ww which is more than three orders of magnitude greater than the maximum reported mean PFHxS concentration in wild avian tissues; 50 ng/g ww in liver tissue of grey herons (Meyer *et al.* 2009). The highest concentration of PFHxA administered, 9,700 ng/g, was

more than 5 orders of magnitude greater than that detected in waterbird eggs; 0.071 ng/g ww in great egrets (Wang *et al.* 2008).

In addition to decreasing pipping success, exposure to 38,000 ng PFHxS/g altered embryonic growth. Mean tarsus length and embryo mass were significantly decreased relative to the DMSO control group. On the other hand, exposure up to the highest dose of 9,700 ng PFHxA/g did not affect any of the growth parameters assessed in this study. Overall, PFHxS was found to alter pipping success and growth/development of embryonic chickens injected prior to incubation. Given the importance of the TH pathway in mediating growth and development in avian species, these findings support further evaluation of TH disruption.

In this study, PFHxS and PFHxA preferentially accumulated in yolk sac > liver > cerebral hemisphere. Concentrations in yolk sac and liver exceeded the whole-egg injection concentration and resulted in maximal enrichment factors (tissue concentration ÷ injected concentration) of 7.8 and 4.5 for PFHxS and 4.4 and 3 for PFHxA. In cerebral hemisphere, levels were consistently lower than the initial injection concentration. The accumulation of PFAAs in hepatic tissue above initial whole-egg concentrations was observed in chicken egg injection studies with PFOS, PFOA, perfluoroundecanoic acid (PFUdA) and perfluorodecane sulfonate (PFDS) in which maximum enrichment factors of 1.5 – 4.5 were reported (O'Brien *et al.* 2009a; O'Brien *et al.* 2009b).

PFAAs are generally highly acidic and exist in aqueous environments as their conjugate bases. Furthermore, the fluorinated hydrocarbon tail of the PFAA conjugate base is lipophilic and the carboxylate or sulfonate functional group is hydrophilic. The polar end of PFAAs preferentially binds with proteins – specifically fatty acid binding proteins, lipoproteins and albumin. PFAAs are sequestered into protein-rich tissues, such as yolk,

liver and blood (Jones *et al.* 2003; Luebker *et al.* 2002). My findings of maximal PFHxS and PFHxA levels in protein-rich compartments (i.e. yolk sac and liver) are consistent with preferential sequestration into protein-rich tissues. The detection of PFHxS and PFHxA in the cerebral hemisphere of chicken embryos demonstrates that they are able to cross the blood-brain barrier. PFOS has also been detected in the brain following laboratory exposures (Austin *et al.* 2003; Sato *et al.* 2009). A dose-dependent accumulation of PFOS was reported in adult female rats intraperitoneally-injected with PFOS at 1 mg/kg body weight (BW) (low dose) and 10 mg/kg BW (high dose) in all brain regions measured (i.e. hypothalamus, cerebral cortex, hippocampus, brain stem, and cerebellum). For instance, in cerebral cortex tissue, the low dose group accumulated 294 ng PFOS/g ww, while the high dose group accumulated 4,487 ng PFOS/g ww. These concentrations are comparable to those observed in the present study. Concentrations of 490 and 3,800 ng PFHxS/g ww were detected in the cerebral hemisphere from the 890 and 9,300 ng PFHxS/g dose groups, respectively. PFHxA accumulation was also observed in the cerebral hemisphere, however to a lesser extent. At the two highest PFHxA dose groups (1,000 ng/g and 9,700 ng/g), PFHxA accumulated to 70 and 800 ng PFHxA/g ww, respectively.

In addition to the overt effects on embryonic development, it was important to assess effects at a more subtle level; i.e. to identify molecular/biochemical effects of exposure that could be linked to the observed response. One of the objectives of this study was to determine the effects of PFHxS and PFHxA treatment on relative mRNA levels of several TH-responsive genes in the liver and cerebral hemisphere of chicken embryos. The molecular mechanisms of action of PFAAs remain unclear, although in recent years the TH pathway has become an evident target (Cheng *et al.* 2011; Lau *et al.* 2003; Thibodeaux *et al.* 2003; Vongphachan *et al.* 2011; Weiss *et al.* 2009; Yu *et al.* 2009).

The mRNA levels of a phase I xenobiotic metabolizing enzyme, cytochrome P450 3A37 (CYP3A37), was induced in response to PFHxS in the liver by 4-fold. CYP3A37 is a chicken xenobiotic-sensing orphan nuclear receptor-regulated enzyme and its up-regulation is associated with increased biotransformation of xenobiotics for detoxication (Goriya *et al.* 2005). The mRNA levels of two enzymes involved in TH homeostasis, D2 and D3, were significantly altered in liver tissue exposed to PFHxS. D2, which converts T4 to its more active form triiodothyronine (T3), was significantly up-regulated in liver tissue of PFHxS-exposed embryos by 5-fold. D3 degrades T4 and/or T3 to form inactive TH derivatives and was also significantly induced in PFHxS-exposed liver tissue by 9-fold, with maximal induction levels greater than those observed for D2 in the liver. Increased D2 and D3 mRNA levels within the liver could lead to altered protein expression and deiodination (outside the scope of the current study), and may be the result of a depletion in circulating T4 levels as T4 would be taken up from the blood stream and into the liver for local deiodination. Future studies would benefit from measuring T4 levels in target tissues (e.g. liver, thyroid gland, cerebral hemisphere) to help determine the cause and effect relationship between reduced T4 levels and altered deiodinase expression. Reduced TH levels can impact overall growth, development, and reproduction of birds.

In the cerebral hemisphere of chicken embryos exposed to PFHxS, TH-responsive genes that were affected included D2, RC3 and OCT1. D2 was induced by PFHxS exposure by 4-fold. Increases in D2 levels in cerebral hemisphere could also lead to diminished circulating T4 levels as a result of augmented, localized outer-ring deiodination of available T4. RC3 is a calmodulin-binding, protein kinase C substrate that is under specific regional and temporal control by T3 (Morte *et al.* 1997). For example, T3 administration increased RC3 mRNA levels up to 30-fold in hypothyroid rats (Iniguez *et al.* 1993). RC3 was up-

regulated 6-fold in cerebral hemisphere in response to PFHxS treatment, a response similar to that observed in CEN cells (i.e. 11-fold induction at 10 μM PFHxS) (Vongphachan *et al.* 2011). Moreover, a commercial mixture of polychlorinated biphenyls (Aroclor 1254) – a class of compounds also suspected of disrupting TH homeostasis – induced RC3 expression in the cerebral cortex of fetal rats demonstrating that RC3 was responsive to an environmental contaminant and that Aroclor 1254 was able to exert TH-like effects via alteration of TH-responsive genes (Gauger *et al.* 2004). Changes in RC3 may also have biological implications in synaptic plasticity, associative learning, and memory (Iniguez *et al.* 1996). OCT1 is a transcription factor involved in cell proliferation and reduced expression is associated with cell cycle arrest and reduced morphological differentiation (Lakin *et al.* 1995). OCT1 expression is responsive to thyroid status – a single dose of T4 increased OCT1 levels in the cortex of athyroid rat pups exposed through the mother during gestation (Dowling *et al.* 2000). In addition, OCT1 has been shown to stimulate thyroid receptor β1 (TRβ1) in cortical neurons and it was suggested that thyroid hormone may act through TRβ1 to enhance OCT1 expression (Nagasawa *et al.* 1997). OCT1 expression was induced 3-fold in response to PFHxS treatment in this study. Furthermore, OCT1 was up-regulated 3- and 5-fold in herring gull embryonic neuronal cells by PFHxS and PFHxA, respectively (Vongphachan *et al.* 2011). OCT1 is also responsive to other environmental contaminants. For example, Aroclor 1254 induced OCT1 expression in the cortex of rodents (Gauger *et al.* 2004). The concordance between the present *in ovo* study and the *in vitro* study by Vongphachan *et al*. (2011) strongly implies that the TH axis is affected by PFAA action.

The observed effects on growth and development combined with the molecular data presented in this study indicate that the TH pathway is a target of PFHxS action. To further

support TH disruption effects, I determined free T4 levels in the plasma of developing chicken embryos exposed to PFHxS and PFHxA. PFHxS significantly decreased plasma free T4 levels in a dose-dependent manner, while PFHxA had no effect on circulating hormone concentration. The depleted free T4 status observed in PFHxS-exposed embryos is in agreement with several of the altered endpoints presented in this study (i.e. reduced pipping success, embryo growth and increased deiodinase expression). The TH axis and the growth hormone (GH) axis are closely related and cross-talk interactions exist between them. GH is required for normal somatic growth in the pre- and post-hatch chicken and there is a critical range of TH levels required for growth; concentrations above or below this range lead to decreased growth (McNabb 2007). Future studies would benefit from a detailed assessment of the cross-talk between the TH and GH axes in avian species as it pertains to altered somatic growth following exposure to environmental contaminants.

The adverse effects in response to PFHxS exposure reported in the present study may, in part, represent an adverse outcome pathway (AOP). An AOP is defined as a sequential series of events that span multiple levels of biological organization used for predictive ecological risk assessment (Ankley *et al.* 2010). PFHxS affected the TH pathway at multiple levels of biological organization – somatic growth, mRNA levels and circulating free T4 concentrations. The lowest PFHxS concentration for which an effect in mRNA levels and circulating free T4 levels was observed was 890 ng/g (injected concentration) or 5100 ng/g ww (liver concentration). These concentrations are 18 or 100 times greater, respectively, than the highest reported mean PFHxS concentration in avian wildlife (50 ng/g ww in liver of grey herons; Meyer *et al.* 2009). TH responses and pathways may be useful in predicting the toxicity of other chemicals in future risk assessments in avian species.

CHAPTER THREE

TRANSCRIPTIONAL PROFILES IN THE CEREBRAL HEMISPHERE OF CHICKEN EMBRYOS FOLLOWING *IN OVO* PERFLUORO-HEXANE SULFONATE EXPOSURE

Modified from Cassone, C.G., Taylor, J.J., O'Brien, J.M., Williams, A., Yauk, C.L., Crump, D., and Kennedy, S.W. (2012). Transcriptional profiles in the cerebral hemisphere of chicken embryos following *in ovo* perfluorohexane sulfonate exposure. *Toxicol. Sci.* (in press).

3.1. ABSTRACT

In a recent egg injection study, I showed that *in ovo* exposure to perfluorohexane sulfonate (PFHxS) affects the pipping success of developing chicken (*Gallus gallus domesticus*) embryos. I also found evidence of thyroid hormone (TH) pathway interference at multiple levels of biological organization (i.e. somatic growth, mRNA levels and circulating free thyroxine levels). Based on these findings, I hypothesize that PFHxS exposure interferes with TH-dependent neurodevelopmental pathways. This study investigates global transcriptional profiles in cerebral hemispheres of chicken embryos following exposure to a solvent control, 890 or 38,000 ng PFHxS/g egg (n=4-5 per group); doses which lead to the adverse effects indicated above. PFHxS significantly alters the expression ($\geq$1.5-fold, $p \leq 0.001$) of 11 transcripts at the low dose (LD; 890 ng/g) and 101 transcripts at the high dose (HD; 38,000 ng/g). Functional enrichment analysis shows that PFHxS affects genes involved in tissue development and morphology, cellular assembly and organization, and cell-to-cell signalling. Pathway and interactome analyses suggest that genes may be affected through several potential regulatory molecules, including integrin receptors, myelocytomatosis viral oncogene and CCAAT/enhancer binding protein. This study identifies key functional and regulatory modes of PFHxS action involving TH-dependent and –independent neurodevelopmental pathways. Some of these TH-dependent

mechanisms that occur during embryonic development include tight junction formation, signal transduction and integrin signaling, while TH-independent mechanisms include gap junction intercellular communication.

3.2. INTRODUCTION

Perfluoroalkyl acids (PFAAs), specifically perfluorinated sulfonates (PFSAs) and carboxylates (PFCAs), are a family of synthetic substances used for their water- and stain-repellent properties. PFAAs have a unique fluorocarbon structure that renders them virtually non-biodegradable and persistent in the environment. Globally, PFSAs and PFCAs have been detected in wildlife and humans and have a tendency to bioaccumulate and biomagnify in food webs (Conder *et al.* 2008). Due to their amphiphilic properties, PFAAs preferentially compartmentalize in protein-rich tissues and have been detected mainly in blood serum, liver and egg samples of wild animal populations worldwide (Giesy and Kannan 2001). Two commonly detected and studied PFAAs, perfluorooctane sulfonate (PFOS) and perfluorooctanoate (PFOA), have been largely phased-out of production in North America; however, certain international manufacturers continue to produce PFOS and its precursors (Wang *et al.* 2010b). Recent production has focused mainly on PFAAs with shorter carbon chain lengths ($C < 8$) to fill market demand.

Perfluorohexane sulfonate (PFHxS) is an example of a PFAA with a shorter carbon chain length ($C = 6$), for which biomonitoring data are limited in wild avian species. PFHxS has been detected in the plasma of herring gulls (*Larus argentatus*) from Lake Huron (Gebbink and Letcher 2012) and in the livers of numerous avian species worldwide at average concentrations ranging from < 0.5 to 50 ng/g wet weight (ww) (Houde *et al.* 2011; Kannan *et al.* 2002; Meyer *et al*. 2009). In herring gull colonies from the Great Lakes,

PFHxS concentrations ranged from below detection limits to 3.8 ng/g ww in whole eggs (Gebbink *et al.* 2011). Although PFHxS is detected in wild avian populations, very little is known about the toxicological effects of exposure. There is a growing body of evidence that suggests various PFAAs can impact neurodevelopment in birds and mammals (Johansson *et al.* 2008; Johansson *et al.* 2009; Lau *et al.* 2003; Lau *et al.* 2004; Lau *et al.* 2007; Lau 2009; Pinkas *et al.* 2010; Slotkin *et al.* 2008; Thibodeaux *et al.* 2003; Wang *et al.* 2010a; Yu *et al.* 2009). Chicken (*Gallus gallus*) egg injection studies report reduced hatching success in response to PFOS and PFOA and higher incidences of physical deformities (Molina *et al.* 2006; O'Brien *et al.* 2009a; O'Brien *et al.* 2009b; Yanai *et al.* 2008). Post-hatch cognitive behaviour (i.e. imprinting behaviour), immune alterations and brain asymmetry changes have also been observed following *in ovo* PFOS and PFOA exposure (Peden-Adams *et al.* 2009; Pinkas *et al.* 2010). Furthermore, PFOS and PFOA have been reported to affect peroxisome proliferator activated receptor alpha (PPARα) activation, lipid metabolism, gap junction intercellular communication (GJIC) and the thyroid hormone (TH) axis (DeWitt *et al.* 2009; Kudo *et al.* 1999; Upham *et al.* 2009; Lau *et al.* 2007).

The reported effects of PFAAs on neurodevelopment led our laboratory to utilize an *in vitro* screening method to determine the effects of 11 short- and long-chained PFAAs on messenger RNA (mRNA) expression of thyroid hormone (TH)-responsive genes in primary cultures of chicken and herring gull embryonic neuronal cells (Vongphachan *et al.* 2011). Effects on the TH pathway were assessed because previous studies reported reduced TH levels (i.e. triiodothyronine [T3] and thyroxine [T4]) in rodents exposed to PFAAs (Chang *et al.* 2008; Martin *et al.* 2007). Vongphachan *et al.* (2011) demonstrated that short-chained PFAAs (< eight carbons) altered the expression of TH-responsive genes, including type II and III 5'-deiodinases (D2 and D3), transthyretin (TTR) and neurogranin (RC3), in chicken

embryonic neuronal cells to a greater extent than long-chained PFAAs (≥ eight carbons). Furthermore, among 24 PFAAs examined, PFHxS had the strongest binding potency for TTR and was able to displace T4 from binding to TTR (Weiss *et al.* 2009). In Chapter 2, *in ovo* exposure to PFHxS reduced the pipping success of chicken embryos and affected the TH pathway at multiple levels of biological organization (i.e. reduced somatic growth, induced gene expression of D2, D3, RC3 and octamer motif binding factor 1 (OCT1) and decreased circulating free T4 levels). Since THs play an essential role in avian brain development (McNabb 2007), disruption of this pathway via PFHxS exposure during neurodevelopment may result in harmful and irreversible effects.

Given that PFHxS affects TH homeostasis in chicken embryos (Chapter 2), I hypothesize that PFHxS exposure interferes with TH-dependent neurodevelopmental pathways. In order to test this hypothesis and to further characterize the effects of PFHxS in the brain, the present study investigates global gene expression profiles in the cerebral hemisphere of chicken embryos from dose groups that demonstrated adverse effects, including a decrease in pipping success and disruptions of the TH system, in my previous study (Chapter 2). The main objectives of this study were to: (1) assess the TH-dependent impacts of PFHxS exposure on gene expression in the brain; and (2) identify novel neurodevelopmental modes of PFHxS action. This study identified potential key functional and regulatory events of PFHxS toxicity during avian neurodevelopment.

3.3. MATERIALS AND METHODS

3.3.1. Chemicals

Linear sodium perfluorohexane sulfonate (PFHxS) was purchased from Wellington Laboratories (Guelph, ON; >98% pure). All stock solutions and serial dilutions were

prepared in dimethyl sulfoxide (DMSO; Fisher Scientific, Ottawa, ON) to yield final in-egg concentrations of 890 and 38,000 ng PFHxS/g egg. The concentrations of the solutions injected into the eggs were determined by high performance liquid chromatography-tandem mass spectrometry (HPLC-MS/MS) as described previously in Chapter 2.

3.3.2. Egg injection and tissue collection

Tissues for gene expression analysis were collected from a PFHxS egg injection experiment described in Chapter 2. In brief, unincubated, fertilized White Leghorn chicken (*Gallus gallus domesticus*) eggs were randomly distributed into the following control and treatment groups: DMSO control (n=20), 890 ng PFHxS/g egg (n=20), and 38,000 ng PFHxS/g egg (n=20), henceforth referred to as the low dose (LD) and the high dose (HD), respectively. An uninjected control group was not included in this study however; previous findings from our laboratory demonstrated a similar pipping success rate among DMSO and uninjected controls (O'Brien *et al.* 2009a; O'Brien *et al.* 2009b). A small hole was drilled through the egg shell at the centre of the air cell and DMSO or PFHxS (~1.0 µl/g egg) was injected into the air cell to attain the desired concentrations described above. After injection, the hole was sealed with filter tape and the eggs were placed horizontally into an incubator (Petersime, Model XI) set at 37.5°C and 58% humidity. During incubation, embryos were monitored frequently by candling and brought to pipping (day 21-22, stage 46 (Hamilton and Hamburger 1951)), at which point embryos were euthanized by decapitation. The left and right cerebral hemispheres were collected; the left was used for chemical residue analysis as described in Chapter 2 and the right was immediately frozen in liquid nitrogen and stored at -80°C for subsequent RNA isolation.

3.3.3. RNA isolation and sample preparation

Total RNA was isolated from a 20-30 mg section of the right cerebral hemisphere (n = 4-5 embryos per treatment group) using RNeasy mini kits according to the manufacturer's instructions (Qiagen). Approximately 5 µg of total RNA was DNase treated using DNA-free kits according to the manufacturer (Ambion, Austin, TX). RNA was quantified with a NanoDrop 2000 spectrophotometer (Thermo Scientific, Wilmington, DE) and RNA quality was assessed using a Bioanalyzer 2100 (Agilent Technologies, Mississauga, ON). Only samples with A260/A280 ratios > 1.8 and an RNA Integrity Number (RIN) > 9 were used for downstream applications. Samples were then prepared by diluting 200 ng RNA to a total volume of 8.3 µL with RNase-free water. A reference pool of RNA for microarray hybridizations was prepared from equal parts of all samples used for microarray analysis and all samples were stored at -80°C for subsequent experiments.

3.3.4. Microarray hybridization

Experimental RNA samples were labeled with Cyanine 5-CTP (Cy5) and chicken reference RNA was labeled with Cyanine 3-CTP (Cy3) using the Quick Amp Labeling Kit (Agilent Technologies), according to manufacturer's instructions. Briefly, double-stranded cDNA was synthesized from 200 ng total RNA using MMLV-RT with T7 promoter primer. Cyanine-labeled cRNA targets were then transcribed *in vitro* using T7 RNA polymerase. The synthesized cRNA was purified using the RNeasy mini kit (Qiagen) and labeled cRNA (825ng) was fragmented at 60°C for 30 min with fragmentation solution. Cy3-reference cRNA and Cy5-sample cRNA were hybridized to Agilent 4X44K chicken gene expression microarrays (containing 44,000 60-mer oligonucleotide probes; Array ID 026441) at 65°C for 17 hours with Agilent hybridization solution and washed according to the manufacturer's

instructions. Arrays were scanned on an Agilent G2505B scanner at 5 μm resolution. Data were acquired with Agilent Feature Extraction software, version 10.7.3.1.

3.3.5. Data analysis for microarrays

A reference design (Kerr 2003; Kerr and Churchill 2001) was used to analyze the gene expression data. Data were pre-processed using R software (http://www.R-project.org). The median signal intensities were normalized using the global locally weighted scatterplot smoothing (LOWESS) method (Yang *et al.* 2002) using the transform.madata function in the microarray analysis of variance (MAANOVA) library (Wu *et al.* 2003). Probes with fluorescent intensity signals significantly greater than the local mean background plus 3 standard deviations (SD) of background intensity were identified as being expressed (denoted as present). Ratio intensity plots were constructed for the raw and normalized data for each array to identify outliers or microarrays with poor data quality. Differentially expressed genes were identified using the MAANOVA library. An ANOVA model including the main effect of treatment and the block effect of the slide was applied. The Fs statistic (Cui *et al.* 2005), a shrinkage estimator, was used for the gene-specific variance components and the associated *p*-values for all the statistical tests were estimated using the permutation method (30,000 permutations with residual shuffling). The least-squares means (LSMeans) (Goodnight and Harvey 1978; Searle *et al.* 1980) was used to estimate the fold changes for each pairwise comparison. Probes were considered differentially expressed if they had absolute fold changes ≥ 1.5 relative to controls and $p \leq 0.001$. The promoter regions (-8kb to +2kb from transcriptional start site) of all differentially expressed genes were scanned for potential TH response elements (TREs), as described in Paquette *et al.* (2011).

Hierarchical clustering was performed using GeneSpring GX ver. 11.0.2 (Agilent Technologies). Clustering was performed on both entities and conditions, using the Euclidian distance metric and the centroid linkage rule.

Functional and canonical pathway analysis was performed in Ingenuity Pathway Analysis (IPA), which identified biological functions/diseases or pathways that were most significant to the dataset. Molecules from the dataset that were recognized as human, mouse or rat orthologs, were differentially expressed and were associated with biological functions and/or diseases in Ingenuity's Knowledgebase were considered for the analysis. A right-tailed Fisher's exact test was used to calculate a *p*-value determining the probability that each biological function/disease or pathway assigned to that dataset was due to chance alone.

For interaction network generation in IPA, differentially expressed genes that mapped into IPA were overlaid onto a global molecular network developed from information contained in Ingenuity's proprietary Knowledgebase. Networks of differentially expressed genes were then algorithmically generated based on their connectivity. Using the Agilent Chicken reference set, only direct interactions between experimentally observed molecules (up to 70 human, rat and mouse orthologs per network) that are expressed in nervous system tissues/primary cells and/or central nervous system (CNS) cell lines were considered. MicroRNAs were not included as a data source for network interactions.

In the network diagrams, genes are represented as nodes and the biological relationship between two nodes is represented as an edge (line). All edges are supported by at least one reference from the literature, a textbook, or from canonical information stored in the Ingenuity Knowledgebase. Nodes are displayed using various shapes that represent the functional class of the gene. The intensity of the node color indicates the degree of up- (red) or down- (green) regulation. Duplicate genes were resolved by using the maximum fold

change value. White and yellow nodes are not differentially expressed, and are added to the network as bridging/connector molecules. Any connector molecule that had direct interactions with four or more disregulated genes was considered to have potential regulatory roles in the PFHxS response and was denoted as a yellow node. IPA was then used to identify all possible direct or indirect interactions between potential regulatory molecules and all disregulated genes in each dose group.

3.3.6. Real-time RT-PCR

Total RNA (375 ng) was reverse transcribed to complementary DNA (cDNA) using SuperScript II reverse transcriptase and random hexamer primers (Invitrogen Canada) as per manufacturer's instructions. Reactions containing an RNA template but lacking reverse transcriptase were run in parallel to verify the absence of contaminating genomic DNA (no-reverse transcriptase control). A 1:20 dilution of cDNA with diethylpyrocarbonate (DEPC)-treated water was prepared and stored at -80°C for subsequent real-time RT-PCR. Changes in mRNA levels were assessed by real-time RT-PCR using the Brilliant Q-PCR Core Reagent Kit (TaqMan assay) or Brilliant SYBR Green Q-PCR Master Mix (SYBR assay) (Agilent Technologies) and MX3000P or MX3005P PCR systems (Stratagene, La Jolla, California). Primer pairs (Invitrogen) and TaqMan fluorogenic probes (Biosearch, Novato, CA) for the transcripts listed in SI Table 3.1 were designed and optimized for real-time RT-PCR.

For TaqMan assays, each 25 µL reaction contained 1X Core PCR buffer, 5 mM $MgCl_2$, 0.8 mM dNTP mix, 8% glycerol, 75 nM ROX reference dye, forward and reverse primers at optimized concentrations (SI Table 3.1), 200 nM fluorogenic probe, 5 µL diluted cDNA (1:20), and 1.25 U SureStart Taq Polymerase. The thermocycler program included an enzyme activation step at 95°C (10 min) and 40 cycles of 95°C (30 sec) and 60°C (1 min).

SYBR assays were used as an alternative to TaqMan assays when fluorogenic probes failed and amplification was non-exponential. Each 25 μL SYBR reaction contained 2X Brilliant SYBR Green QPCR Master Mix, 75 nM ROX reference dye, forward and reverse primers at optimized concentrations (SI Table 3.1) and 5 μL diluted cDNA (1:20). The thermocycler program included an enzyme activation step at 95°C (10 min) and 40 cycles of 95°C (30 sec), 60°C (1 min) and 72°C (30 sec). All reactions were performed using cDNA from the same 4-5 embryos per treatment group used for microarray analysis. All PCR products were sequenced to verify that each primer pair was amplifying the intended gene target. All gene targets were normalized to β-actin (internal control) as its expression was invariable across treatment groups. An identical reaction was conducted, in parallel, for each assay by replacing cDNA template with DEPC water (no template control, NTC) to monitor for contamination. Cycle threshold (Ct) data were normalized to β-actin using the $2^{-\Delta Ct}$ equation (Schmittgen and Livak 2008). The fold change in target gene mRNA abundance in PFAA treatment groups was expressed relative to the solvent control group. Statistically significant differences in mRNA levels were identified by performing a one-way ANOVA to $2^{-\Delta Ct}$-transformed data followed by a Bonferroni's t-test for multiple comparisons versus the solvent control (SigmaStat v2.03; SPSS). Changes were considered statistically significant if $p \leq 0.05$.

3.4. RESULTS

3.4.1. Differentially expressed genes

Changes in gene transcription in the cerebral hemisphere of chicken embryos exposed to PFHxS were identified using Agilent 4x44K chicken gene expression microarrays. The

data discussed in this publication have been deposited in the National Centre for Biotechnology Information (NCBI) Gene Expression Omnibus (series accession GSE37339) (Edgar *et al.* 2002). A total of 106 probes (representing 78 unique genes) were differentially expressed (fold change≥1.5, $p \leq 0.001$) in the cerebral hemisphere following exposure to PFHxS. Of these differentially expressed probes, the majority (94/106 = 89%) were down-regulated by PFHxS in the developing chicken brain while only 12 probes (11%) were up-regulated. A Venn diagram showing the number of probes that were up- or down-regulated by the 890 ng/g (LD) and 38,000 ng/g (HD) of PFHxS is depicted in Figure 3.1. A detailed list of all probes that were differentially expressed following PFHxS exposure is included in the Supplementary Information (SI Table 3.2). Hierarchical clustering was conducted using the list of differentially expressed genes and revealed two main branches dividing the HD group from the solvent control group (Figure 3.2).

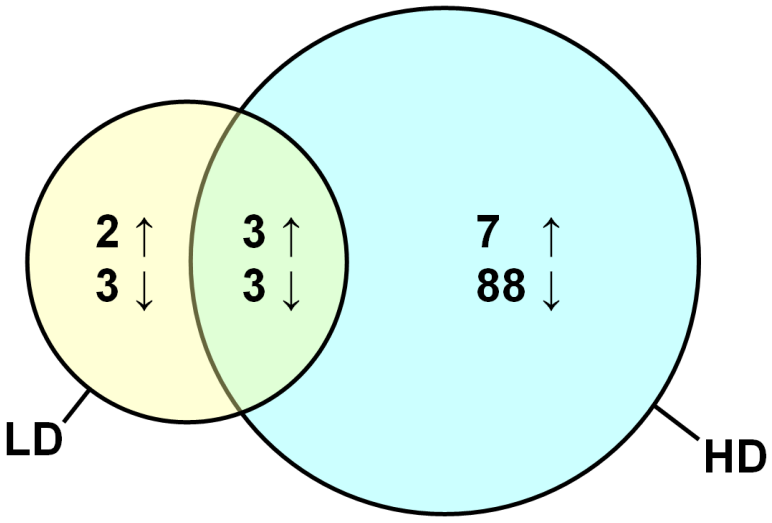

Figure 3.1. Venn diagram illustrating the number of genes up-(↑) or down-(↓) regulated (fold change≥1.5, $p \leq 0.001$) by either 890 ng/g (LD) or 38,000 ng/g (HD) perfluorohexane sulfonate in the cerebral hemisphere of embryonic chickens.

The two largest significant decreases in expression in response to PFHxS exposure were for two splice variants of nephroblastoma overexpressed gene (NOV), which were down-regulated by 4.3- and 5.2-fold at the HD. Both NOV splice variants were also decreased in the LD by 1.6- and 2-fold although the expression changes were not statistically significant. The third largest significant decrease in expression in response to PFHxS exposure was for claudin 11 (CLDN11), which was reduced by 3.2-fold at the HD. A duplicate probe for CLDN11 was also decreased significantly by 2.4-fold at the HD. At the LD, both CLDN11 probes were also decreased by 1.4-fold, but not significantly. Few of the differentially expressed genes determined by the microarray analysis were up-regulated by PFHxS exposure. The largest significant increase in expression in response to PFHxS exposure was for heparan sulfate 6-O-sulfotransferase 2 (HS6ST2), which was up-regulated by 4.9- and 2.4-fold at the LD and HD, respectively.

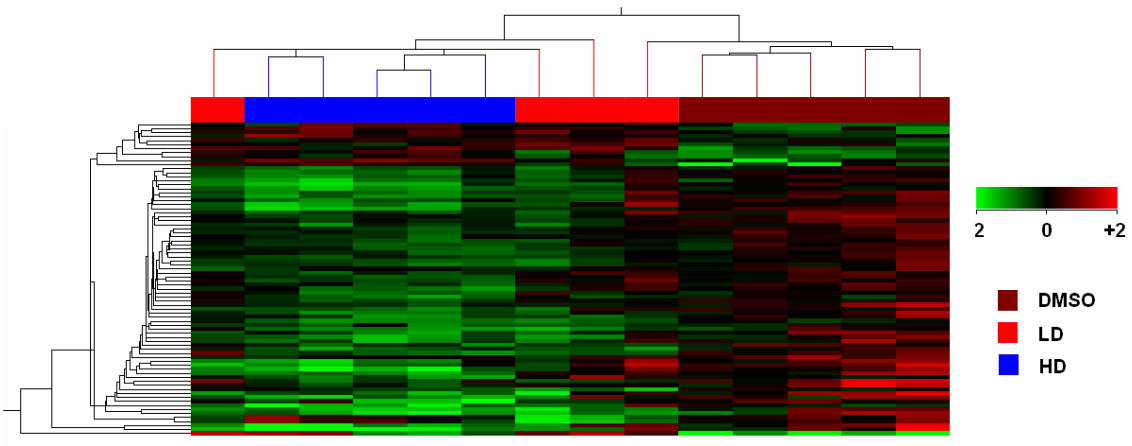

Figure 3.2. Hierarchical clustering of expression profiles from the cerebral hemisphere of chicken embryos exposed to the dimethyl sulfoxide (DMSO) solvent control, 890 ng/g (LD) or 38,000 ng/g (HD) perfluorohexane sulfonate. Clustering was based on 78 unique and differentially expressed genes (fold change$\geq$1.5, $p\leq$0.001).

The expression of several differentially expressed genes identified via microarray analysis was assessed using real-time RT-PCR. The expression of CLDN11, desmoplakin (DSP), and NOV were consistent between approaches (Figure 3.3). An additional nine transcripts, selected for their role in the interaction networks discussed below, were also analyzed by real-time RT-PCR to assess concordance with microarray results (SI Figure 3.1).

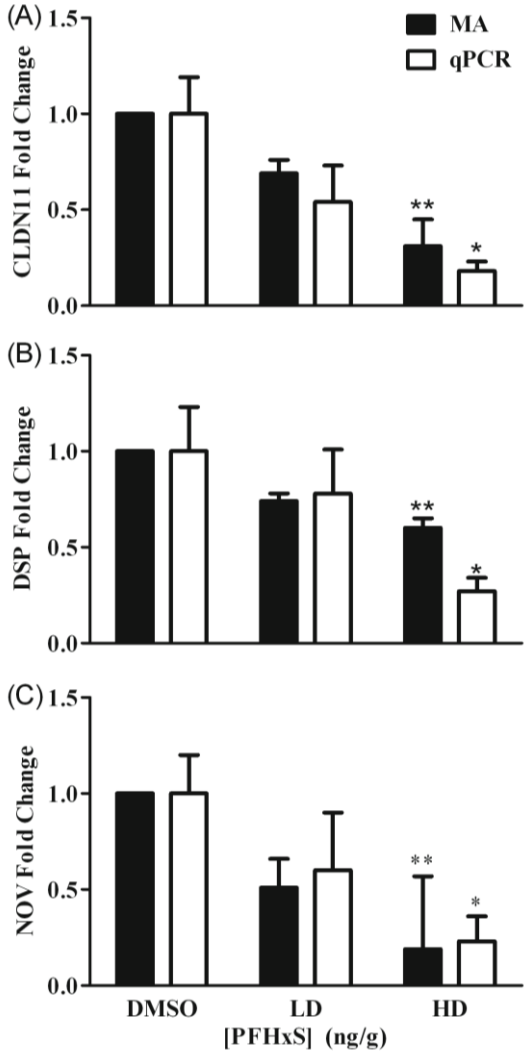

Figure 3.3. The relative mRNA levels of neuronal transcripts following *in ovo* exposure of chicken embryos to 890 ng/g (LD) or 38,000 ng/g (HD) perfluorohexane sulfonate. Messenger RNA levels of [A] claudin 11 (CLDN11); [B] desmoplakin (DSP); and [C] nephroblastoma overexpressed gene (NOV) were determined by microarray (MA, black bars) and real-time RT-PCR (qPCR, white bars) (n=4-5; error bars represent SEM; *$p \leq 0.05$; **$p \leq 0.001$).

A complete list of transcripts assessed is included in SI Table 3.1. Transcripts assessed by real-time RT-PCR were directionally consistent with microarray data for 17 out of 24 conditions (i.e. 12 genes at two dose groups). This level of concordance between real-time RT-PCR and microarray data is comparable to a study by Wang *et al.* (2010a) which showed that gene expression profiles in the rat brain were directionally consistent for 11 out of 14 conditions.

3.4.2. Functional analysis and canonical pathway mapping

For all probes on the chicken array, 29,985 out of 43,603 (69%) were recognized by IPA as gene orthologs in human, rat or mouse. Of all disregulated genes, 86 of 106 probes (81%) were mapped as orthologs in IPA (shown in SI Table 3.2). The majority of unmapped IDs correspond to probes for hypothetical proteins and ESTs with unknown function and therefore could not be included in downstream functional, pathway, and interactome analysis.

Functional enrichment analysis of the differentially expressed genes was performed using IPA. The relevant functional categories are summarized in Table 3.1. Detailed lists of the specific significantly enriched functions and genes within each category are included in SI Table 3.3. The top functional categories, based on significance ($p \leq 0.05$), were: tissue development and morphology, cellular assembly and organization, cell-to-cell signalling and interaction, cellular movement, and nervous system development and function. Many of the tissue development and morphology functions that were enriched were involved in adherence, adhesion, assembly and cell-cell contact of astrocytes, glioma cells and neuroepithelial cells.

Table 3.1. Enriched functional categories for genes differentially expressed in chicken embryonic cerebral hemisphere following exposure to 890 ng/g (LD) or 38,000 ng/g (HD) perfluorohexane sulfonate.

Rank	Category	LD				HD			
		p-value Range			# Genes	*p*-value Range			# Genes
1	Tissue Development and Morphology	7.59E-04	—	4.49E-02	4	5.58E-04	—	4.61E-02	18
2	Cellular Assembly and Organization	7.59E-04	—	4.62E-02	2	5.58E-04	—	4.61E-02	13
3	Cell-To-Cell Signaling and Interaction	7.57E-03	—	4.18E-02	2	5.58E-04	—	4.61E-02	8
4	Cellular Movement	2.28E-03	—	4.77E-02	2	6.06E-04	—	4.16E-02	11
5	Nervous System Development and Function	7.59E-04	—	4.62E-02	2	6.06E-04	—	4.61E-02	5
6	Cell Development and Morphology	7.59E-04	—	4.03E-02	3	7.56E-04	—	4.36E-02	19
7	Molecular Transport	1.52E-03	—	1.36E-02	3	2.17E-03	—	3.25E-02	7
8	Lipid Metabolism	7.59E-04	—	3.79E-03	2	2.17E-03	—	3.70E-02	4
9	Cellular Growth and Proliferation	7.59E-04	—	4.03E-02	4	4.26E-03	—	4.67E-02	12
10	Endocrine System Development and Disorders	7.59E-04	—	7.59E-04	1	4.67E-03	—	4.69E-02	10
11	Protein Synthesis and Trafficking	1.36E-02	—	1.36E-02	1	4.71E-03	—	1.28E-02	4
12	Gene Expression	3.79E-03	—	3.79E-03	1	4.71E-03	—	3.25E-02	3
13	Amino Acid Metabolism	7.59E-04	—	1.52E-03	1	4.71E-03	—	3.25E-02	2
14	Embryonic Development	7.59E-04	—	4.40E-02	2	4.71E-03	—	3.40E-02	14
15	Nucleic Acid Metabolism	1.52E-03	—	1.36E-02	2	4.71E-03	—	3.70E-02	2
16	Carbohydrate Metabolism	1.52E-03	—	1.52E-03	1	9.39E-03	—	3.70E-02	2
17	Cancer	4.40E-02	—	4.77E-02	1	9.39E-03	—	4.61E-02	19
18	Cellular Function and Maintenance					1.41E-02	—	1.41E-02	1
19	DNA Replication, Recombination, and Repair					1.87E-02	—	1.87E-02	1
20	Organismal Survival					3.01E-02	—	3.01E-02	2

Differentially expressed genes were mapped to canonical pathways using Ingenuity's Knowledgebase in IPA, which revealed that exposure to PFHxS disregulated genes belonging to several pathways. Canonical pathways that were significantly affected are summarized in Table 3.2. Pathways that were most significantly disrupted by PFHxS exposure include dendritic cell maturation, integrin-linked kinase (ILK) signaling (SI Figure 3.2), and virus entry via endocytic pathways.

Table 3.2. Enriched canonical pathways for genes that were differentially expressed in the cerebral hemisphere of chicken embryos exposed to 38,000 ng/g perfluorohexane sulfonate. Only pathways with two or more affected genes were reported.

Ingenuity Canonical Pathways	***p*-value**	**# Genes**	**Genes**	**# Molecules in Pathway**
Dendritic Cell Maturation	2.57E-03	3	PIK3R1, HLA-C, COL3A1	110
ILK Signaling	1.20E-02	5	DSP, PIK3R1, FN1, VIM, PGF	159
Virus Entry via Endocytic Pathways	2.82E-02	2	PIK3R1, HLA-C	83
Role of Macrophages, Fibroblasts and Endothelial Cells in Rheumatoid Arthritis	3.63E-02	4	PIK3R1, FN1, SFRP2, PGF	247
IGF-1 Signaling	3.72E-02	2	PIK3R1, NOV	93
Hereditary Breast Cancer Signaling	4.27E-02	2	PIK3R1, SLC19A1	109
Relaxin Signaling	4.57E-02	2	PIK3R1, PDE5A	127
Hepatic Fibrosis / Hepatic Stellate Cell Activation	4.90E-02	3	FN1, COL3A1, PGF	122

3.4.3. Interaction networks and potential regulatory molecules

Interaction networks were generated in IPA using mapped orthologs of differentially expressed genes from the HD treatment group. Interaction networks for the LD group were not identified as too few genes were disregulated and connections could not be established. The network generated is shown in Figure 3.4, where only direct interactions with gene products that occur in the brain were considered. Indirect interactions were not considered

because they do not require evidence that a physical interactuion exist between genes or gene products and, therefore, can lead to uncertainties regarding the nature of the interaction because of the potential involvement of one or multiple intermediary factor(s). A summary of potential regulatory molecules (i.e. interactions with four or more genes that were differentially expressed by PFHxS exposure) is listed in Table 3.3 and a detailed list of the interacting genes is included in SI Table 3.4. The potential regulatory molecules identified through interactome analysis include integrin beta 1 (ITGβ1), myelocytomatosis viral oncogene (MYC) and CCAAT/enhancer binding protein beta (C/EBPβ).

Table 3.3. Molecules from networks generated in Ingenuity Pathway Analysis that had interactions with four or more genes that were differentially expressed (DE) in the cerebral hemisphere of chicken embryos exposed to 38,000 ng/g perfluorohexane sulfonate. Fold change (FC) and *p*-values from microarray are also reported.

Molecule	Entrez Name	FC	*p*-value	# Interacting DE Genes		
				Direct	Indirect	Total
MYC	Myelocytomatosis viral oncogene homolog (avian)	-1.13	0.021	6	1	7
SRC	Sarcoma viral oncogene homolog (avian)	1.11	0.007	5	2	7
HIF1α	Hypoxia inducible factor 1, alpha	1.17	0.169	4	2	6
HNF4α	Hepatocyte nuclear factor 4, alpha	-1.15	0.061	5	0	5
C/EBPβ	CCAAT/enhancer binding protein (C/EBP), beta	-1.05	0.538	3	1	4
SP1	Specificity protein 1 transcription factor	-1.18	0.214	4	0	4
ITGβ1	Integrin, beta 1	-1.26	0.189	3	1	4
THBS1	Thrombospondin 1	-1.48	0.002	4	0	4

3.5. DISCUSSION

This study determined the effects of exposure to two PFHxS doses on global transcription profiles in the cerebral hemisphere of developing chicken embryos. Other

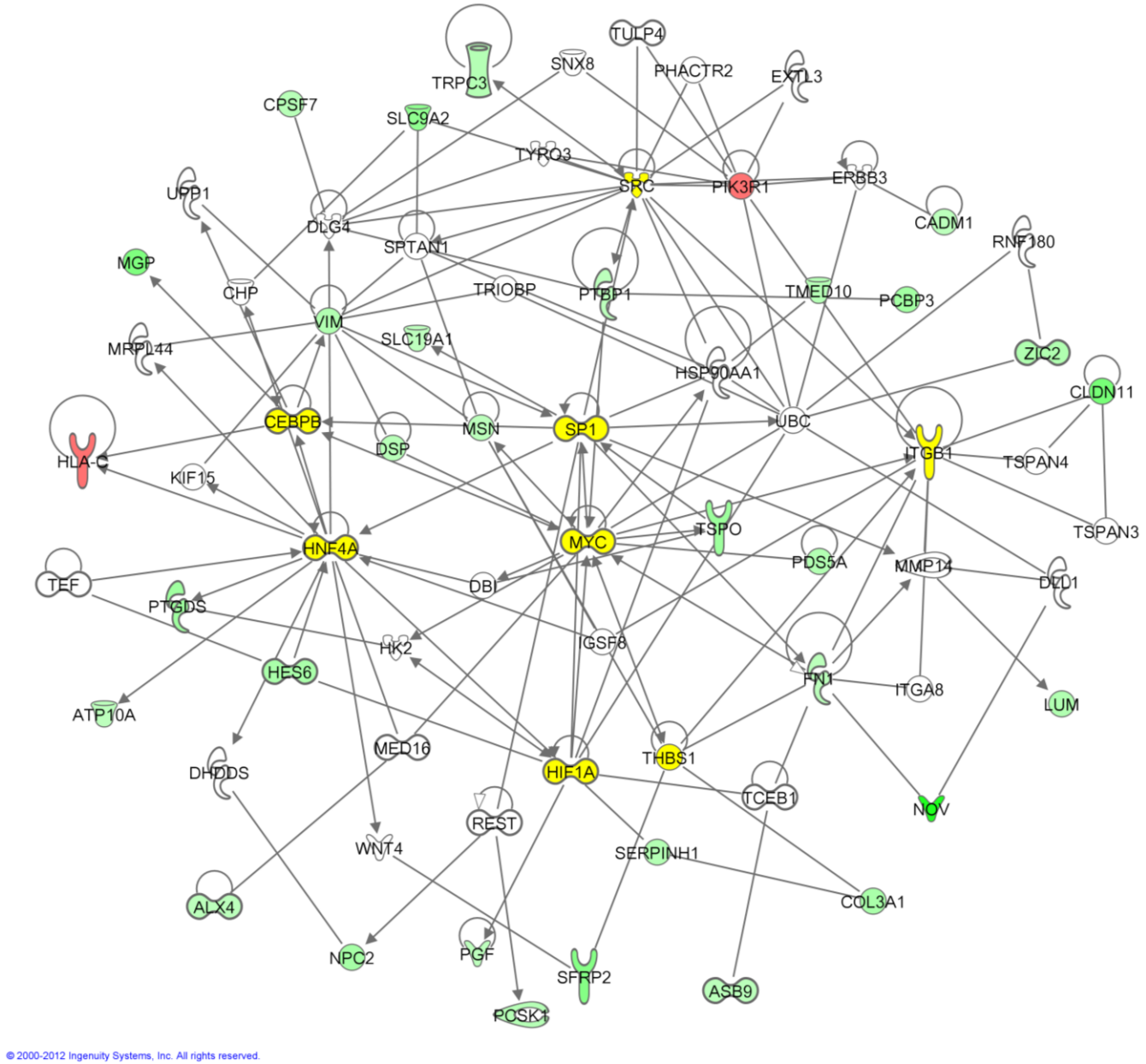

Figure 3.4. Ingenuity Pathway Analysis (IPA)-generated interaction network for genes disregulated by exposure to 38,000 ng/g perfluorohexane sulfonate. Red nodes represent genes that were significantly up-regulated and green nodes represent genes that were significantly down-regulated. Connecting lines (edges) represent direct interactions between genes that are documented in the Ingenuity Knowledgebase. White and yellow nodes are genes that were added to the network by IPA based on their connectivity to disregulated genes, where yellow nodes are considered potential regulatory molecules (see Table 3.3).

genomic studies in avian species include the development, annotation and utilization of microarrays to determine molecular perturbations in Northern bobwhite (*Colinus virginianus*) following 2,6-dinitrotoluene (Rawat *et al.* 2010a; Rawat *et al.* 2010b). The analysis revealed 78 genes that were differentially expressed, the majority of which were responsive only at the HD (86%) and were primarily down-regulated (89%). Cluster analysis on the differentially expressed genes separated DMSO-exposed cerebral hemisphere from all except one of the PFHxS-treated embryos. Hierarchical clustering could not separate two LD samples from the HD treatment groups. The clustering results demonstrate a clear dose-response relationship, with the HD clustering furthest from the DMSO group and the LD having an intermediate expression profile.

The NOV transcript had the largest significant decrease in expression levels following PFHxS exposure, a result that was confirmed by real-time RT-PCR. Nephroblastoma overexpressed gene is involved in organogenesis and regulation of various cellular processes such as adhesion, migration, proliferation, differentiation and survival (Le Dreau *et al.* 2010b). A microarray study on liver tissue of 14-week-old chickens revealed induction of NOV expression after four weeks of PFOS and PFOA exposure at 0.1 and 0.5 mg/mL, respectively, followed by four weeks of depuration (Yeung *et al.* 2007). The results from this study and Yeung *et al.* 2007 indicate that NOV expression is altered following exposure to various PFAAs. The variability in direction of disregulation could be based on differences in life-history stage (pipping embryo vs. 14-week-old chickens), tissue type (cerebral hemisphere vs. liver), and PFAA (PFHxS vs. PFOS and PFOA) between the two studies. Furthermore, NOV may play a role in GJIC, where the anti-proliferative activity of NOV affects reorganization of cellular contacts (Gupta *et al.* 2001). It is well documented that PFAAs can influence GJIC (Hu *et al.* 2002; Upham *et al.* 2009; Yoo *et al.* 2008) and

chronic GJIC disruption could lead to serious neurological and endocrinological problems (Hu *et al.* 2002). In rat liver and dolphin kidney epithelial cell lines, PFHxS inhibits GJIC in a rapid and reversible dose-dependent manner, although the mechanism is not fully understood (Hu *et al.* 2002; Yoo *et al.* 2008). It is plausible that the effects of PFHxS on GJIC in the brain are related to NOV down-regulation. In addition, altered GJIC activity may partly explain the reduced growth observed in chicken embryos from the PFHxS egg injection study (Chapter 2) as GJIC is known to be essential for normal growth and development (Fu *et al.* 2004). Overall, the utility of NOV expression as an indicator of PFAA exposure warrants further investigation (e.g. mechanistic *in vitro* studies) given the variable expression results in two avian studies following exposure to various PFAAs (this study vs. Yeung *et al.* 2007).

Claudin 11 is a transmembrane protein that functions within the myelin sheaths of the brain and its transcript levels were significantly diminished in response to the HD of PFHxS, a result that was confirmed by real-time RT-PCR. Claudin 11 plays a critical role in tight junction (TJ) formation. TJs are composed partly of claudins and when formed between the blood-brain barrier (BBB) endothelial cells, lead to high endothelial electrical resistance and low paracellular permeability (Stamatovic *et al.* 2008). Claudin 11-null mice exhibit a 60% decrease in nerve conduction (Devaux and Gow 2008) and absent CNS myelin and TJ formation, leading to neurological deficiencies (Tiwari-Woodruff *et al.* 2001). PFOS treatment of human brain microvascular endothelial cells – major components of the BBB – results in disassembly (i.e. "opening") of endothelial TJs and increases in permeability; claudin 5 distribution is also disrupted (Stamatovic *et al.* 2008). Desmoplakin, another important player in endothelial junctions, was also significantly decreased in the HD PFHxS group and validated by real-time RT-PCR. Desmoplakin is involved in cellular structure and

is an indispensable component of functional desmosomes, intercellular junctions that tightly link adjacent cells. Desmoplakin knockout mice demonstrate increased embryonic death (Gallicano *et al.* 1998; Vasioukhin *et al.* 2001). Taken together, my results indicate that PFHxS may act on CLDN11 and/or DSP, which affects TJ formation and may facilitate transport across the BBB. This hypothesis is in agreement with the dose-dependent PFHxS accumulation observed in cerebral hemispheres of chicken embryos reported in Chapter 2.

Functional enrichment analysis identified the top functional categories to be tissue development and morphology, cellular assembly and organization, cell-to-cell signalling and interaction, cellular movement, and nervous system development and function. To my knowledge, only one other study has investigated gene expression profiles in the brain in response to PFAA treatment (Wang *et al.* 2010a). Wang *et al.* (2010a) demonstrated similar functional enrichment in the cortex of rat pups exposed prenatally to PFOS, where the top functional categories were cell cycle, tight junction and cell communication. As such, the functional profiles determined by the present avian study are consistent with the gene expression study using mammalian models.

The functions described above are essential to embryonic development; perturbation of the associated genes may result in abnormal maturation and function of the CNS. Developmental neurotoxicity has been reported previously in response to PFAA exposure (Lau *et al.* 2004; Lau *et al.* 2007). At a cellular level, PFAAs have negative effects on cell growth and replication as well as cell numbers and viability in undifferentiated and differentiated PC12 cells (a neuronotypic cell line used to characterize neurotoxicity) (Slotkin *et al.* 2008). These findings agree with the cellular growth and proliferation functional category that was significantly enriched by PFHxS exposure in the present study. In neonatal mice given a single, oral dose of PFOS or PFOA, levels of proteins important in

normal brain development (i.e. neuronal growth and synaptogenesis) were altered in the hippocampus and cerebral cortex (Johansson *et al.* 2009), which supports the functional categories enriched in the present study (i.e. tissue development and morphology and nervous system development and function). Furthermore, prolonged PFAA treatment moderately inhibited neurite growth and dramatically suppressed synaptogenesis in cultured neurons in a chain length- and functional group-dependent manner, where PFHxS suppressed the neurite sum lengths by ~10% (Liao *et al.* 2009). This reduction suggests that long-term exposure may result in serious neurodevelopmental damage.

3.5.1. Integrin receptors and signaling

Integrins are transmembrane receptors essential to embryonic development and necessary for neuronal cells to attach, spread, migrate and extend processes on extracellular matrix molecules and mediate cell-cell and cell-matrix adhesion events (Wu and Reddy 2012). Mice lacking extracellular matrix components, such as fibronectin, or lacking β1 integrins die during the early stages of embryonic development. Fibronectin 1 (FN1) was significantly decreased by the HD of PFHxS via microarray. This decrease was confirmed by real-time RT-PCR. Integrins were also found to interact with many of the top differentially expressed genes in my study, providing further support to their involvement in PFHxS response. Nephroblastoma overexpressed gene is a putative ligand for integrin receptors, including β1 and β5 (ITGβ1 and ITGβ5, respectively), and mediates several cellular actions such as cell adhesion and proliferation (Le Dreau *et al.* 2010a; Le Dreau *et al.* 2010b; Sin *et al.* 2009). Claudin 11 forms a complex with ITGβ1 to regulate proliferation and migration of oligodendrocytes (Tiwari-Woodruff *et al.* 2001; Tiwari-Woodruff *et al.* 2004). Therefore, decreased FN1 transcript levels and integrin-mediated response genes may contribute to the reduced pipping success observed in chicken embryos at the HD in Chapter 2.

Among enriched canonical pathways, ILK signaling had the largest number of perturbed genes (i.e. DSP, phosphoinositide-3-kinase, regulatory subunit 1 [PIK3R1], FN1, vimentin [VIM] and placental growth factor [PGF]) following PFHxS treatment. Most of the genes that were disrupted are downstream products of ILK activation, as opposed to genes that interact directly with ILK. The expression of these downstream genes – DSP, FN1, VIM and PGF – is directly regulated, at the transcriptional level, by snail homolog 2 (SLUG) or hypoxia inducible factor 1 alpha (HIF1α) (Jethwa *et al.* 2008; Savagner *et al.* 1997; Tan *et al.* 2004; Vuoriluoto *et al.* 2011). SLUG is a transcription factor required for the development of neural crest cells, which give rise to many tissues and cells during embryonic development (Cohen *et al.* 1998). HIF1α is a transcription factor that functions in reduced oxygen conditions to induce the transcription of various target genes involved in tumor angiogenesis, invasion, cell survival and glucose metabolism (Kaur *et al.* 2005). SLUG and HIF1α are two of the most overexpressed transcription factors in human glioblastomas when compared to non-tumor brains (Yang *et al.* 2010). Furthermore, PFOS and perfluorodecanoic acid (PFDA) both stimulate glioblastoma cell proliferation (Merritt and Foran 2007).

Detailed network analysis of my dataset revealed that an integrin receptor (i.e. ITGβ1) may be a potential regulatory molecule (i.e. ITGβ1 had interactions with four or more genes that were differentially expressed by PFHxS exposure) driving the observed integrin-associated responses in PFHxS-exposed embryos. ITGβ1 has been implicated in regulating the morphology of cortical development and dendritic spines, formation of synapses in neurons and mediating neurite outgrowth after injury. Taken together, these data provide further evidence to suggest that integrin receptors and signaling play an integral role in PFHxS action.

3.5.2. Thyroid-dependent effects

Thyroid hormones are important for the control of growth and development in birds because they directly trigger cellular differentiation and maturation in a number of tissues, but are especially important in neurodevelopment (McNabb 2007). Previously, I reported that PFHxS adversely affects the TH pathway of developing chicken embryos at multiple levels of biological organization (Chapter 2). At concentrations ≥ 890 ng/g, PFHxS induced the expression of TH-responsive genes (D2, D3, RC3 and OCT1) in liver and the cerebral hemisphere and diminished circulating free T4 levels. It was hypothesized that increases in D2 and D3 levels led to reduced free T4 levels as a result of augmented, localized metabolism of available T4. Furthermore, at 38,000 ng/g, PFHxS decreased pipping success and reduced the mass and tarsus length of surviving embryos. In the present study, I examined the cerebral hemispheres from dose groups in Chapter 2 that demonstrated adverse TH-related effects using microarrays, thereby phenotypically anchoring gene expression data to these toxicologically relevant endpoints.

The top differentially expressed genes were hypothesized to be associated with TH-dependent effects. As NOV expression is not known to be directly or indirectly mediated by TH, it is unclear whether this effect is a TH-specific or independent process. However, the promoter region of NOV was scanned for TRE consensus sequences and 8 potential TREs were found. Future studies investigating whether these TREs are active sites of TH receptor binding and transcriptional control would be valuable to further elucidate PFHxS mode of action. Claudin 11 and DSP also contain 2 potential TREs in the promoter region of each gene. Furthermore, TJ opening is hypothesized to occur via the phosphatidylinositol 3-kinase (PI3K) signaling pathway (Wang *et al.* 2011), which plays a role in non-genomic TH action. In addition to the perturbation of CLDN11 expression observed in this study, PIK3R1

was significantly induced in response to the HD of PFHxS, a result that was directionally consistent with real-time RT-PCR data. THs activate the PI3K pathway at the cell surface via integrins, which ultimately increases transcription of various genes (Davis *et al.* 2009; Di, I 2008; Lu and Cheng 2010; Moeller and Broecker-Preuss 2011; Sheng *et al.* 2012). Thus, TH-driven perturbations in PIK3R1 may lead to changes in CLDN11 and DSP expression, and reflect important neurotoxicological events in the TH-dependent mode of action of PFHxS. Moreover, non-genomic mechanisms of TH action have been described in many tissues, including the brain, some of which appear to be mediated by integrins (Di, I 2008; Moeller and Broecker-Preuss 2011; Sheng *et al.* 2012). This suggests that disruption of ILK signaling in response to PFHxS may also result from TH-dependent pathways. Protein binding studies with integrins and THs, in response to PFHxS exposure, would offer further clarification on this mechanism.

Enriched functional categories can also be linked to the TH effects observed in my previous egg injection study (Chapter 2). Tissue-specific differentiation and maturation is a TH-dependent function in birds (McNabb 2007) and appears to be affected by the LD and HD of PFHxS. At the LD of PFHxS, few genes with known functions were altered. Wingless-type MMTV integration site family, member 5A (WNT5A) was significantly decreased and HS6ST2 and gamma-glutamyltransferase 1 (GGT1) were significantly increased by PFHxS at the LD. Together, WNT5A, HS6ST2 and GGT1 are involved in tissue development and proliferation of cells. These altered genes and enriched functions were affected at the same dose group that demonstrated a decrease in free T4 levels in chicken embryos (Chapter 2). Diminished free T4 levels may result in reduced embryonic growth, which corresponds with the enriched functions observed at the LD in the present study, as well as effects observed at the HD. At the HD, tissue development and morphology

was also enriched via interference with intercellular interactions. Furthermore, the cellular assembly and organization category had several enriched functions relating to formation of intercellular junctions, further supporting the role of PFHxS in disrupting cell-cell interactions. In addition, this category comprised many enriched functions involved in the reorganization of F-actin, morphology of actin filaments, formation of actin cytoskeleton and organization of actin stress fibres. Diminished circulating free T4 levels can influence actin and tubulin expression (Smith *et al.* 2002), and further supports a TH-dependent mode of action. Since THs regulate neurodevelopment, it can be hypothesized that the reduced free T4 levels observed in response to PFHxS exposure could be a factor explaining the enriched functional categories described in the present study.

The potential regulatory molecules identified in the current study are also linked to TH-dependent effects. Thyroxine is able to induce short-term responses in both neurons and astrocytes by binding to integrins; T4 induces integrin binding to its ligand, laminin (Farwell *et al.* 2005). Farwell *et al.* (2005) demonstrate that T4 (but not T3) directly regulates F-actin content of elongating neurites and promotes extensive granule cell migration and neuronal process outgrowth, which are attenuated by anti-ITGβ1 antibodies. These data suggest that T4 influences neuronal process outgrowth via integrin receptors. Overall, the results of my study support a causal association between THs and integrin signaling at the molecular level (i.e. individual gene expression changes and perturbed pathways) and phenotypic level (i.e. decreased embryo growth and reduced free T4 levels) in response to PFHxS exposure in developing chicken embryos (Chapter 2).

Other regulatory molecules identified include MYC and C/EBPβ, receptor pathways that were suppressed in response to PFHxS exposure. MYC is a transcription factor that plays an important role in growth control, differentiation and apoptosis and is believed to

regulate the expression of 10-15% of all cellular genes (Hoffman and Liebermann 2008). The MYC protein is one of the most frequently affected in a variety of cancers and its target genes participate in functions including cell cycle, survival, protein synthesis and cell adhesion (Hoffman and Liebermann 2008). The majority of genes that were disregulated by PFHxS and that interact with MYC are involved in tissue development and apoptosis functions. Although MYC expression was not significantly altered in this study, it was implicated as a regulatory molecule in response to PFHxS treatment. PFOS exposure was found to upregulate MYC expression in the spleen of adult male mice (Dong *et al.* 2012). The variability in gene expression response between this study and the Dong *et al.* 2012 study may be based on differences in species (i.e. chicken vs. mouse) and life-history stage (i.e. embryo vs. adult). In addition, MYC expression can be directly regulated by THs; neuroblastoma cells treated with T3 rapidly down-regulate MYC (Puzianowska-Kuznicka *et al.* 2006). C/EBPβ protein plays a pivotal role in the control of cellular growth, proliferation and differentiation (Ramji and Foka 2002). In the brain, C/EBPβ functions in neuronal differentiation, learning and memory processes, glial or neuronal cell functions and synaptic plasticity (Calella *et al.* 2007; Sterneck and Johnson 1998). All of the genes that were disregulated by PFHxS and interact with C/EBPβ are involved in cell death (i.e. down-regulation of these genes increases apoptosis). In mammalian cells, C/EBPβ binds the promoter region of the MYC gene and represses expression (Berberich-Siebelt *et al.* 2006; Gutsch *et al.* 2011; Sebastian *et al.* 2005). Furthermore, C/EBPβ plays a role in TH-dependent transactivation and its expression can also be mediated by THs (Wang *et al.* 2009). These data taken together suggest a TH-dependent mode of action in the regulation of cellular growth and survival mediated via MYC and C/EBPβ following PFHxS exposure in the developing chicken brain.

3.5.3. Conclusion

Due to the voluntary phase-out of PFOS and PFOA, short-chain PFAAs are being manufactured as replacement substances. PFHxS is an example of a short-chained PFSA that has been detected in the environment and biota, for which few toxicological studies exist. Previously, I reported TH-disrupting effects of PFHxS in developing chicken embryos (Chapter 2) with a lowest observable adverse effect level (890 ng/g) that was 18 times greater than the highest reported mean concentration in avian wildlife (50 ng/g ww in liver of grey herons (Meyer *et al.* 2009)). Effects on the TH pathway at 890 ng/g PFHxS led to the genome-wide evaluation of transcription profiles of PFHxS action in the present study; however, effects on gene expression and molecular mechanisms were minimal in the cerebral hemisphere at 890 ng/g PFHxS. At 38,000 ng/g, functional enrichment analysis revealed effects on genes associated with tissue development and morphology and cellular assembly and organization, two categories that are TH-dependent. Interactome analysis further suggested that genes may be affected through integrin receptors and integrin signaling pathways, which can be TH-dependent via non-genomic mechanisms. These transcriptional responses support my hypothesis that TH-dependent neurodevelopmental pathways are affected in developing chicken embryos exposed to PFHxS. One TH-independent mode of PFHxS action identified was gap junction intercellular communication via NOV down-regulation. Overall, the use of microarray technology enabled the identification of novel modes of PFHxS action, including developmental and cellular processes and expanded our understanding concerning the molecular effects of PFHxS.

CHAPTER FOUR

GENERAL CONCLUSIONS AND FUTURE DIRECTIONS

4.1. CONCLUSIONS

The majority of PFAA research conducted to date has been on PFOS and PFOA, the two most frequently used and detected chemicals from this family of substances. Studies on PFOS and PFOA including animal toxicity, biomonitoring, endocrine disruption, and toxicokinetics have been conducted; however, the specific modes of action of PFAAs are not well established. With the phase-out of PFOS and PFOA, substitute compounds (i.e. PFAAs with < eight carbons) have been used as replacements. There are still many information gaps concerning the effects of short-chained PFAAs, including PFHxS and PFHxA, especially in non-mammalian species. Despite the wide-spread detection of PFHxS in birds, very few studies investigate its toxicity and mode of action in avian species. The results from this thesis may help advance the current understanding of effects of short-chained PFAAs in avian species; however, many challenges remain to fully understand the biological processes of PFAA action. The main objectives of this thesis were to determine the embryotoxic effects of PFHxS and PFHxA in developing chicken embryos and to gain insight into their potential modes of action.

In Chapter 2, I demonstrated that PFHxS and PFHxA accumulated in the yolk sac > liver > cerebral hemisphere of developing chicken embryos in a dose-dependent manner following injection into the egg prior to incubation. PFHxS (but not PFHxA) decreased the pipping success and overall growth of chicken embryos at whole-egg concentrations of 38,000 ng/g. These results indicated that short-chained PFAAs were able to accumulate in important tissues and exert adverse effects in avian species. Furthermore, PFHxS induced the

expression of TH-responsive transcripts in the liver and brain and diminished circulating free T4 levels in chicken embryos. Taken together, the results indicate that the TH axis is a target for PFHxS action, as the TH pathway was affected at multiple levels of biological organization (i.e. somatic growth, mRNA levels and TH homeostasis). I also demonstrated that PFHxS alters the expression of several genes involved in tight junction formation, signal transduction, tissue development, cellular assembly and organization and integrin signaling in the cerebral hemispheres of adversely affected chicken embryos (Chapter 3). These enriched functional categories and pathways can be related to TH-dependent mechanisms via genomic and non-genomic TH action and I hypothesize that the transcriptional responses are elicited by a decrease in circulating free T4 levels caused by PFHxS exposure (Chapter 2). TH-independent pathways of PFHxS action were also reported, including gap junction intercellular communication via NOV down-regulation. Thus, the exact modes of action of PFHxS remain unclear and additional studies should be conducted in order to provide further evidence to support TH pathway disruption.

4.2. RESEARCH NEEDS AND FUTURE DIRECTIONS

Due to their historic and continued manufacture and use, their resistance to biodegradation and poor elimination rates, PFAAs will likely persist in the environment and biota for an extended amount of time. Despite the substantial research being conducted on PFAAs, there remain numerous gaps relating to their modes of action and toxicity in animals, including humans. Such research gaps and recommendations for future PFAA research, based on the results and discussion from this M.Sc. thesis, include:

- Determine the uptake and distribution of PFAAs in biota. While the results from Chapter 2 of this thesis suggest that PFHxS and PFHxA partition into the yolk sac > liver > cerebral hemisphere of chicken embryos, not all compartments of the embryo were assessed. Future work should address the distribution of these compounds into other compartments (i.e. heart, kidney, thyroid, etc.). In order to reduce the number of embryos sacrificed for analysis, assessing plasma samples for PFAA levels would be a useful and less invasive method for obtaining an estimate of exposure levels. Plasma levels can then be compared to tissue levels to determine how well this method reflects whole body burden. Furthermore, species-specific differences in uptake and distribution should be addressed and if they exist, the biological reasons for these differences should be examined.

- Measure the concentrations of PFHxS and PFHxA in the brain tissue of wild avian species. Given that PFHxS and PFHxA were measured in the cerebral hemisphere of chicken embryos following egg injection, it can be hypothesized that these substances will be detected in wild birds that are exposed to them in the environment. Recent monitoring studies have detected PFOS in the brain of various wildlife species providing evidence that this compound can cross the blood-brain barrier. However, new and emerging PFAAs are not often measured in the brain tissue of wild avian species.

- Investigate the relative accumulation, metabolism and toxicity of linear and branched chain isomers. This thesis does not assess the impacts of linear vs. branched PFHxS or

PFHxA; however, structure-specific differences have been observed previously (Gebbink and Letcher 2010; O'Brien *et al.* 2011).

- Determine the effects of chemical mixtures, which can have combined toxicological interactions (i.e. synergism, potentiation or antagonism) (Cassee *et al.* 1998; Silva *et al.* 2002). Future studies should examine the impact of a mixture of PFAAs and other substances in birds, as opposed to single chemical studies as done in this thesis. In addition, comparing the effects of a PFAA mixture and a single substance at environmentally-relevant exposure levels would give insight into synergistic or antagonistic mixture effects.

- Target mechanistic investigations to hypotheses derived from the microarray results (Chapter 3). For example, design studies to assess the mechanisms for PFHxS toxicity via integrin signaling. Furthermore, egg injection experiments at varying developmental stages should be performed to dissect the various mechanisms and interactions. In addition, effects at environmentally-relevant concentrations should be addressed.

- Measure the protein levels for transcripts that were found to be the most responsive in this study. Protein expression does not always correspond with mRNA level patterns. Thus, examining the protein expression patterns in brain tissue following PFHxS exposure would help support the mRNA level results presented in Chapters 2 and 3.

- Conduct protein binding studies to determine interactions between PFHxS and other implicated receptors (i.e. integrins, TH receptors, C/EBPs and/or MYC). Knockout or knockdown studies for these various receptors would also clarify their involvement in PFHxS toxicity.

- Determine the activity of enzymes involved in various TH functions such as deiodination following PFAA exposure. Enzyme activity assays would help corroborate the mRNA level results presented in Chapter 2.

- Measure the T4 levels in target tissues (e.g. liver, thyroid gland, cerebral hemisphere) to help determine the cause and effect relationship between reduced T4 levels and altered deiodinase expression. Reduced TH levels can impact overall growth, development, and reproduction of birds. Additionally, measuring T3 and thyroid stimulating hormone (TSH) in conjunction with T4 would help establish a stronger case for TH disruption.

- Determine the utility of NOV expression as an indicator of PFAA exposure using mechanistic *in vitro* studies (e.g. reporter gene assay). Given that NOV expression was affected by PFAA exposure in two separate avian studies (this thesis and Yeung *et al.* 2007) and that NOV plays a role in GJIC (which is inhibited by PFAA exposure), it can be hypothesized that NOV plays an important role in PFAA action.

REFERENCES

Austin, M. E., Kasturi, B. S., Barber, M., Kannan, K., MohanKumar, P. S., and MohanKumar, S. M. (2003). Neuroendocrine effects of perfluorooctane sulfonate in rats. *Environ Health Perspect* **111**(12), 1485-1489.

Berberich-Siebelt, F., Berberich, I., Andrulis, M., Santner-Nanan, B., Jha, M. K., Klein-Hessling, S., Schimpl, A., and Serfling, E. (2006). SUMOylation interferes with CCAAT/enhancer-binding protein beta-mediated c-myc repression, but not IL-4 activation in T cells. *J Immunol.* **176**(8), 4843-4851.

Buck, R. C., Franklin, J., Berger, U., Conder, J. M., Cousins, I. T., de, V. P., Jensen, A. A., Kannan, K., Mabury, S. A., and van Leeuwen, S. P. (2011). Perfluoroalkyl and polyfluoroalkyl substances in the environment: terminology, classification, and origins. *Integr Environ Assess. Manag.* **7**(4), 513-541.

Bustnes, J. O., Borga, K., Erikstad, K. E., Lorentsen, S. H., and Herzke, D. (2008). Perfluorinated, brominated, and chlorinated contaminants in a population of lesser black-backed gulls (Larus fuscus). *Environ Toxicol Chem* **27**(6), 1383-1392.

Butenhoff, J. L., Chang, S. C., Ehresman, D. J., and York, R. G. (2009a). Evaluation of potential reproductive and developmental toxicity of potassium perfluorohexanesulfonate in Sprague Dawley rats. *Reprod Toxicol* **27**(3-4), 331-341.

Butenhoff, J. L., Ehresman, D. J., Chang, S. C., Parker, G. A., and Stump, D. G. (2009b). Gestational and lactational exposure to potassium perfluorooctanesulfonate (K+PFOS) in rats: developmental neurotoxicity. *Reprod Toxicol* **27**(3-4), 319-330.

Calella, A. M., Nerlov, C., Lopez, R. G., Sciarretta, C., von Bohlen und, H. O., Bereshchenko, O., and Minichiello, L. (2007). Neurotrophin/Trk receptor signaling mediates C/EBPalpha, -beta and NeuroD recruitment to immediate-early gene promoters in neuronal cells and requires C/EBPs to induce immediate-early gene transcription. *Neural Dev.* **2**, 4.

Cassee, F. R., Groten, J. P., van Bladeren, P. J., and Feron, V. J. (1998). Toxicological evaluation and risk assessment of chemical mixtures. *Crit Rev Toxicol* **28**(1), 73-101.

Chang, S. C., Ehresman, D. J., Bjork, J. A., Wallace, K. B., Parker, G. A., Stump, D. G., and Butenhoff, J. L. (2009). Gestational and lactational exposure to potassium perfluorooctanesulfonate (K+PFOS) in rats: toxicokinetics, thyroid hormone status, and related gene expression. *Reprod Toxicol* **27**(3-4), 387-399.

Chang, S. C., Thibodeaux, J. R., Eastvold, M. L., Ehresman, D. J., Bjork, J. A., Froehlich, J. W., Lau, C., Singh, R. J., Wallace, K. B., and Butenhoff, J. L. (2008). Thyroid hormone status and pituitary function in adult rats given oral doses of perfluorooctanesulfonate (PFOS). *Toxicology* **243**(3), 330-339.

Chang, S. C., Thibodeaux, J. R., Eastvold, M. L., Ehresman, D. J., Bjork, J. A., Froehlich, J. W., Lau, C. S., Singh, R. J., Wallace, K. B., and Butenhoff, J. L. (2007). Negative bias from analog methods used in the analysis of free thyroxine in rat serum containing perfluorooctanesulfonate (PFOS). *Toxicology* **234**(1-2), 21-33.

Cheng, Y., Cui, Y., Chen, H. M., and Xie, W. P. (2011). Thyroid disruption effects of environmental level perfluorooctane sulfonates (PFOS) in Xenopus laevis. *Ecotoxicology.*

Chengelis, C. P., Kirkpatrick, J. B., Radovsky, A., and Shinohara, M. (2009). A 90-day repeated dose oral (gavage) toxicity study of perfluorohexanoic acid (PFHxA) in rats (with functional observational battery and motor activity determinations). *Reprod Toxicol* **27**(3-4), 342-351.

Cohen, M. E., Yin, M., Paznekas, W. A., Schertzer, M., Wood, S., and Jabs, E. W. (1998). Human SLUG gene organization, expression, and chromosome map location on 8q. *Genomics* **51**(3), 468-471.

Conder, J. M., Hoke, R. A., De, W. W., Russell, M. H., and Buck, R. C. (2008). Are PFCAs bioaccumulative? A critical review and comparison with regulatory criteria and persistent lipophilic compounds. *Environ Sci Technol* **42**(4), 995-1003.

Crump, D., Chiu, S., Egloff, C., and Kennedy, S. W. (2008). Effects of hexabromocyclododecane and polybrominated diphenyl ethers on mRNA expression in chicken (Gallus domesticus) hepatocytes. *Toxicol. Sci.* **106**(2), 479-487.

Crump, D., Chiu, S., Gauthier, L. T., Hickey, N. J., Letcher, R. J., and Kennedy, S. W. (2011). The effects of Dechlorane Plus on toxicity and mRNA expression in chicken embryos: A comparison of in vitro and in ovo approaches. *Comp Biochem Physiol C Toxicol Pharmacol* **154**(2), 129-134.

Crump, D., Egloff, C., Chiu, S., Letcher, R. J., Chu, S., and Kennedy, S. W. (2010). Pipping success, isomer-specific accumulation, and hepatic mRNA expression in chicken embryos exposed to HBCD. *Toxicol. Sci.* **115**(2), 492-500.

Cui, X., Hwang, J. T., Qiu, J., Blades, N. J., and Churchill, G. A. (2005). Improved statistical tests for differential gene expression by shrinking variance components estimates. *Biostatistics* **6**(1), 59-75.

Custer, T. W., Kannan, K., Tao, L., Yun, S. H., and Trowbridge, A. (2010). Perfluorinated compounds amd polybrominated diphenyl ethers in great blue heron eggs from three colonies on the Mississippi River, Minnesota. *Waterbirds* **33**(1), 86-95.

Davis, P. J., Davis, F. B., Lin, H. Y., Mousa, S. A., Zhou, M., and Luidens, M. K. (2009). Translational implications of nongenomic actions of thyroid hormone initiated at its integrin receptor. *Am J Physiol Endocrinol Metab* **297**(6), E1238-E1246.

Devaux, J., and Gow, A. (2008). Tight junctions potentiate the insulative properties of small CNS myelinated axons. *J Cell Biol* **183**(5), 909-921.

Di, L., I (2008). Thyroid hormones and the central nervous system of mammals (Review). *Mol Med Report.* **1**(3), 279-295.

Dong, G. H., Zhang, Y. H., Zheng, L., Liang, Z. F., Jin, Y. H., and He, Q. C. (2012). Subchronic effects of perfluorooctanesulfonate exposure on inflammation in adult male C57BL/6 mice. *Environ Toxicol* **27**(5), 285-296.

Dowling, A. L., Martz, G. U., Leonard, J. L., and Zoeller, R. T. (2000). Acute changes in maternal thyroid hormone induce rapid and transient changes in gene expression in fetal rat brain. *J Neurosci.* **20**(6), 2255-2265.

Edgar, R., Domrachev, M., and Lash, A. E. (2002). Gene Expression Omnibus: NCBI gene expression and hybridization array data repository. *Nucleic Acids Res* **30**(1), 207-210.

Falandysz, J., Taniyasu, S., Yamashita, N., Rostkowski, P., Zalewski, K., and Kannan, K. (2007). Perfluorinated compounds in some terrestrial and aquatic wildlife species from Poland. *J Environ Sci Health A Tox Hazard Subst Environ Eng* **42**(6), 715-719.

Farwell, A. P., Dubord-Tomasetti, S. A., Pietrzykowski, A. Z., Stachelek, S. J., and Leonard, J. L. (2005). Regulation of cerebellar neuronal migration and neurite outgrowth by thyroxine and 3,3',5'-triiodothyronine. *Brain Res Dev. Brain Res* **154**(1), 121-135.

Fu, C. T., Bechberger, J. F., Ozog, M. A., Perbal, B., and Naus, C. C. (2004). CCN3 (NOV) interacts with connexin43 in C6 glioma cells: possible mechanism of connexin-mediated growth suppression. *J Biol Chem* **279**(35), 36943-36950.

Fuentes, S., Colomina, M. T., Vicens, P., Franco-Pons, N., and Domingo, J. L. (2007). Concurrent exposure to perfluorooctane sulfonate and restraint stress during pregnancy in mice: effects on postnatal development and behavior of the offspring. *Toxicol Sci* **98**(2), 589-598.

Gallicano, G. I., Kouklis, P., Bauer, C., Yin, M., Vasioukhin, V., Degenstein, L., and Fuchs, E. (1998). Desmoplakin is required early in development for assembly of desmosomes and cytoskeletal linkage. *J Cell Biol* **143**(7), 2009-2022.

Gauger, K. J., Kato, Y., Haraguchi, K., Lehmler, H. J., Robertson, L. W., Bansal, R., and Zoeller, R. T. (2004). Polychlorinated biphenyls (PCBs) exert thyroid hormone-like effects in the fetal rat brain but do not bind to thyroid hormone receptors. *Environ Health Perspect* **112**(5), 516-523.

Gebbink, W. A., Hebert, C. E., and Letcher, R. J. (2009). Perfluorinated carboxylates and sulfonates and precursor compounds in herring gull eggs from colonies spanning the Laurentian Great Lakes of North America. *Environ Sci Technol* **43**(19), 7443-7449.

Gebbink, W. A., and Letcher, R. J. (2010). Linear and branched perfluorooctane sulfonate isomer patterns in herring gull eggs from colonial sites across the Laurentian Great Lakes. *Environ Sci Technol* **44**(10), 3739-3745.

Gebbink, W. A., and Letcher, R. J. (2012). Comparative tissue and body compartment accumulation and maternal transfer to eggs of perfluoroalkyl sulfonates and carboxylates in Great Lakes herring gulls. *Environ Pollut* **162**, 40-47.

Gebbink, W. A., Letcher, R. J., Hebert, C. E., and Chip Weseloh, D. V. (2011). Twenty years of temporal change in perfluoroalkyl sulfonate and carboxylate contaminants in herring gull eggs from the Laurentian Great Lakes. *J Environ Monit.* **13**(12), 3365-3372.

Giesy, J. P., and Kannan, K. (2001). Global distribution of perfluorooctane sulfonate in wildlife. *Environ Sci Technol* **35**(7), 1339-1342.

Goodnight, J. H., and Harvey, W. R. Least-Squares Means in the Fixed-Effects General Linear Models. R-103. 1978. Cary, NC, SAS Institute Inc. SAS Technical Report.
Ref Type: Report

Goriya, H. V., Kalia, A., Bhavsar, S. K., Joshi, C. G., Rank, D. N., and Thaker, A. M. (2005). Comparative evaluation of phenobarbital-induced CYP3A and CYP2H1 gene expression by quantitative RT-PCR in Bantam, Bantamized White Leghorn and White Leghorn chicks. *J Vet. Sci* **6**(4), 279-285.

Gupta, N., Wang, H., McLeod, T. L., Naus, C. C., Kyurkchiev, S., Advani, S., Yu, J., Perbal, B., and Weichselbaum, R. R. (2001). Inhibition of glioma cell growth and tumorigenic potential by CCN3 (NOV). *Mol Pathol* **54**(5), 293-299.

Gutsch, R., Kandemir, J. D., Pietsch, D., Cappello, C., Meyer, J., Simanowski, K., Huber, R., and Brand, K. (2011). CCAAT/enhancer-binding protein beta inhibits proliferation in monocytic cells by affecting the retinoblastoma protein/E2F/cyclin E pathway but is not directly required for macrophage morphology. *J Biol Chem* **286**(26), 22716-22729.

Hamilton, V., and Hamburger, H. L. (1951). A series of normal stages in the development of the chick embryo. *J. Morphol.* **88**, 49-92.

Herzke, D., Nygard, T., Berger, U., Huber, S., and Rov, N. (2009). Perfluorinated and other persistent halogenated organic compounds in European shag (Phalacrocorax aristotelis) and common eider (Somateria mollissima) from Norway: a suburban to remote pollutant gradient. *Sci Total Environ* **408**(2), 340-348.

Hickey, N. J., Crump, D., Jones, S. P., and Kennedy, S. W. (2009). Effects of 18 perfluoroalkyl compounds on mRNA expression in chicken embryo hepatocyte cultures. *Toxicol. Sci.* **111**(2), 311-320.

Hoffman, B., and Liebermann, D. A. (2008). Apoptotic signaling by c-MYC. *Oncogene* **27**(50), 6462-6472.

Holmstrom, K. E., Jarnberg, U., and Bignert, A. (2005). Temporal trends of PFOS and PFOA in guillemot eggs from the Baltic Sea, 1968--2003. *Environ Sci Technol* **39**(1), 80-84.

Houde, M., De Silva, A. O., Muir, D. C., and Letcher, R. J. (2011). Monitoring of perfluorinated compounds in aquatic biota: an updated review. *Environ Sci Technol* **45**(19), 7962-7973.

Houde, M., Martin, J. W., Letcher, R. J., Solomon, K. R., and Muir, D. C. (2006). Biological monitoring of polyfluoroalkyl substances: A review. *Environ Sci Technol* **40**(11), 3463-3473.

Hu, W., Jones, P. D., Upham, B. L., Trosko, J. E., Lau, C., and Giesy, J. P. (2002). Inhibition of gap junctional intercellular communication by perfluorinated compounds in rat liver and dolphin kidney epithelial cell lines in vitro and Sprague-Dawley rats in vivo. *Toxicol Sci* **68**(2), 429-436.

Iniguez, M. A., De, L. L., Guadano-Ferraz, A., Morte, B., Gerendasy, D., Sutcliffe, J. G., and Bernal, J. (1996). Cell-specific effects of thyroid hormone on RC3/neurogranin expression in rat brain. *Endocrinology* **137**(3), 1032-1041.

Iniguez, M. A., Rodriguez-Pena, A., Ibarrola, N., Aguilera, M., Munoz, A., and Bernal, J. (1993). Thyroid hormone regulation of RC3, a brain-specific gene encoding a protein kinase-C substrate. *Endocrinology* **133**(2), 467-473.

Jensen, A. A., and Leffers, H. (2008). Emerging endocrine disrupters: perfluoroalkylated substances. *Int J Androl* **31**(2), 161-169.

Jethwa, P., Naqvi, M., Hardy, R. G., Hotchin, N. A., Roberts, S., Spychal, R., and Tselepis, C. (2008). Overexpression of Slug is associated with malignant progression of esophageal adenocarcinoma. *World J Gastroenterol.* **14**(7), 1044-1052.

Johansson, N., Eriksson, P., and Viberg, H. (2009). Neonatal exposure to PFOS and PFOA in mice results in changes in proteins which are important for neuronal growth and synaptogenesis in the developing brain. *Toxicol Sci* **108**(2), 412-418.

Johansson, N., Fredriksson, A., and Eriksson, P. (2008). Neonatal exposure to perfluorooctane sulfonate (PFOS) and perfluorooctanoic acid (PFOA) causes neurobehavioural defects in adult mice. *Neurotoxicology* **29**(1), 160-169.

Jones, P. D., Hu, W., De, C. W., Newsted, J. L., and Giesy, J. P. (2003). Binding of perfluorinated fatty acids to serum proteins. *Environ Toxicol Chem* **22**(11), 2639-2649.

Kannan, K., Choi, J. W., Iseki, N., Senthilkumar, K., Kim, D. H., and Giesy, J. P. (2002a). Concentrations of perfluorinated acids in livers of birds from Japan and Korea. *Chemosphere* **49**(3), 225-231.

Kannan, K., Corsolini, S., Falandysz, J., Oehme, G., Focardi, S., and Giesy, J. P. (2002b). Perfluorooctanesulfonate and related fluorinated hydrocarbons in marine mammals, fishes, and birds from coasts of the Baltic and the Mediterranean Seas. *Environ Sci Technol* **36**(15), 3210-3216.

Kannan, K., Franson, J. C., Bowerman, W. W., Hansen, K. J., Jones, P. D., and Giesy, J. P. (2001a). Perfluorooctane sulfonate in fish-eating water birds including bald eagles and albatrosses. *Environ Sci Technol* **35**(15), 3065-3070.

Kannan, K., Koistinen, J., Beckmen, K., Evans, T., Gorzelany, J. F., Hansen, K. J., Jones, P. D., Helle, E., Nyman, M., and Giesy, J. P. (2001b). Accumulation of perfluorooctane sulfonate in marine mammals. *Environ Sci Technol* **35**(8), 1593-1598.

Kannan, K., Tao, L., Sinclair, E., Pastva, S. D., Jude, D. J., and Giesy, J. P. (2005). Perfluorinated compounds in aquatic organisms at various trophic levels in a Great Lakes food chain. *Arch Environ Contam Toxicol* **48**(4), 559-566.

Karrman, A., Domingo, J. L., Llebaria, X., Nadal, M., Bigas, E., van, B. B., and Lindstrom, G. (2010). Biomonitoring perfluorinated compounds in Catalonia, Spain: concentrations and trends in human liver and milk samples. *Environ Sci Pollut Res Int* **17**(3), 750-758.

Kaur, B., Khwaja, F. W., Severson, E. A., Matheny, S. L., Brat, D. J., and Van Meir, E. G. (2005). Hypoxia and the hypoxia-inducible-factor pathway in glioma growth and angiogenesis. *Neuro. Oncol.* **7**(2), 134-153.

Kerr, M. K. (2003). Design considerations for efficient and effective microarray studies. *Biometrics* **59**(4), 822-828.

Kerr, M. K., and Churchill, G. A. (2001). Statistical design and the analysis of gene expression microarray data. *Genet Res* **77**(2), 123-128.

Lakin, N. D., Palmer, R., Lillycrop, K. A., Howard, M. K., Burke, L. C., Thomas, N. S., and Latchman, D. S. (1995). Down regulation of the octamer binding protein Oct-1 during growth arrest and differentiation of a neuronal cell line. *Brain Res Mol Brain Res* **28**(1), 47-54.

Lau, C. (2009). Perfluoroalkyl acids: recent activities and research progress. *Reprod Toxicol* **27**(3-4), 209-211.

Lau, C., Anitole, K., Hodes, C., Lai, D., Pfahles-Hutchens, A., and Seed, J. (2007). Perfluoroalkyl acids: a review of monitoring and toxicological findings. *Toxicol Sci* **99**(2), 366-394.

Lau, C., Butenhoff, J. L., and Rogers, J. M. (2004). The developmental toxicity of perfluoroalkyl acids and their derivatives. *Toxicol Appl Pharmacol* **198**(2), 231-241.

Lau, C., Thibodeaux, J. R., Hanson, R. G., Rogers, J. M., Grey, B. E., Stanton, M. E., Butenhoff, J. L., and Stevenson, L. A. (2003). Exposure to perfluorooctane sulfonate during pregnancy in rat and mouse. II: postnatal evaluation. *Toxicol Sci* **74**(2), 382-392.

Le Dreau, G., Kular, L., Nicot, A. B., Calmel, C., Melik-Parsadaniantz, S., Kitabgi, P., Laurent, M., and Martinerie, C. (2010a). NOV/CCN3 upregulates CCL2 and CXCL1 expression in astrocytes through beta1 and beta5 integrins. *Glia* **58**(12), 1510-1521.

Le Dreau, G., Nicot, A., Benard, M., Thibout, H., Vaudry, D., Martinerie, C., and Laurent, M. (2010b). NOV/CCN3 promotes maturation of cerebellar granule neuron precursors. *Mol Cell Neurosci.* **43**(1), 60-71.

Liao, C., Wang, T., Cui, L., Zhou, Q., Duan, S., and Jiang, G. (2009). Changes in synaptic transmission, calcium current, and neurite growth by perfluorinated compounds are dependent on the chain length and functional group. *Environ Sci Technol* **43**(6), 2099-2104.

Loveless, S. E., Slezak, B., Serex, T., Lewis, J., Mukerji, P., O'Connor, J. C., Donner, E. M., Frame, S. R., Korzeniowski, S. H., and Buck, R. C. (2009). Toxicological evaluation of sodium perfluorohexanoate. *Toxicology* **264**(1-2), 32-44.

Lu, C., and Cheng, S. Y. (2010). Thyroid hormone receptors regulate adipogenesis and carcinogenesis via crosstalk signaling with peroxisome proliferator-activated receptors. *J Mol Endocrinol* **44**(3), 143-154.

Luebker, D. J., Hansen, K. J., Bass, N. M., Butenhoff, J. L., and Seacat, A. M. (2002). Interactions of fluorochemicals with rat liver fatty acid-binding protein. *Toxicology* **176**(3), 175-185.

Martin, J. W., Asher, B. J., Beesoon, S., Benskin, J. P., and Ross, M. S. (2010). PFOS or PreFOS? Are perfluorooctane sulfonate precursors (PreFOS) important determinants of human and environmental perfluorooctane sulfonate (PFOS) exposure? *J Environ Monit.* **12**(11), 1979-2004.

Martin, M. T., Brennan, R. J., Hu, W., Ayanoglu, E., Lau, C., Ren, H., Wood, C. R., Corton, J. C., Kavlock, R. J., and Dix, D. J. (2007). Toxicogenomic study of triazole fungicides and perfluoroalkyl acids in rat livers predicts toxicity and categorizes chemicals based on mechanisms of toxicity. *Toxicol Sci* **97**(2), 595-613.

McNabb, F. M. (2007). The hypothalamic-pituitary-thyroid (HPT) axis in birds and its role in bird development and reproduction. *Crit Rev Toxicol* **37**(1-2), 163-193.

Merritt, R. L., and Foran, C. M. (2007). Influence of persistent contaminants and steroid hormones on glioblastoma cell growth. *J Toxicol Environ Health A* **70**(1), 19-27.

Meyer, J., Jaspers, V. L., Eens, M., and De Coen, W. (2009). The relationship between perfluorinated chemical levels in the feathers and livers of birds from different trophic levels. *Sci Total Environ* **407**(22), 5894-5900.

Moeller, L. C., and Broecker-Preuss, M. (2011). Transcriptional regulation by nonclassical action of thyroid hormone. *Thyroid Res* **4 Suppl 1**, S6.

Molina, E. D., Balander, R., Fitzgerald, S. D., Giesy, J. P., Kannan, K., Mitchell, R., and Bursian, S. J. (2006). Effects of air cell injection of perfluorooctane sulfonate before incubation on development of the white leghorn chicken (Gallus domesticus) embryo. *Environ Toxicol Chem* **25**(1), 227-232.

Morte, B., Iniguez, M. A., Lorenzo, P. I., and Bernal, J. (1997). Thyroid hormone-regulated expression of RC3/neurogranin in the immortalized hypothalamic cell line GT1-7. *J Neurochem.* **69**(3), 902-909.

Nagasawa, T., Takeda, T., Minemura, K., and DeGroot, L. J. (1997). Oct-1, silencer sequence, and GC box regulate thyroid hormone receptor beta1 promoter. *Mol Cell Endocrinol* **130**(1-2), 153-165.

Nakata, H., Kannan, K., Nasu, T., Cho, H. S., Sinclair, E., and Takemurai, A. (2006). Perfluorinated contaminants in sediments and aquatic organisms collected from shallow water and tidal flat areas of the Ariake Sea, Japan: environmental fate of perfluorooctane sulfonate in aquatic ecosystems. *Environ Sci Technol* **40**(16), 4916-4921.

Nakayama, K., Iwata, H., Tao, L., Kannan, K., Imoto, M., Kim, E. Y., Tashiro, K., and Tanabe, S. (2008). Potential effects of perfluorinated compounds in common cormorants from Lake Biwa, Japan: an implication from the hepatic gene expression profiles by microarray. *Environ Toxicol Chem* **27**(11), 2378-2386.

National Toxicology Program. Testing status of agents at NTP. 18-7-2011. 17-8-2011.
Ref Type: Online Source

O'Brien, J. M., Austin, A. J., Williams, A., Yauk, C. L., Crump, D., and Kennedy, S. W. (2011). Technical-grade perfluorooctane sulfonate alters the expression of more transcripts in cultured chicken embryonic hepatocytes than linear perfluorooctane sulfonate. *Environ Toxicol Chem* **30**(12), 2846-2859.

O'Brien, J. M., Carew, A. C., Chu, S., Letcher, R. J., and Kennedy, S. W. (2009a). Perfluorooctane sulfonate (PFOS) toxicity in domestic chicken (Gallus gallus domesticus) embryos in the absence of effects on peroxisome proliferator activated receptor alpha (PPARalpha)-regulated genes. *Comp Biochem Physiol C Toxicol Pharmacol* **149**(4), 524-530.

O'Brien, J. M., Crump, D., Mundy, L. J., Chu, S., McLaren, K. K., Vongphachan, V., Letcher, R. J., and Kennedy, S. W. (2009b). Pipping success and liver mRNA expression in chicken embryos exposed in ovo to C8 and C11 perfluorinated carboxylic acids and C10 perfluorinated sulfonate. *Toxicol Lett* **190**(2), 134-139.

OECD. Hazard assessment of perfluorooctane sulfonate (PFOS) and its salts. ENV/JM/RD(2002)17/FINAL. 2002. 10-2-2012.
Ref Type: Report

Paquette, M. A., Dong, H., Gagne, R., Williams, A., Malowany, M., Wade, M. G., and Yauk, C. L. (2011). Thyroid Hormone-Regulated Gene Expression in Juvenile Mouse Liver: Identification of Thyroid Response Elements Using Microarray Profiling and In Silico Analyses. *BMC Genomics* **12**(1), 634.

Paul, A. G., Jones, K. C., and Sweetman, A. J. (2009). A first global production, emission, and environmental inventory for perfluorooctane sulfonate. *Environ Sci Technol* **43**(2), 386-392.

Peden-Adams, M. M., Stuckey, J. E., Gaworecki, K. M., Berger-Ritchie, J., Bryant, K., Jodice, P. G., Scott, T. R., Ferrario, J. B., Guan, B., Vigo, C., Boone, J. S., McGuinn, W. D., DeWitt, J. C., and Keil, D. E. (2009). Developmental toxicity in white leghorn chickens following in ovo exposure to perfluorooctane sulfonate (PFOS). *Reprod Toxicol* **27**(3-4), 307-318.

Pinkas, A., Slotkin, T. A., Brick-Turin, Y., Van der Zee, E. A., and Yanai, J. (2010). Neurobehavioral teratogenicity of perfluorinated alkyls in an avian model. *Neurotoxicol. Teratol.* **32**(2), 182-186.

Prevedouros, K., Cousins, I. T., Buck, R. C., and Korzeniowski, S. H. (2006). Sources, fate and transport of perfluorocarboxylates. *Environ Sci Technol* **40**(1), 32-44.

Puzianowska-Kuznicka, M., Pietrzak, M., Turowska, O., and Nauman, A. (2006). Thyroid hormones and their receptors in the regulation of cell proliferation. *Acta Biochim. Pol.* **53**(4), 641-650.

Ramji, D. P., and Foka, P. (2002). CCAAT/enhancer-binding proteins: structure, function and regulation. *Biochem J* **365**(Pt 3), 561-575.

Sato, I., Kawamoto, K., Nishikawa, Y., Tsuda, S., Yoshida, M., Yaegashi, K., Saito, N., Liu, W., and Jin, Y. (2009). Neurotoxicity of perfluorooctane sulfonate (PFOS) in rats and mice after single oral exposure. *J Toxicol Sci* **34**(5), 569-574.

Savagner, P., Yamada, K. M., and Thiery, J. P. (1997). The zinc-finger protein slug causes desmosome dissociation, an initial and necessary step for growth factor-induced epithelial-mesenchymal transition. *J Cell Biol* **137**(6), 1403-1419.

Schiavone, A., Corsolini, S., Kannan, K., Tao, L., Trivelpiece, W., Torres, D., Jr., and Focardi, S. (2009). Perfluorinated contaminants in fur seal pups and penguin eggs from South Shetland, Antarctica. *Sci Total Environ* **407**(12), 3899-3904.

Schmittgen, T. D., and Livak, K. J. (2008). Analyzing real-time PCR data by the comparative C(T) method. *Nat. Protoc.* **3**(6), 1101-1108.

Searle, S. R., Speed, F. M., and Milliken, G. A. (1980). The population marginal means in the linear model: An alternative to least squares means. *Amer Statistician* **34**(4), 216-221.

Sebastian, T., Malik, R., Thomas, S., Sage, J., and Johnson, P. F. (2005). C/EBPbeta cooperates with RB:E2F to implement Ras(V12)-induced cellular senescence. *EMBO J* **24**(18), 3301-3312.

Senthilkumar, K., Ohi, E., Sajwan, K., Takasuga, T., and Kannan, K. (2007). Perfluorinated compounds in river water, river sediment, market fish, and wildlife samples from Japan. *Bull. Environ Contam Toxicol* **79**(4), 427-431.

Sheng, Z. G., Tang, Y., Liu, Y. X., Yuan, Y., Zhao, B. Q., Chao, X. J., and Zhu, B. Z. (2012). Low concentrations of bisphenol a suppress thyroid hormone receptor transcription through a nongenomic mechanism. *Toxicol Appl Pharmacol* **259**(1), 133-142.

Shi, X., Du, Y., Lam, P. K., Wu, R. S., and Zhou, B. (2008). Developmental toxicity and alteration of gene expression in zebrafish embryos exposed to PFOS. *Toxicol Appl Pharmacol* **230**(1), 23-32.

Silva, E., Rajapakse, N., and Kortenkamp, A. (2002). Something from "nothing"--eight weak estrogenic chemicals combined at concentrations below NOECs produce significant mixture effects. *Environ Sci Technol* **36**(8), 1751-1756.

Sin, W. C., Tse, M., Planque, N., Perbal, B., Lampe, P. D., and Naus, C. C. (2009). Matricellular protein CCN3 (NOV) regulates actin cytoskeleton reorganization. *J Biol Chem* **284**(43), 29935-29944.

Sinclair, E., Mayack, D. T., Roblee, K., Yamashita, N., and Kannan, K. (2006). Occurrence of perfluoroalkyl surfactants in water, fish, and birds from New York State. *Arch Environ Contam Toxicol* **50**(3), 398-410.

Slotkin, T. A., MacKillop, E. A., Melnick, R. L., Thayer, K. A., and Seidler, F. J. (2008). Developmental neurotoxicity of perfluorinated chemicals modeled in vitro. *Environ Health Perspect* **116**(6), 716-722.

Smith, J. W., Evans, A. T., Costall, B., and Smythe, J. W. (2002). Thyroid hormones, brain function and cognition: a brief review. *Neurosci. Biobehav. Rev* **26**(1), 45-60.

Stamatovic, S. M., Keep, R. F., and Andjelkovic, A. V. (2008). Brain endothelial cell-cell junctions: how to "open" the blood brain barrier. *Curr. Neuropharmacol.* **6**(3), 179-192.

Sterneck, E., and Johnson, P. F. (1998). CCAAT/enhancer binding protein beta is a neuronal transcriptional regulator activated by nerve growth factor receptor signaling. *J Neurochem.* **70**(6), 2424-2433.

Tan, C., Cruet-Hennequart, S., Troussard, A., Fazli, L., Costello, P., Sutton, K., Wheeler, J., Gleave, M., Sanghera, J., and Dedhar, S. (2004). Regulation of tumor angiogenesis by integrin-linked kinase (ILK). *Cancer Cell* **5**(1), 79-90.

Tao, L., Kannan, K., Kajiwara, N., Costa, M. M., Fillmann, G., Takahashi, S., and Tanabe, S. (2006). Perfluorooctanesulfonate and related fluorochemicals in albatrosses, elephant seals, penguins, and polar skuas from the Southern Ocean. *Environ Sci Technol* **40**(24), 7642-7648.

Thibodeaux, J. R., Hanson, R. G., Rogers, J. M., Grey, B. E., Barbee, B. D., Richards, J. H., Butenhoff, J. L., Stevenson, L. A., and Lau, C. (2003). Exposure to perfluorooctane sulfonate

during pregnancy in rat and mouse. I: maternal and prenatal evaluations. *Toxicol Sci* **74**(2), 369-381.

Tiwari-Woodruff, S. K., Buznikov, A. G., Vu, T. Q., Micevych, P. E., Chen, K., Kornblum, H. I., and Bronstein, J. M. (2001). OSP/claudin-11 forms a complex with a novel member of the tetraspanin super family and beta1 integrin and regulates proliferation and migration of oligodendrocytes. *J Cell Biol* **153**(2), 295-305.

Tiwari-Woodruff, S. K., Kaplan, R., Kornblum, H. I., and Bronstein, J. M. (2004). Developmental expression of OAP-1/Tspan-3, a member of the tetraspanin superfamily. *J Neurosci. Res* **77**(2), 166-173.

Tomy, G. T., Pleskach, K., Ferguson, S. H., Hare, J., Stern, G., Macinnis, G., Marvin, C. H., and Loseto, L. (2009). Trophodynamics of some PFCs and BFRs in a western Canadian Arctic marine food web. *Environ Sci Technol* **43**(11), 4076-4081.

Upham, B. L., Park, J. S., Babica, P., Sovadinova, I., Rummel, A. M., Trosko, J. E., Hirose, A., Hasegawa, R., Kanno, J., and Sai, K. (2009). Structure-activity-dependent regulation of cell communication by perfluorinated fatty acids using in vivo and in vitro model systems. *Environ Health Perspect* **117**(4), 545-551.

Van de Vijver, K. I., Holsbeek, L., Das, K., Blust, R., Joiris, C., and De, C. W. (2007). Occurrence of perfluorooctane sulfonate and other perfluorinated alkylated substances in harbor porpoises from the Black Sea. *Environ Sci Technol* **41**(1), 315-320.

Vasioukhin, V., Bowers, E., Bauer, C., Degenstein, L., and Fuchs, E. (2001). Desmoplakin is essential in epidermal sheet formation. *Nat Cell Biol* **3**(12), 1076-1085.

Verreault, J., Houde, M., Gabrielsen, G. W., Berger, U., Haukas, M., Letcher, R. J., and Muir, D. C. (2005). Perfluorinated alkyl substances in plasma, liver, brain, and eggs of glaucous gulls (Larus hyperboreus) from the Norwegian arctic. *Environ Sci Technol* **39**(19), 7439-7445.

Verreault, J., Skaare, J. U., Jenssen, B. M., and Gabrielsen, G. W. (2004). Effects of organochlorine contaminants on thyroid hormone levels in Arctic breeding glaucous gulls, Larus hyperboreus. *Environ Health Perspect* **112**(5), 532-537.

Vongphachan, V., Cassone, C. G., Wu, D., Chiu, S., Crump, D., and Kennedy, S. W. (2011). Effects of perfluoroalkyl compounds on mRNA expression levels of thyroid hormone-responsive genes in primary cultures of avian neuronal cells. *Toxicol. Sci.* **120**(2), 392-402.

Vuoriluoto, K., Haugen, H., Kiviluoto, S., Mpindi, J. P., Nevo, J., Gjerdrum, C., Tiron, C., Lorens, J. B., and Ivaska, J. (2011). Vimentin regulates EMT induction by Slug and oncogenic H-Ras and migration by governing Axl expression in breast cancer. *Oncogene* **30**(12), 1436-1448.

Wallington, T. J., Hurley, M. D., Xia, J., Wuebbles, D. J., Sillman, S., Ito, A., Penner, J. E., Ellis, D. A., Martin, J., Mabury, S. A., Nielsen, O. J., and Sulbaek Andersen, M. P. (2006).

Formation of C7F15COOH (PFOA) and other perfluorocarboxylic acids during the atmospheric oxidation of 8:2 fluorotelomer alcohol. *Environ Sci Technol* **40**(3), 924-930.

Wang, F., Liu, W., Jin, Y., Dai, J., Yu, W., Liu, X., and Liu, L. (2010a). Transcriptional effects of prenatal and neonatal exposure to PFOS in developing rat brain. *Environ Sci Technol* **44**(5), 1847-1853.

Wang, S., Zhang, S., Zhao, B., and Lun, L. (2009). Up-regulation of C/EBP by thyroid hormones: a case demonstrating the vertebrate-like thyroid hormone signaling pathway in amphioxus. *Mol Cell Endocrinol* **313**(1-2), 57-63.

Wang, X., Li, B., Zhao, W. D., Liu, Y. J., Shang, D. S., Fang, W. G., and Chen, Y. H. (2011). Perfluorooctane sulfonate triggers tight junction "opening" in brain endothelial cells via phosphatidylinositol 3-kinase. *Biochem Biophys. Res Commun.* **410**(2), 258-263.

Wang, Y., Fu, J., Wang, T., Liang, Y., Pan, Y., Cai, Y., and Jiang, G. (2010b). Distribution of perfluorooctane sulfonate and other perfluorochemicals in the ambient environment around a manufacturing facility in China. *Environ Sci Technol* **44**(21), 8062-8067.

Wang, Y., Yeung, L. W., Taniyasu, S., Yamashita, N., Lam, J. C., and Lam, P. K. (2008). Perfluorooctane sulfonate and other fluorochemicals in waterbird eggs from south China. *Environ Sci Technol* **42**(21), 8146-8151.

Weiss, J. M., Andersson, P. L., Lamoree, M. H., Leonards, P. E., van Leeuwen, S. P., and Hamers, T. (2009). Competitive binding of poly- and perfluorinated compounds to the thyroid hormone transport protein transthyretin. *Toxicol Sci* **109**(2), 206-216.

Wu, H., Kerr, M. K., Cui, X., and Churchill, G. A. (2003). MAANOVA: A Software Package for the Analysis of Spotted cDNA Microarray Experiments. In *The Analysis of Gene Expression Data: Methods and Software* (G.Parmigiani, E.S.Garrett, R.A.Irizarry, and S.Zeger, Eds.), pp. 313-431. Springer-Verlag, New York, NY.

Wu, X., and Reddy, D. S. (2012). Integrins as receptor targets for neurological disorders. *Pharmacol Ther* **134**(1), 68-81.

Yamashita, N., Kannan, K., Taniyasu, S., Horii, Y., Petrick, G., and Gamo, T. (2005). A global survey of perfluorinated acids in oceans. *Mar. Pollut. Bull.* **51**(8-12), 658-668.

Yanai, J., Dotan, S., Goz, R., Pinkas, A., Seidler, F. J., Slotkin, T. A., and Zimmerman, F. (2008). Exposure of developing chicks to perfluorooctanoic acid induces defects in prehatch and early posthatch development. *J Toxicol Environ Health A* **71**(2), 131-133.

Yang, H. W., Menon, L. G., Black, P. M., Carroll, R. S., and Johnson, M. D. (2010). SNAI2/Slug promotes growth and invasion in human gliomas. *BMC Cancer* **10**, 301.

Yang, Y. H., Dudoit, S., Luu, P., Lin, D. M., Peng, V., Ngai, J., and Speed, T. P. (2002). Normalization for cDNA microarray data: a robust composite method addressing single and multiple slide systematic variation. *Nucleic Acids Res* **30**(4), e15.

Yeung, L. W., Guruge, K. S., Yamanaka, N., Miyazaki, S., and Lam, P. K. (2007). Differential expression of chicken hepatic genes responsive to PFOA and PFOS. *Toxicology* **237**(1-3), 111-125.

Yeung, L. W., Loi, E. I., Wong, V. Y., Guruge, K. S., Yamanaka, N., Tanimura, N., Hasegawa, J., Yamashita, N., Miyazaki, S., and Lam, P. K. (2009). Biochemical responses and accumulation properties of long-chain perfluorinated compounds (PFOS/PFDA/PFOA) in juvenile chickens (Gallus gallus). *Arch Environ Contam Toxicol* **57**(2), 377-386.

Yoo, H., Kannan, K., Kim, S. K., Lee, K. T., Newsted, J. L., and Giesy, J. P. (2008). Perfluoroalkyl acids in the egg yolk of birds from Lake Shihwa, Korea. *Environ Sci Technol* **42**(15), 5821-5827.

Young, C. J., Furdui, V. I., Franklin, J., Koerner, R. M., Muir, D. C., and Mabury, S. A. (2007). Perfluorinated acids in Arctic snow: new evidence for atmospheric formation. *Environ Sci Technol* **41**(10), 3455-3461.

Yu, W. G., Liu, W., and Jin, Y. H. (2009). Effects of perfluorooctane sulfonate on rat thyroid hormone biosynthesis and metabolism. *Environ Toxicol Chem* **28**(5), 990-996.

Zoeller, R. T., Tan, S. W., and Tyl, R. W. (2007). General background on the hypothalamic-pituitary-thyroid (HPT) axis. *Crit Rev Toxicol* **37**(1-2), 11-53.

APPENDIX I

SUPPLEMENTARY INFORMATION

The following tables and figures contain data pertaining to Chapter Three

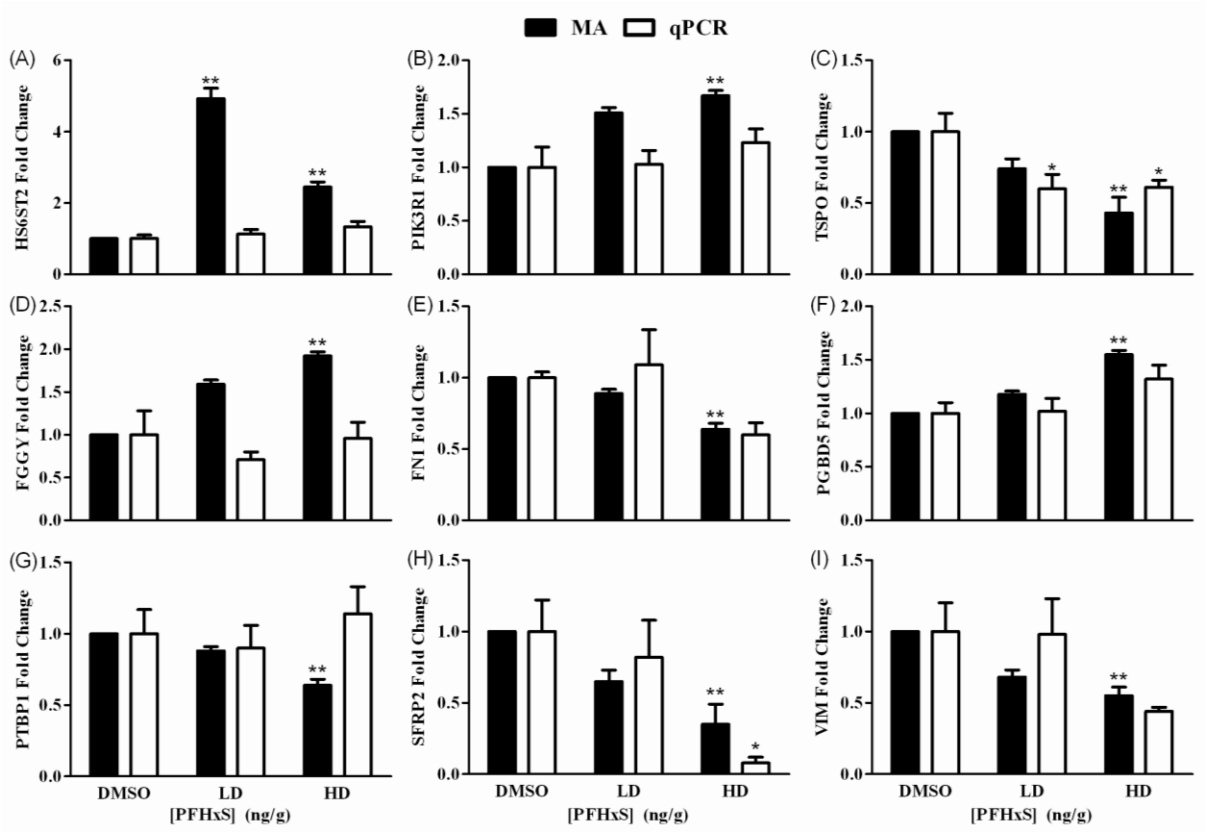

SI Figure 3.1. The relative mRNA levels of neuronal transcripts following *in ovo* exposure of chicken embryos to 890 ng/g (LD) or 38,000 ng/g (HD) perfluorohexane sulfonate. Messenger RNA levels of [A] heparan sulfate 6-O-sulfotransferase 2 (HS6ST2); [B] phosphoinositide-3-kinase, regulatory subunit 1 (PIK3R1); [C] translocator protein (TSPO); [D] FGGY carbohydrate kinase domain containing (FGGY); [E] fibronectin 1 (FN1); [F] piggyBac transposable element derived 5 (PGBD5); [G] polypyrimidine tract binding protein 1 (PTBP1); [H] secreted frizzled-related protein 2 (SFRP2); and [I] vimentin (VIM) were determined by microarray (MA, black bars) and real-time RT-PCR (qPCR, white bars) (n=4-5; error bars represent SEM; *$p \leq 0.05$; **$p \leq 0.001$).

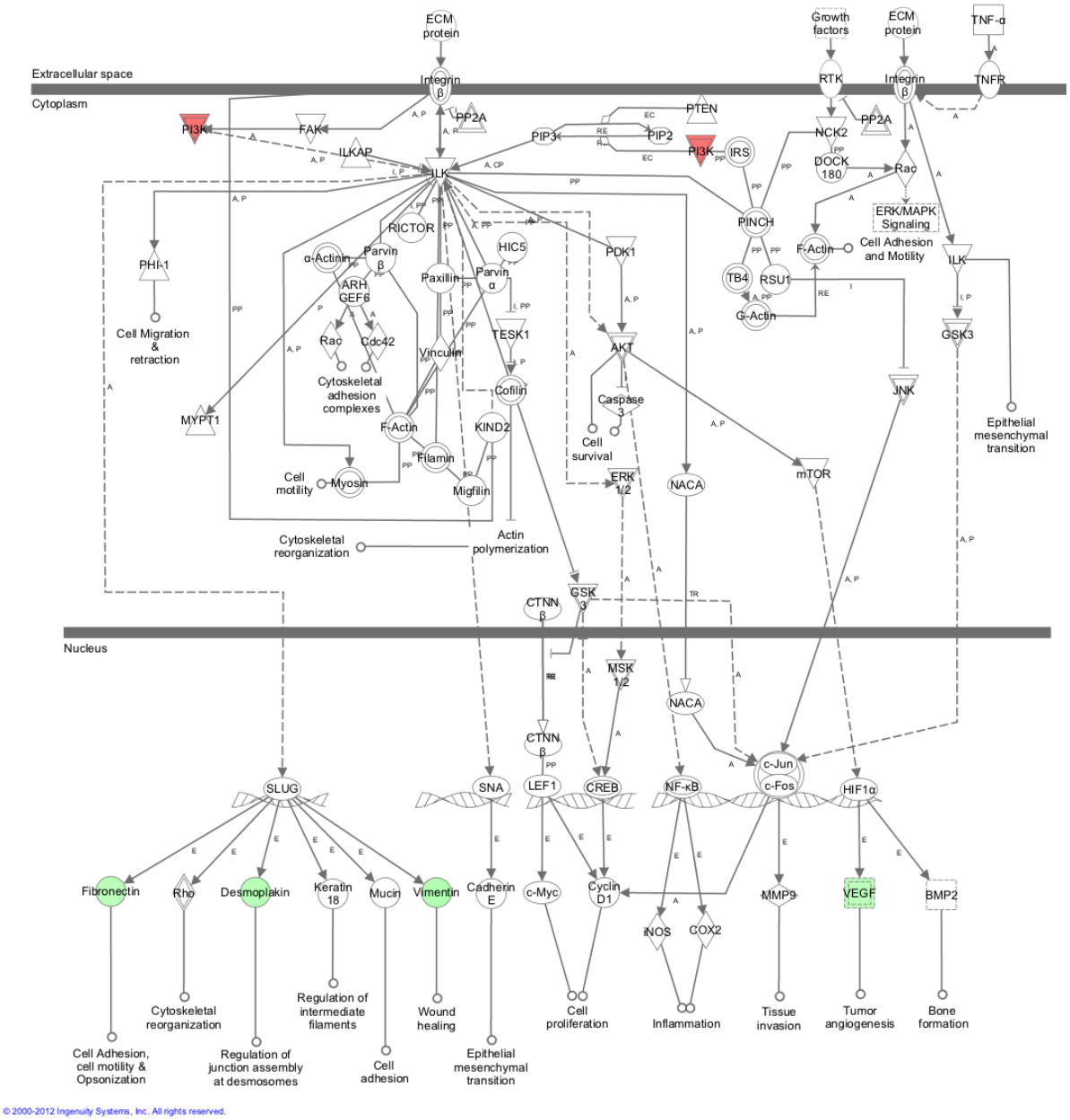

SI Figure 3.2. Integrin-linked kinase (ILK) signaling pathway as depicted in the Ingenuity canonical pathways library. The ILK signaling pathway was overlaid with differentially expressed genes resulting from exposure to 38,000 ng/g perfluorohexane sulfonate. Red or green nodes represent genes that were significantly up- or down-regulated, respectively.

SI Table 3.1. List of genes examined by real-time RT-PCR and their gene symbols, accession numbers, primer and probe sequences, and reaction concentrations.

Gene Name	Symbol	Accession Number	Assay(s)	Oligo	Sequence (5'-3')	Reaction Concentration
β-actin	BA	X00182.1	TaqMan SYBR	FWD primer	AAATTGTGCGTGACATCAAGGA	50
				REV primer	GAGGCAGCTGTGGCCATCT	50
				Probe	TGCTACGTCGCACTGGATTTGGAGC	200
Claudin 11	CLDN11	XM_422797.3	TaqMan	FWD primer	TCATGAGCTTCGGCTACTCC	300
				REV primer	TAGTAGAAGCGGTTCTCGCC	300
				Probe	CGGGCTGGATCGGCTCTGCCCTCTGCC	200
Desmoplakin	DSP	XM_418957.2	TaqMan	FWD primer	GTCATCAAGGAGAAGGAGTACG	300
				REV primer	ACTCATCTCCTCGCTAAACTG	300
				Probe	TGCAGGATGAAGGCACACGGAAGAGGG	200
FGGY carbohydrate kinase domain containing	FGGY	XM_001235528.1	TaqMan	FWD primer	AATGGGAAAAATCGGGCGAG	300
				REV primer	AGATGAAATTAGCCTCGTCGTAG	300
				Probe	AGTGGCATCTTCTGGGAACGGCAGGG	200
Fibronectin 1	FN1	NM_001198712.1	SYBR	FWD primer	GCACTTGTTACGGAGGACAG	150
				REV primer	CCGTGGATGTTGTGTGTCTG	150
Heparan sulfate 6-O-sulfotransferase 2	HS6ST2	NM_204490.1	SYBR	FWD primer	TACATGAGGCAGAAGGAGCAC	900
				REV primer	CACGTTCCCCAGGTAGTCC	900
Nephroblastoma overexpressed gene	NOV	NM_205268.1	TaqMan	FWD primer	GCAGACTTACAAACCTCGTTACTG	300
				REV primer	ACTCTGAGGACAGTTACCATGAC	300
				Probe	GGGCGATGCTGTACCCCACACAACACC	200
PiggyBac transposable element derived 5	PGBD5	BX931270.1	SYBR	FWD primer	TTCGGTGAAAGACTTGTAAAGGAG	300
				REV primer	GGCATCACTTGGTGTTTTTGG	900
Phosphoinositide-3-kinase, regulatory subunit 1	PIK3R1	XM_424759.3	SYBR	FWD primer	AGACATTGACTTGCACTTAGGAG	900
				REV primer	ACTTGGTGCTACAGGAAGGG	900
Polypyrimidine tract binding protein 1	PTBP1	NM_001030935.1	SYBR	FWD primer	ACAGGCTATGTGTGTATCTTGC	150
				REV primer	GCCCCCTCATGTCTTACAAC	150
Secreted frizzled-related protein 2	SFRP2	NM_204773.1	TaqMan	FWD primer	GCATGTTTGTTGTGCAAAAGTAG	300
				REV primer	GCAAGCAATTTCACCTCAGTG	300
				Probe	CGTGTGCCACTGGCTTGTCACAAGGGG	200

Gene Name	Symbol	Accession Number	Assay(s)	Oligo	Sequence (5'-3')	Reaction Concentration
Translocator protein (18kDa)	TSPO	XM_416451.3	TaqMan	FWD primer	GACTGTGGTCTGAATTGGTCC	300
				REV primer	CGCAAACTGTGAAAAAGATGTGG	150
				Probe	TCTCACTGCAGCAGCCGCGTCTTCTGA	200
Vimentin	VIM	NM_001048076.1	TaqMan	FWD primer	CCAGATGCGTGAAATGGAGG	300
				REV primer	GGCGAGCCATTTCTTCCTTC	300
				Probe	ACCAGGACACTATTGGCCGCCTGCAGG	200

SI Table 3.2. Detailed list of probes that were differentially expressed following exposure to 890 (LD) and 38,000 (HD) ng/g perfluorohexane sulfonate. Ingenuity Pathway Analysis (IPA) mappings are also included: mapped (M) and duplicate gene (*). FC = fold change.

Probe ID	GenBank ID	Gene Symbol	Gene Name/Description	LD		HD		IPA
				FC	*p*-value	FC	*p*-value	
A_87_P121103	CR385595		gallus gallus finished cDNA, clone ChEST853e7	-2.45	0.0000	-2.69	0.0000	
A_87_P121103	CR385595	SLC13A3	solute carrier family 13 (sodium-dependent dicarboxylate transporter), member 3	-1.68	0.0004	-2.71	0.0000	M*
A_87_P003051	XM_416881	ATP10A	rep: probable phospholipid-transporting ATPase VA (ATPVA)	-1.51	0.0002	-1.53	0.0000	M
A_87_P017320	CR385143		gallus gallus finished cDNA, clone ChEST402l8	1.77	0.0003	1.73	0.0001	
A_87_P018199	CR353040		gallus gallus finished cDNA, clone ChEST219m12	2.23	0.0000	1.87	0.0000	M
A_87_P056341	NM_204490	HS6ST2	heparan sulfate 6-O-sulfotransferase 2	4.93	0.0000	2.45	0.0009	M
A_87_P008904	NM_205268	NOV	nephroblastoma overexpressed gene	-1.96	0.0518	-5.22	0.0000	M*
A_87_P105138	NM_205268	NOV	nephroblastoma overexpressed gene	-1.63	0.1874	-4.32	0.0000	M*
A_87_P019855	CO762861	CLDN11	claudin 11	-1.44	0.1120	-3.18	0.0000	M*
A_87_P008735	NM_205044	MGP	matrix Gla protein	-2.39	0.0025	-2.99	0.0001	M
A_87_P059436	NM_204773	SFRP2	secreted frizzled-related protein 2	-1.55	0.0760	-2.84	0.0000	M
A_87_P110388	BX266614	SLC9A2	solute carrier family 9 (sodium/hydrogen exchanger), member 2	-1.60	0.0998	-2.58	0.0004	M
A_87_P011657	CR523375		gallus gallus finished cDNA, clone ChEST875h18	-2.34	0.0033	-2.57	0.0005	
A_87_P059166	NM_204624	MOXD1	monooxygenase, DBH-like 1	-1.39	0.1183	-2.45	0.0000	M
A_87_P147108	CO762861	CLDN11	claudin 11	-1.39	0.1963	-2.44	0.0002	M*
A_87_P108093	XM_416451	TSPO	translocator protein (18kDa)	-1.36	0.1862	-2.30	0.0003	M*
A_87_P022211	BX935212	SLC13A3	solute carrier family 13 (sodium-dependent dicarboxylate transporter), member 3	-1.15	0.4868	-2.25	0.0000	M*
A_87_P038127	NM_204259	PTGDS	prostaglandin D2 synthase 21kDa (brain)	-1.51	0.0284	-2.24	0.0000	M
A_87_P016610	CR386251		gallus gallus finished cDNA, clone ChEST129f19	-1.93	0.0084	-2.22	0.0007	M
A_87_P149458	XR_026692	SLC13A3	solute carrier family 13 (sodium-dependent dicarboxylate transporter), member 3	-1.13	0.5459	-2.16	0.0001	M*
A_87_P118208	BX950459		hypothetical protein LOC771263	-1.53	0.0134	-2.15	0.0000	M
A_87_P012359	CR407022		gallus gallus finished cDNA, clone ChEST914e18	-1.43	0.0408	-2.09	0.0000	
A_87_P036466	NM_001031203	NPC2	Niemann-Pick disease, type C2	-1.65	0.0181	-2.07	0.0004	M*

Probe ID	GenBank ID	Gene Symbol	Gene Name/Description	LD		HD		IPA
				FC	*p*-value	FC	*p*-value	
A_87_P017920	CR353470	SLC16A12	solute carrier family 16, member 12 (monocarboxylic acid transporter 12)	-1.50	0.0558	-2.06	0.0003	M
A_87_P016382	CR386573		gallus gallus finished cDNA, clone ChEST762g9	-1.73	0.0051	-2.06	0.0001	
A_87_P024236	BX930604	C1H2ORF40	chromosome 2 open reading frame 40	-1.49	0.0555	-2.03	0.0004	M
A_87_P238018	NM_205380	COL3A1	collagen, type III, alpha 1	-1.46	0.0279	-1.98	0.0000	M
A_87_P021968	BX935736	HES6	hairy and enhancer of split 6 (drosophila)	-1.54	0.0176	-1.97	0.0001	M
A_87_P231498	NM_204636	MXRA8	matrix-remodelling associated 8	-1.22	0.1113	-1.90	0.0000	M
A_87_P193998	NM_205316	CALB2	calbindin 2, 29kDa (calretinin)	-1.24	0.2735	-1.87	0.0007	M
A_87_P037810	AF188735		gallus gallus ZIC2 gene, partial 3'UTR	-1.66	0.0026	-1.84	0.0001	M
A_87_P058361	NM_001048076	VIM	vimentin	-1.47	0.0358	-1.81	0.0007	M
A_87_P146353	M80584	LUM	lumican	-1.43	0.0581	-1.81	0.0010	M
A_87_P056766	NM_205138	FOXC2	forkhead box C2 (MFH-1, mesenchyme forkhead 1)	-1.46	0.0208	-1.78	0.0001	M
A_87_P021702	NM_001199522	GCHFR	GTP cyclohydrolase I feedback regulator	-1.34	0.0638	-1.78	0.0001	M
A_87_P035695	NM_001012580	PDS5A	PDS5, regulator of cohesion maintenance, homolog A (S. cerevisiae)	-1.16	0.3198	-1.76	0.0001	M
A_87_P008913	NM_205291	SERPINH1	serpin peptidase inhibitor, clade H, member 1 (collagen binding protein 1)	-1.55	0.0082	-1.74	0.0003	M
A_87_P052351	NM_001079487	CBLN4	cerebellin 4 precursor	-1.55	0.0083	-1.74	0.0006	M
A_87_P145043	XM_426322	TRPC3	transient receptor potential cation channel, subfamily C, member 3	-1.32	0.0992	-1.72	0.0007	M
A_87_P017434	CR354268		gallus gallus finished cDNA, clone ChEST292g23	-1.61	0.0044	-1.71	0.0006	
A_87_P257763	XR_026679	PCSK1	proprotein convertase subtilisin/kexin type 1	-1.49	0.0106	-1.70	0.0004	M
A_87_P012448	CR406902		gallus gallus finished cDNA, clone ChEST927k17	-1.29	0.0574	-1.70	0.0000	
A_87_P050131	NM_001006482	TMED10	transmembrane emp24-like trafficking protein 10 (yeast)	-1.27	0.0806	-1.69	0.0001	M*
A_87_P050131	NM_001006482	TMED10	transmembrane emp24-like trafficking protein 10 (yeast)	-1.27	0.0806	-1.69	0.0001	M*
A_87_P050131	NM_001006482	TMED10	transmembrane emp24-like trafficking protein 10 (yeast)	-1.27	0.0806	-1.69	0.0001	M*
A_87_P050131	NM_001006482	TMED10	transmembrane emp24-like trafficking protein 10 (yeast)	-1.27	0.0806	-1.69	0.0001	M*
A_87_P050131	NM_001006482	TMED10	transmembrane emp24-like trafficking protein 10 (yeast)	-1.27	0.0806	-1.69	0.0001	M*
A_87_P050131	NM_001006482	TMED10	transmembrane emp24-like trafficking protein 10 (yeast)	-1.38	0.0362	-1.68	0.0006	M*
A_87_P050131	NM_001006482	TMED10	transmembrane emp24-like trafficking protein 10 (yeast)	-1.38	0.0362	-1.68	0.0006	M*

Probe ID	GenBank ID	Gene Symbol	Gene Name/Description	LD		HD		IPA
				FC	*p*-value	FC	*p*-value	
A_87_P050131	NM_001006482	TMED10	transmembrane emp24-like trafficking protein 10 (yeast)	-1.38	0.0362	-1.68	0.0006	M*
A_87_P050131	NM_001006482	TMED10	transmembrane emp24-like trafficking protein 10 (yeast)	-1.38	0.0362	-1.68	0.0006	M*
A_87_P050131	NM_001006482	TMED10	transmembrane emp24-like trafficking protein 10 (yeast)	-1.38	0.0362	-1.68	0.0006	M*
A_87_P132438	AJ002600		gallus gallus domesticus, peripheral Retina, embryonal stage E6-cDNA, PEV16/8	-1.59	0.0016	-1.68	0.0002	
A_87_P050951	NM_001031203	NPC2	Niemann-Pick disease, type C2	-1.25	0.0898	-1.66	0.0002	M*
A_87_P050951	NM_001031203	NPC2	Niemann-Pick disease, type C2	-1.25	0.0898	-1.66	0.0002	M*
A_87_P050951	NM_001031203	NPC2	Niemann-Pick disease, type C2	-1.25	0.0898	-1.66	0.0002	M*
A_87_P050951	NM_001031203	NPC2	Niemann-Pick disease, type C2	-1.25	0.0898	-1.66	0.0002	M*
A_87_P050951	NM_001031203	NPC2	Niemann-Pick disease, type C2	-1.25	0.0898	-1.66	0.0002	M*
A_87_P050131	NM_001006482	TMED10	transmembrane emp24-like trafficking protein 10 (yeast)	-1.34	0.0250	-1.66	0.0001	M*
A_87_P050131	NM_001006482	TMED10	transmembrane emp24-like trafficking protein 10 (yeast)	-1.34	0.0250	-1.66	0.0001	M*
A_87_P050131	NM_001006482	TMED10	transmembrane emp24-like trafficking protein 10 (yeast)	-1.34	0.0250	-1.66	0.0001	M*
A_87_P050131	NM_001006482	TMED10	transmembrane emp24-like trafficking protein 10 (yeast)	-1.34	0.0250	-1.66	0.0001	M*
A_87_P050131	NM_001006482	TMED10	transmembrane emp24-like trafficking protein 10 (yeast)	-1.34	0.0250	-1.66	0.0001	M*
A_87_P242263	XM_418957	DSP	desmoplakin	-1.36	0.0500	-1.66	0.0005	M
A_87_P118508	BX950758	CPSF7	cleavage and polyadenylation specific factor 7, 59kDa	-1.62	0.0033	-1.66	0.0010	M
A_87_P017273	CR385213		gallus gallus finished cDNA, clone ChEST545m21	1.30	0.0947	-1.64	0.0008	
A_87_P022251	NM_001199625	CPM	carboxypeptidase M	-1.42	0.0014	-1.64	0.0000	M
A_87_P012208	CR407231		gallus gallus finished cDNA, clone ChEST417p21	-1.46	0.0151	-1.64	0.0008	
A_87_P050131	NM_001006482	TMED10	transmembrane emp24-like trafficking protein 10 (yeast)	-1.42	0.0024	-1.60	0.0001	M*
A_87_P050131	NM_001006482	TMED10	transmembrane emp24-like trafficking protein 10 (yeast)	-1.42	0.0024	-1.60	0.0001	M*
A_87_P050131	NM_001006482	TMED10	transmembrane emp24-like trafficking protein 10 (yeast)	-1.42	0.0024	-1.60	0.0001	M*
A_87_P050131	NM_001006482	TMED10	transmembrane emp24-like trafficking protein 10 (yeast)	-1.42	0.0024	-1.60	0.0001	M*
A_87_P050131	NM_001006482	TMED10	transmembrane emp24-like trafficking protein 10 (yeast)	-1.42	0.0024	-1.60	0.0001	M*
A_87_P036388	NM_001006262	ASB9	ankyrin repeat and SOCS box-containing 9	-1.46	0.0079	-1.59	0.0004	M
A_87_P125298	CR390846		gallus gallus finished cDNA, clone ChEST968j13	-1.40	0.0028	-1.58	0.0000	

Probe ID	GenBank ID	Gene Symbol	Gene Name/Description	LD		HD		IPA
				FC	*p*-value	FC	*p*-value	
A_87_P016728	CR386059		gallus gallus finished cDNA, clone ChEST217j10	-1.04	0.7231	-1.57	0.0000	
A_87_P081761	NM_001198712	FN1	fibronectin 1	-1.12	0.3894	-1.57	0.0005	M
A_87_P019710	XM_420631	PDE5A	rep: cGMP-specific 3',5'-cyclic phosphodiesterase (CGB-PDE)	-1.38	0.0032	-1.57	0.0000	M
A_87_P035530	NM_001031112	MSN	moesin	-1.21	0.0896	-1.57	0.0000	M
A_87_P035772	NM_001030935	PTBP1	polypyrimidine tract binding protein 1	-1.14	0.3460	-1.56	0.0006	M
A_87_P124058	CR389565	CADM1	cell adhesion molecule 1	1.08	0.5030	-1.56	0.0001	M
A_87_P016302	CR386696		gallus gallus finished cDNA, clone ChEST298l12	-1.38	0.0130	-1.55	0.0006	M
A_87_P050951	NM_001031203	NPC2	Niemann-Pick disease, type C2	-1.39	0.0153	-1.54	0.0008	M*
A_87_P050951	NM_001031203	NPC2	Niemann-Pick disease, type C2	-1.39	0.0153	-1.54	0.0008	M*
A_87_P050951	NM_001031203	NPC2	Niemann-Pick disease, type C2	-1.39	0.0153	-1.54	0.0008	M*
A_87_P050951	NM_001031203	NPC2	Niemann-Pick disease, type C2	-1.39	0.0153	-1.54	0.0008	M*
A_87_P050951	NM_001031203	NPC2	Niemann-Pick disease, type C2	-1.39	0.0153	-1.54	0.0008	M*
A_87_P124648	CR390194		hypothetical protein LOC771832	-1.39	0.0126	-1.53	0.0008	M
A_87_P011537	CR523549		gallus gallus finished cDNA, clone ChEST859n24	1.05	0.6873	-1.53	0.0001	
A_87_P121153	CR385665		gallus gallus finished cDNA, clone ChEST578n21	1.00	0.9551	-1.52	0.0000	
A_87_P016580	CR386291		gallus gallus finished cDNA, clone ChEST55l7	-1.26	0.0662	-1.52	0.0004	
A_87_P023207	BX933089	FAM84A	family with sequence similarity 84, member A	1.06	0.6584	-1.52	0.0008	M
A_87_P015719	CR387580		gallus gallus finished cDNA, clone ChEST49c14	-1.24	0.0679	-1.51	0.0003	
A_87_P022359	NM_001006513	SLC19A1	solute carrier family 19 (folate transporter), member 1	-1.27	0.0396	-1.50	0.0001	M
A_87_P023990	BX931270	PGBD5	piggyBac transposable element derived 5	1.18	0.2167	1.55	0.0009	M
A_87_P284823	XM_424759	PIK3R1	phosphoinositide-3-kinase, regulatory subunit 1 (p85 alpha)	1.51	0.0132	1.67	0.0009	M
A_87_P060016	CR733267	HLA-C	major histocompatibility complex, class I, C	1.36	0.0360	1.70	0.0001	M
A_87_P060279	CR733267		PREDICTED: gallus gallus similar to MHC Rfp-Y class I alpha chain (LOC417053), mRNA	1.48	0.0382	1.81	0.0006	
A_87_P016101	CR387009	FGGY	FGGY carbohydrate kinase domain containing	1.59	0.0026	1.92	0.0000	M
A_87_P135483	BX930765	TSPO	translocator protein (18kDa)	1.27	0.2721	2.12	0.0004	M*
A_87_P017972	CR353391		gallus gallus finished cDNA, clone ChEST489n5	1.96	0.0200	2.55	0.0007	

Probe ID	GenBank ID	Gene Symbol	Gene Name/Description	LD		HD		IPA
				FC	*p*-value	FC	*p*-value	
A_87_P122215	CR387022		gallus gallus finished cDNA, clone ChEST435b7	-2.50	0.0000	-1.06	0.7680	
A_87_P123661	CR389160		gallus gallus finished cDNA, clone ChEST278g5	-2.48	0.0000	-1.02	0.9374	
A_87_P038213	NM_204887	WNT5A	wingless-type MMTV integration site family, member 5A	-1.73	0.0007	-1.29	0.0859	M
A_87_P308552	XM_001235792		sia-alpha-2,3-Gal-beta-1,4-GlcNAc-R:alpha 2,8-sialyltransferase-like	1.51	0.0005	1.19	0.1110	M
A_87_P027490	XM_415238	GGT1	gamma-glutamyltransferase 1	1.73	0.0009	1.19	0.2436	M

SI Table 3.3A. Detailed list of functions and genes within each functional enrichment category for chicken cerebral hemispheres exposed to 890 ng/g perfluorohexane sulfonate.

Category	Subcategory	Function	Function Annotation	*p*-value	Genes	# Genes
Tissue Development and Morphology	Tissue Development	morphogenesis	morphogenesis of mesencephalon	7.59E-04	WNT5A	1
Tissue Development and Morphology	Tissue Development	morphogenesis	morphogenesis of pituitary gland	7.59E-04	WNT5A	1
Tissue Development and Morphology	Tissue Development	regeneration	regeneration of hypoglossal nerve	7.59E-04	ST8SIA1	1
Tissue Development and Morphology	Tissue Development	formation	formation of primitive streak	3.79E-03	WNT5A	1
Tissue Development and Morphology	Tissue Development	synaptogenesis	synaptogenesis	1.36E-02	WNT5A	1
Tissue Development and Morphology	Tissue Development	morphogenesis	morphogenesis of epithelial tissue	2.26E-02	WNT5A	1
Tissue Development and Morphology	Tissue Development	formation	formation of tissue	2.85E-02	GGT1, WNT5A	2
Tissue Development and Morphology	Tissue Development	closure	closure of neural tube	3.81E-02	WNT5A	1
Tissue Development and Morphology	Tissue Development	development	development of neural tube	3.81E-02	WNT5A	1
Tissue Development and Morphology	Tissue Development	development	tissue development	4.49E-02	GGT1, HS6ST2, WNT5A	3
Tissue Development and Morphology	Tissue Morphology	degeneration	degeneration of peripheral nerve	7.59E-04	ST8SIA1	1
Tissue Development and Morphology	Tissue Morphology	quantity	quantity of dopaminergic neurons	7.57E-03	WNT5A	1
Cellular Assembly and Organization		proliferation	proliferation of axons	7.59E-04	ST8SIA1	1
Cellular Assembly and Organization		reorientation	reorientation of centrosome	3.03E-03	WNT5A	1
Cellular Assembly and Organization		synaptogenesis	synaptogenesis	1.36E-02	WNT5A	1
Cellular Assembly and Organization		formation	formation of neurites	4.62E-02	ST8SIA1	1
Cell-To-Cell Signaling and Interaction		synaptic transmission	synaptic transmission of hippocampal neurons	7.57E-03	WNT5A	1
Cell-To-Cell Signaling and Interaction		synaptogenesis	synaptogenesis	1.36E-02	WNT5A	1
Cell-To-Cell Signaling and Interaction		activation	activation of cells	3.06E-02	GGT1, WNT5A	2
Cell-To-Cell Signaling and Interaction		activation	activation of macrophages	4.18E-02	WNT5A	1
Cellular Movement		dissemination	dissemination of tumor cells	2.28E-03	WNT5A	1
Cellular Movement		invasion	invasion of tumor cell lines	1.52E-02	ST8SIA1, WNT5A	2
Cellular Movement		migration	migration of carcinoma cell lines	2.26E-02	WNT5A	1
Cellular Movement		invasion	invasion of carcinoma cell lines	2.78E-02	WNT5A	1
Cellular Movement		invasion	invasion of tumor cells	4.77E-02	WNT5A	1

Category	Subcategory	Function	Function Annotation	*p*-value	Genes	# Genes
Nervous System Development and Function		morphogenesis	morphogenesis of mesencephalon	7.59E-04	WNT5A	1
Nervous System Development and Function		proliferation	proliferation of axons	7.59E-04	ST8SIA1	1
Nervous System Development and Function		regeneration	regeneration of hypoglossal nerve	7.59E-04	ST8SIA1	1
Nervous System Development and Function		expansion	expansion of dopaminergic neurons	1.52E-03	WNT5A	1
Nervous System Development and Function		proliferation	proliferation of dopaminergic neurons	1.52E-03	WNT5A	1
Nervous System Development and Function		S phase	entry into S phase of cortical neurons	1.52E-03	ST8SIA1	1
Nervous System Development and Function		branching	branching of sympathetic neuron	3.03E-03	WNT5A	1
Nervous System Development and Function		differentiation	differentiation of dopaminergic neurons	6.81E-03	WNT5A	1
Nervous System Development and Function		quantity	quantity of dopaminergic neurons	7.57E-03	WNT5A	1
Nervous System Development and Function		synaptic transmission	synaptic transmission of hippocampal neurons	7.57E-03	WNT5A	1
Nervous System Development and Function		synaptogenesis	synaptogenesis	1.36E-02	WNT5A	1
Nervous System Development and Function		branching	branching of axons	1.81E-02	WNT5A	1
Nervous System Development and Function		length	length of neurites	3.07E-02	WNT5A	1
Nervous System Development and Function		formation	formation of neurites	4.62E-02	ST8SIA1	1
Cell Development and Morphology	Cell Morphology	innervation	innervation of olfactory epithelium	7.59E-04	WNT5A	1
Cell Development and Morphology	Cell Morphology	reorientation	reorientation of centrosome	3.03E-03	WNT5A	1
Cell Development and Morphology	Cell Morphology	morphology	morphology of neuroblastoma cell lines	5.30E-03	ST8SIA1	1
Cell Development and Morphology	Cell Morphology	morphology	morphology of cells	1.78E-02	ST8SIA1, WNT5A	2
Cell Development and Morphology	Cell Morphology	length	length of neurites	3.07E-02	WNT5A	1
Cell Development and Morphology	Cellular Development	expansion	expansion of dopaminergic neurons	1.52E-03	WNT5A	1
Cell Development and Morphology	Cellular Development	growth	growth of tumor cell lines	2.98E-03	GGT1, ST8SIA1, WNT5A	3
Cell Development and Morphology	Cellular Development	branching	branching of sympathetic neuron	3.03E-03	WNT5A	1
Cell Development and Morphology	Cellular Development	growth	growth of pheochromocytoma cell lines	6.06E-03	ST8SIA1	1
Cell Development and Morphology	Cellular Development	differentiation	differentiation of dopaminergic neurons	6.81E-03	WNT5A	1
Cell Development and Morphology	Cellular Development	growth	growth of neuroblastoma cell lines	1.36E-02	ST8SIA1	1
Cell Development and Morphology	Cellular Development	branching	branching of axons	1.81E-02	WNT5A	1
Cell Development and Morphology	Cellular Development	growth	growth of epithelial cell lines	4.03E-02	WNT5A	1

Category	Subcategory	Function	Function Annotation	*p*-value	Genes	# Genes
Molecular Transport		quantity	quantity of ganglioside GD1b	1.52E-03	ST8SIA1	1
Molecular Transport		quantity	quantity of ganglioside GD2	1.52E-03	ST8SIA1	1
Molecular Transport		quantity	quantity of ganglioside GT1	1.52E-03	ST8SIA1	1
Molecular Transport		quantity	quantity of L-cysteine	1.52E-03	GGT1	1
Molecular Transport		quantity	quantity of ganglioside GD3	3.03E-03	ST8SIA1	1
Molecular Transport		quantity	quantity of ganglioside GM3	3.79E-03	ST8SIA1	1
Molecular Transport		quantity	quantity of cyclic GMP	1.36E-02	WNT5A	1
Lipid Metabolism		sialylation	sialylation of ganglioside GM3	7.59E-04	ST8SIA1	1
Lipid Metabolism		cleavage	cleavage of leukotriene C4	1.52E-03	GGT1	1
Lipid Metabolism		cleavage	cleavage of leukotriene D4	1.52E-03	GGT1	1
Lipid Metabolism		quantity	quantity of ganglioside GD1b	1.52E-03	ST8SIA1	1
Lipid Metabolism		quantity	quantity of ganglioside GD2	1.52E-03	ST8SIA1	1
Lipid Metabolism		quantity	quantity of ganglioside GT1	1.52E-03	ST8SIA1	1
Lipid Metabolism		synthesis	synthesis of ganglioside GD3	2.28E-03	ST8SIA1	1
Lipid Metabolism		quantity	quantity of ganglioside GD3	3.03E-03	ST8SIA1	1
Lipid Metabolism		synthesis	synthesis of ganglioside GM3	3.03E-03	ST8SIA1	1
Lipid Metabolism		quantity	quantity of ganglioside GM3	3.79E-03	ST8SIA1	1
Cellular Growth and Proliferation	Cell Cycle	S phase	entry into S phase of cortical neurons	1.52E-03	ST8SIA1	1
Cellular Growth and Proliferation	Cell Death	apoptosis	apoptosis of neurons	9.32E-03	ST8SIA1, WNT5A	2
Cellular Growth and Proliferation	Cell Death	apoptosis	apoptosis of organ	2.27E-02	ST8SIA1, WNT5A	2
Cellular Growth and Proliferation	Cell Death	apoptosis	apoptosis of cortical neurons	2.78E-02	ST8SIA1	1
Cellular Growth and Proliferation		clonogenicity	clonogenicity of carcinoma cell lines	7.59E-04	WNT5A	1
Cellular Growth and Proliferation		expansion	expansion of dopaminergic neurons	1.52E-03	WNT5A	1
Cellular Growth and Proliferation		proliferation	proliferation of dopaminergic neurons	1.52E-03	WNT5A	1
Cellular Growth and Proliferation		growth	growth of tumor cell lines	2.98E-03	GGT1, ST8SIA1, WNT5A	3
Cellular Growth and Proliferation		proliferation	proliferation of cells	9.22E-03	GGT1, HS6ST2, ST8SIA1, WNT5A	4
Cellular Growth and Proliferation		growth	growth of neuroblastoma cell lines	1.36E-02	ST8SIA1	1

Category	Subcategory	Function	Function Annotation	*p*-value	Genes	# Genes
Cellular Growth and Proliferation		growth	growth of epithelial cell lines	4.03E-02	WNT5A	1
Endocrine System Development and Disorders		morphogenesis	morphogenesis of pituitary gland	7.59E-04	WNT5A	1
Protein Synthesis and Trafficking		metabolism	metabolism of glutathione	1.36E-02	GGT1	1
Gene Expression		activation	activation of T-cell factor responsive element	3.79E-03	WNT5A	1
Amino Acid Metabolism		quantity	quantity of L-cysteine	1.52E-03	GGT1	1
Amino Acid Metabolism		utilization	utilization of glutamine	7.59E-04	GGT1	1
Embryonic Development		elongation	elongation of ectoderm	7.59E-04	WNT5A	1
Embryonic Development		morphogenesis	morphogenesis of mesencephalon	7.59E-04	WNT5A	1
Embryonic Development		morphogenesis	morphogenesis of pituitary gland	7.59E-04	WNT5A	1
Embryonic Development		development	development of gland	1.68E-03	HS6ST2, WNT5A	2
Embryonic Development		formation	formation of primitive streak	3.79E-03	WNT5A	1
Embryonic Development		specification	specification of rostrocaudal axis	8.32E-03	WNT5A	1
Embryonic Development		somitogenesis	somitogenesis	2.03E-02	WNT5A	1
Embryonic Development		closure	closure of neural tube	3.81E-02	WNT5A	1
Embryonic Development		development	development of neural tube	3.81E-02	WNT5A	1
Embryonic Development		patterning	patterning of rostrocaudal axis	4.40E-02	WNT5A	1
Nucleic Acid Metabolism		synthesis	synthesis of CMP-sialic acid	1.52E-03	ST8SIA1	1
Nucleic Acid Metabolism		quantity	quantity of cyclic GMP	1.36E-02	WNT5A	1
Carbohydrate Metabolism		synthesis	synthesis of CMP-sialic acid	1.52E-03	ST8SIA1	1
Cancer	Tumor Morphology	invasion	invasion of tumor cells	4.77E-02	WNT5A	1
Cancer		neuroblastoma	neuroblastoma	4.40E-02	WNT5A	1

SI Table 3.3B. Detailed list of functions and genes within each functional enrichment category for chicken cerebral hemispheres exposed to 38,000 ng/g perfluorohexane sulfonate.

Category	Subcategory	Function	Function Annotation	*p*-value	Genes	# Genes
Tissue Development and Morphology	Tissue Development	accumulation	accumulation of extracellular matrix	2.33E-02	FN1	1
Tissue Development and Morphology	Tissue Development	adherence	adherence of astrocytes	9.39E-03	CADM1	1
Tissue Development and Morphology	Tissue Development	adherence	adherence of cells	9.42E-04	CADM1, FN1	2
Tissue Development and Morphology	Tissue Development	adhesion	adhesion of astrocytes	9.39E-03	FN1	1
Tissue Development and Morphology	Tissue Development	adhesion	adhesion of brain cancer cell lines	2.79E-02	FN1	1
Tissue Development and Morphology	Tissue Development	adhesion	adhesion of cell-associated matrix	5.58E-04	COL3A1, FN1, PIK3R1	3
Tissue Development and Morphology	Tissue Development	adhesion	adhesion of glioma cells	9.39E-03	FN1	1
Tissue Development and Morphology	Tissue Development	adhesion	adhesion of neuroepithelial cells	9.39E-03	FN1	1
Tissue Development and Morphology	Tissue Development	aggregation	aggregation of cells	2.94E-02	CADM1, FN1, PIK3R1	3
Tissue Development and Morphology	Tissue Development	assembly	assembly of desmosomes	4.71E-03	DSP	1
Tissue Development and Morphology	Tissue Development	assembly	assembly of fibronectin matrix	4.61E-02	FN1	1
Tissue Development and Morphology	Tissue Development	assembly	assembly of intercellular junctions	6.49E-03	CADM1, DSP	2
Tissue Development and Morphology	Tissue Development	assembly	assembly of synapse	4.61E-02	CADM1	1
Tissue Development and Morphology	Tissue Development	attachment	attachment of brain cancer cell lines	1.87E-02	FN1	1
Tissue Development and Morphology	Tissue Development	attachment	attachment of carcinoma cell lines	4.71E-03	FN1	1
Tissue Development and Morphology	Tissue Development	attachment	attachment of cells	3.30E-02	CADM1, FN1	2
Tissue Development and Morphology	Tissue Development	attachment	attachment of epithelial cell lines	9.39E-03	FN1	1
Tissue Development and Morphology	Tissue Development	binding	binding of focal adhesions	1.41E-02	FN1	1
Tissue Development and Morphology	Tissue Development	cell-cell adhesion	cell-cell adhesion	2.37E-02	CADM1, PIK3R1	2
Tissue Development and Morphology	Tissue Development	cell-cell contact	cell-cell contact	4.01E-03	CADM1, DSP, FN1	3
Tissue Development and Morphology	Tissue Development	cell-cell contact	cell-cell contact of astrocytes	4.71E-03	CADM1	1
Tissue Development	Tissue Development	cell-cell contact	cell-cell contact of nervous tissue	9.39E-03	CADM1	1

Category	Subcategory	Function	Function Annotation	*p*-value	Genes	# Genes
and Morphology			cell lines			
Tissue Development and Morphology	Tissue Development	density	density of neuromuscular junctions	4.71E-03	HLA-C	1
Tissue Development and Morphology	Tissue Development	development	development of neural tube	2.37E-02	FN1, SFRP2	2
Tissue Development and Morphology	Tissue Development	development	tissue development	1.67E-02	ALX4, CADM1, COL3A1, DSP, FN1, HS6ST2, MGP, MSN, NOV, PGF, PIK3R1, SFRP2, SLC19A1, ZIC2	14
Tissue Development and Morphology	Tissue Development	developmental process	developmental process of extracellular matrix	9.39E-03	FN1	1
Tissue Development and Morphology	Tissue Development	fibrogenesis	fibrogenesis of fibronectin matrix	4.71E-03	FN1	1
Tissue Development and Morphology	Tissue Development	formation	delay in formation of focal adhesions	9.39E-03	FN1	1
Tissue Development and Morphology	Tissue Development	formation	formation of focal complexes	3.70E-02	FN1	1
Tissue Development and Morphology	Tissue Development	formation	formation of intercellular junctions	1.25E-02	CADM1, CLDN11, DSP	3
Tissue Development and Morphology	Tissue Development	maturation	maturation of focal adhesions	4.71E-03	FN1	1
Tissue Development and Morphology	Tissue Development	quantity	quantity of desmosomes	1.41E-02	DSP	1
Tissue Development and Morphology	Tissue Development	segmentation	segmentation of somites	2.33E-02	SFRP2	1
Tissue Development and Morphology	Tissue Development	size	size of focal adhesions	1.87E-02	PTBP1	1
Tissue Development and Morphology	Tissue Morphology	morphology	morphology of basement membrane	4.71E-03	SERPINH1	1
Tissue Development and Morphology	Tissue Morphology	quantity	quantity of lesion	8.04E-03	PIK3R1, SLC19A1	2
Tissue Development and Morphology	Tissue Morphology	morphology	morphology of visceral endoderm	1.41E-02	SERPINH1	1
Tissue Development and Morphology	Tissue Morphology	quantity	quantity of endothelial cell lines	4.61E-02	FN1	1
Cellular Assembly and Organization		adhesion	adhesion of cell-associated matrix	5.58E-04	COL3A1, FN1, PIK3R1	3
Cellular Assembly and Organization		morphology	morphology of filaments	7.56E-04	LUM, PIK3R1	2
Cellular Assembly and Organization		organization	organization of filaments	8.75E-04	COL3A1, FN1, MSN, SERPINH1, SFRP2, VIM	6
Cellular Assembly and Organization		organization	organization of organelle	1.36E-03	COL3A1, DSP, FN1, MSN, SERPINH1, SFRP2, TMED10, VIM	8
Cellular Assembly and Organization		quantity	quantity of filaments	3.53E-03	DSP, FN1, SERPINH1, VIM	4
Cellular Assembly and Organization		quantity	quantity of keratin filaments	4.71E-03	DSP	1

Category	Subcategory	Function	Function Annotation	*p*-value	Genes	# Genes
Cellular Assembly and Organization		assembly	assembly of desmosomes	4.71E-03	DSP	1
Cellular Assembly and Organization		attachment	attachment of desmosomes	4.71E-03	DSP	1
Cellular Assembly and Organization		attachment	attachment of intermediate filaments	4.71E-03	DSP	1
Cellular Assembly and Organization		fibrogenesis	fibrogenesis of fibronectin matrix	4.71E-03	FN1	1
Cellular Assembly and Organization		stabilization	stabilization of desmosomes	4.71E-03	DSP	1
Cellular Assembly and Organization		assembly	assembly of intercellular junctions	6.49E-03	CADM1, DSP	2
Cellular Assembly and Organization		quantity	quantity of adherens junctions	9.39E-03	DSP	1
Cellular Assembly and Organization		quantity	quantity of intermediate filaments	9.39E-03	DSP, VIM	2
Cellular Assembly and Organization		assembly	delay in assembly of actin stress fibers	9.39E-03	FN1	1
Cellular Assembly and Organization		formation	delay in formation of focal adhesions	9.39E-03	FN1	1
Cellular Assembly and Organization		elongation	elongation of lamellipodia	9.39E-03	PIK3R1	1
Cellular Assembly and Organization		outgrowth	outgrowth of growth cone	9.39E-03	FN1	1
Cellular Assembly and Organization		rearrangement	delay in rearrangement of cytoskeleton	9.39E-03	FN1	1
Cellular Assembly and Organization		reorganization	reorganization of F-actin	9.39E-03	FN1	1
Cellular Assembly and Organization		transport	transport of nucleus	9.39E-03	FN1	1
Cellular Assembly and Organization		formation	formation of intercellular junctions	1.25E-02	CADM1, CLDN11, DSP	3
Cellular Assembly and Organization		quantity	quantity of desmosomes	1.41E-02	DSP	1
Cellular Assembly and Organization		binding	binding of focal adhesions	1.41E-02	FN1	1
Cellular Assembly and Organization		morphology	morphology of Golgi apparatus	1.87E-02	TMED10	1
Cellular Assembly and Organization		formation	formation of cell-matrix contacts	1.87E-02	FN1	1
Cellular Assembly and Organization		formation	formation of lipid bodies	1.87E-02	PIK3R1	1
Cellular Assembly and Organization		binding	binding of Golgi membranes	1.87E-02	TMED10	1
Cellular Assembly and Organization		size	size of focal adhesions	1.87E-02	PTBP1	1

Category	Subcategory	Function	Function Annotation	*p*-value	Genes	# Genes
Cellular Assembly and Organization		sealing	sealing of cellular membrane	2.33E-02	DSP	1
Cellular Assembly and Organization		organization	organization of adherens junctions	2.79E-02	DSP	1
Cellular Assembly and Organization		morphology	morphology of actin filaments	2.79E-02	PIK3R1	1
Cellular Assembly and Organization		formation	formation of focal complexes	3.70E-02	FN1	1
Cellular Assembly and Organization		organization	organization of actin stress fibers	4.16E-02	FN1	1
Cellular Assembly and Organization		assembly	assembly of fibronectin matrix	4.61E-02	FN1	1
Cellular Assembly and Organization		assembly	assembly of synapse	4.61E-02	CADM1	1
Cellular Assembly and Organization		formation	formation of actin cytoskeleton	4.61E-02	FN1	1
Cellular Assembly and Organization		formation	formation of nucleus	4.61E-02	FN1	1
Cell-To-Cell Signaling and Interaction		adhesion	adhesion of cell-associated matrix	5.58E-04	COL3A1, FN1, PIK3R1	3
Cell-To-Cell Signaling and Interaction		cell-cell contact	cell-cell contact	4.01E-03	CADM1, DSP, FN1	3
Cell-To-Cell Signaling and Interaction		cell-cell contact	cell-cell contact of astrocytes	4.71E-03	CADM1	1
Cell-To-Cell Signaling and Interaction		assembly	assembly of desmosomes	4.71E-03	DSP	1
Cell-To-Cell Signaling and Interaction		attachment	attachment of carcinoma cell lines	4.71E-03	FN1	1
Cell-To-Cell Signaling and Interaction		density	density of neuromuscular junctions	4.71E-03	HLA-C	1
Cell-To-Cell Signaling and Interaction		maturation	maturation of focal adhesions	4.71E-03	FN1	1
Cell-To-Cell Signaling and Interaction		stabilization	stabilization of desmosomes	4.71E-03	DSP	1
Cell-To-Cell Signaling and Interaction		assembly	assembly of intercellular junctions	6.49E-03	CADM1, DSP	2
Cell-To-Cell Signaling and Interaction		adhesion	adhesion of astrocytes	9.39E-03	FN1	1
Cell-To-Cell Signaling and Interaction		adhesion	adhesion of glioma cells	9.39E-03	FN1	1
Cell-To-Cell Signaling and Interaction		adhesion	adhesion of neuroepithelial cells	9.39E-03	FN1	1
Cell-To-Cell Signaling and Interaction		cell-cell contact	cell-cell contact of nervous tissue cell lines	9.39E-03	CADM1	1
Cell-To-Cell Signaling and Interaction		activation	activation of carcinoma cell lines	9.39E-03	CADM1	1

Category	Subcategory	Function	Function Annotation	*p*-value	Genes	# Genes
Cell-To-Cell Signaling and Interaction		dynamics	dynamics of cell-matrix contacts	9.39E-03	FN1	1
Cell-To-Cell Signaling and Interaction		formation	delay in formation of focal adhesions	9.39E-03	FN1	1
Cell-To-Cell Signaling and Interaction		quantity	quantity of adherens junctions	9.39E-03	DSP	1
Cell-To-Cell Signaling and Interaction		stimulation	stimulation of microglia	9.39E-03	FN1	1
Cell-To-Cell Signaling and Interaction		transduction	transduction of multilineage progenitor cells	9.39E-03	FN1	1
Cell-To-Cell Signaling and Interaction		formation	formation of intercellular junctions	1.25E-02	CADM1, CLDN11, DSP	3
Cell-To-Cell Signaling and Interaction		binding	binding of focal adhesions	1.41E-02	FN1	1
Cell-To-Cell Signaling and Interaction		quantity	quantity of desmosomes	1.41E-02	DSP	1
Cell-To-Cell Signaling and Interaction		attachment	attachment of brain cancer cell lines	1.87E-02	FN1	1
Cell-To-Cell Signaling and Interaction		formation	formation of cell-matrix contacts	1.87E-02	FN1	1
Cell-To-Cell Signaling and Interaction		size	size of focal adhesions	1.87E-02	PTBP1	1
Cell-To-Cell Signaling and Interaction		cell-cell adhesion	cell-cell adhesion	2.37E-02	CADM1, PIK3R1	2
Cell-To-Cell Signaling and Interaction		adhesion	adhesion of brain cancer cell lines	2.79E-02	FN1	1
Cell-To-Cell Signaling and Interaction		organization	organization of adherens junctions	2.79E-02	DSP	1
Cell-To-Cell Signaling and Interaction		attachment	attachment of cells	3.30E-02	CADM1, FN1	2
Cell-To-Cell Signaling and Interaction		formation	formation of focal complexes	3.70E-02	FN1	1
Cell-To-Cell Signaling and Interaction	Cell Signaling	insulin-like growth factor receptor signaling pathway	insulin-like growth factor receptor signaling pathway	4.16E-02	PIK3R1	1
Cell-To-Cell Signaling and Interaction		assembly	assembly of fibronectin matrix	4.61E-02	FN1	1
Cell-To-Cell Signaling and Interaction		assembly	assembly of synapse	4.61E-02	CADM1	1
Cellular Movement		migration	migration of neuroglia	6.06E-04	CLDN11, FN1, TSPO	3
Cellular Movement		mobility	mobility of cells	1.88E-03	CADM1, FN1	2
Cellular Movement		migration	migration of pyramidal neurons	9.39E-03	FN1	1
Cellular Movement		mobility	mobility of carcinoma cell lines	9.39E-03	CADM1	1
Cellular Movement		haptotaxis	haptotaxis of neuroblastoma cell lines	1.41E-02	FN1	1

Category	Subcategory	Function	Function Annotation	*p*-value	Genes	# Genes
Cellular Movement		migration	migration of phagocytes	1.63E-02	FN1, LUM, PIK3R1	3
Cellular Movement		cell movement	cell movement of glioma cells	2.33E-02	SFRP2	1
Cellular Movement		movement	movement of cells	2.55E-02	CADM1, CLDN11, FN1, LUM, MGP, NOV, PGF, PIK3R1, SFRP2, TSPO, VIM	11
Cellular Movement		invasion	invasion of tumor cells	3.61E-02	FN1, NOV	2
Cellular Movement		migration	migration of oligodendrocytes	4.16E-02	CLDN11	1
Cellular Movement		dissemination	dissemination of cells	4.16E-02	FN1	1
Nervous System Development and Function		migration	migration of neuroglia	6.06E-04	CLDN11, FN1, TSPO	3
Nervous System Development and Function		migration	migration of pyramidal neurons	9.39E-03	FN1	1
Nervous System Development and Function		adhesion	adhesion of astrocytes	9.39E-03	FN1	1
Nervous System Development and Function		cell-cell contact	cell-cell contact of nervous tissue cell lines	9.39E-03	CADM1	1
Nervous System Development and Function		outgrowth	outgrowth of growth cone	9.39E-03	FN1	1
Nervous System Development and Function		stimulation	stimulation of microglia	9.39E-03	FN1	1
Nervous System Development and Function		ensheathment	ensheathment of axons	1.87E-02	CLDN11	1
Nervous System Development and Function		proliferation	proliferation of neuroglia	2.63E-02	CLDN11, TRPC3, TSPO	3
Nervous System Development and Function		differentiation	differentiation of neural precursor cells	3.70E-02	FN1	1
Nervous System Development and Function		migration	migration of oligodendrocytes	4.16E-02	CLDN11	1
Nervous System Development and Function		assembly	assembly of synapse	4.61E-02	CADM1	1
Cell Development and Morphology	Cell Morphology	morphology	morphology of filaments	7.56E-04	LUM, PIK3R1	2

Category	Subcategory	Function	Function Annotation	*p*-value	Genes	# Genes
Cell Development and Morphology	Cell Morphology	polarization	polarization of phagocytes	1.88E-03	FN1, PIK3R1	2
Cell Development and Morphology	Cell Morphology	extension	extension of microvascular endothelial cells	4.71E-03	FN1	1
Cell Development and Morphology	Cell Morphology	cell spreading	cell spreading of endothelial cell lines	9.39E-03	FN1	1
Cell Development and Morphology	Cell Morphology	elongation	elongation of lamellipodia	9.39E-03	PIK3R1	1
Cell Development and Morphology	Cell Morphology	reorganization	reorganization of F-actin	9.39E-03	FN1	1
Cell Development and Morphology	Cell Morphology	morphology	morphology of Golgi apparatus	1.87E-02	TMED10	1
Cell Development and Morphology	Cell Morphology	polarization	polarization of macrophage cancer cell lines	1.87E-02	PIK3R1	1
Cell Development and Morphology	Cell Morphology	cell spreading	cell spreading of embryonic cell lines	1.87E-02	FN1, VIM	2
Cell Development and Morphology	Cell Morphology	size	size of focal adhesions	1.87E-02	PTBP1	1
Cell Development and Morphology	Cell Morphology	morphology	morphology of actin filaments	2.79E-02	PIK3R1	1
Cell Development and Morphology	Cell Morphology	cell spreading	cell spreading of epithelial cell lines	2.79E-02	FN1, VIM	2
Cell Development and Morphology	Cell Morphology	cell spreading	cell spreading of brain cancer cell lines	3.70E-02	FN1	1
Cell Development and Morphology	Cellular Development	development	development of cells	1.79E-02	CADM1, FN1, HLA-C, MGP, NOV, PGF, PIK3R1, SFRP2, SLC19A1, VIM	10
Cell Development and Morphology	Cellular Development	developmental process	developmental process of embryonic stem cells	3.40E-02	PIK3R1, SFRP2	2
Cell Development and Morphology	Cellular Development	differentiation	differentiation of neural precursor cells	3.70E-02	FN1	1
Cell Development and Morphology	Cellular Development	growth	growth of carcinoma cell lines	4.14E-02	NOV, PIK3R1	2
Cell Development and Morphology	Cellular Development	differentiation	differentiation	4.36E-02	DSP, FN1, HES6, HLA-C, MGP, PDE5A, PGF, PIK3R1, PTGDS, SERPINH1, SFRP2, VIM, ZIC2	13
Molecular Transport		transport	transport of cholesterol	2.17E-03	NPC2, TSPO	2
Molecular Transport		accumulation	accumulation of protein fragment	4.71E-03	FN1	1
Molecular Transport		accumulation	accumulation of sphingomyelin	4.71E-03	NPC2	1
Molecular Transport		accumulation	accumulation of thiamine	4.71E-03	SLC19A1	1
Molecular Transport		influx	influx of methotrexate	4.71E-03	SLC19A1	1
Molecular Transport		localization	localization of protein fragment	4.71E-03	HLA-C	1
Molecular Transport		uptake	uptake of methotrexate	4.71E-03	SLC19A1	1

Category	Subcategory	Function	Function Annotation	*p*-value	Genes	# Genes
Molecular Transport		uptake	uptake of thiamine	4.71E-03	SLC19A1	1
Molecular Transport		accumulation	accumulation of phospholipid	5.10E-03	NPC2, PIK3R1	2
Molecular Transport		accumulation	accumulation of ganglioside GM3	9.39E-03	NPC2	1
Molecular Transport		accumulation	accumulation of lysobisphosphatidic acid	9.39E-03	NPC2	1
Molecular Transport		import	import of cholesterol	9.39E-03	TSPO	1
Molecular Transport		release	release of proteoglycan	9.39E-03	FN1	1
Molecular Transport		localization	localization of protein	1.28E-02	HLA-C, PIK3R1, SLC9A2	3
Molecular Transport		transport	transport of glycolipid	1.41E-02	NPC2	1
Molecular Transport		accumulation	accumulation of asialo GM2 ganglioside	1.41E-02	NPC2	1
Molecular Transport		accumulation	accumulation of glucosylceramide	1.41E-02	NPC2	1
Molecular Transport		accumulation	accumulation of lactosylceramide	1.41E-02	NPC2	1
Molecular Transport		transport	transport of leucovorin	1.87E-02	SLC19A1	1
Molecular Transport		accumulation	accumulation of ganglioside GM2	1.87E-02	NPC2	1
Molecular Transport		accumulation	accumulation of phosphatidylinositol-3-phosphate	1.87E-02	PIK3R1	1
Molecular Transport		movement	movement of cholesterol	1.87E-02	NPC2	1
Molecular Transport		quantity	quantity of 5,6,7,8-tetrahydrobiopterin	1.87E-02	PIK3R1	1
Molecular Transport		accumulation	accumulation of lipid	2.94E-02	FN1, NPC2, PIK3R1	3
Molecular Transport		transport	transport of folic acid	3.25E-02	SLC19A1	1
Molecular Transport		transport	transport of methotrexate	3.25E-02	SLC19A1	1
Molecular Transport		release	release of leukotriene C4	3.25E-02	PIK3R1	1
Lipid Metabolism		transport	transport of cholesterol	2.17E-03	NPC2, TSPO	2
Lipid Metabolism		accumulation	accumulation of sphingomyelin	4.71E-03	NPC2	1
Lipid Metabolism		loading	loading of ganglioside GM3	4.71E-03	NPC2	1
Lipid Metabolism		unloading	unloading of ganglioside GT1	4.71E-03	NPC2	1
Lipid Metabolism		accumulation	accumulation of phospholipid	5.10E-03	NPC2, PIK3R1	2
Lipid Metabolism		accumulation	accumulation of ganglioside GM3	9.39E-03	NPC2	1

Category	Subcategory	Function	Function Annotation	*p*-value	Genes	# Genes
Lipid Metabolism		accumulation	accumulation of lysobisphosphatidic acid	9.39E-03	NPC2	1
Lipid Metabolism		import	import of cholesterol	9.39E-03	TSPO	1
Lipid Metabolism		transport	transport of glycolipid	1.41E-02	NPC2	1
Lipid Metabolism		accumulation	accumulation of asialo GM2 ganglioside	1.41E-02	NPC2	1
Lipid Metabolism		accumulation	accumulation of glucosylceramide	1.41E-02	NPC2	1
Lipid Metabolism		accumulation	accumulation of lactosylceramide	1.41E-02	NPC2	1
Lipid Metabolism		trafficking	trafficking of cholesterol	1.41E-02	NPC2	1
Lipid Metabolism		accumulation	accumulation of ganglioside GM2	1.87E-02	NPC2	1
Lipid Metabolism		accumulation	accumulation of phosphatidylinositol-3-phosphate	1.87E-02	PIK3R1	1
Lipid Metabolism		binding	binding of phosphatidylinositol 4,5-diphosphate	1.87E-02	FN1	1
Lipid Metabolism		formation	formation of lipid bodies	1.87E-02	PIK3R1	1
Lipid Metabolism		movement	movement of cholesterol	1.87E-02	NPC2	1
Lipid Metabolism		accumulation	accumulation of lipid	2.94E-02	FN1, NPC2, PIK3R1	3
Lipid Metabolism		release	release of leukotriene C4	3.25E-02	PIK3R1	1
Lipid Metabolism		synthesis	synthesis of pregnenolone	3.70E-02	TSPO	1
Cellular Growth and Proliferation	Cell Cycle	G0/G1 phase transition	arrest in G0/G1 phase transition of embryonic stem cells	4.71E-03	PIK3R1	1
Cellular Growth and Proliferation	Cell Cycle	G1/S phase transition	entry into G1/S phase transition of microvascular endothelial cells	4.71E-03	FN1	1
Cellular Growth and Proliferation	Cell Cycle	mid-G1 phase	arrest in mid-G1 phase of microvascular endothelial cells	4.71E-03	FN1	1
Cellular Growth and Proliferation	Cell Cycle	senescence	senescence of nervous tissue cell lines	4.71E-03	C2ORF40	1
Cellular Growth and Proliferation	Cell Cycle	senescence	senescence of oligodendrocyte precursor cells	4.71E-03	C2ORF40	1
Cellular Growth and Proliferation	Cell Death	apoptosis	apoptosis of stem cells	4.26E-03	PIK3R1, SFRP2	2
Cellular Growth and Proliferation	Cell Death	survival	survival of cancer cells	8.04E-03	PIK3R1, SFRP2	2
Cellular Growth and Proliferation	Cell Death	apoptosis	apoptosis of embryonic cells	2.03E-02	ALX4, PIK3R1	2
Cellular Growth and Proliferation	Cell Death	survival	survival of glioma cells	2.33E-02	SFRP2	1
Cellular Growth and Proliferation	Cell Death	inhibition	inhibition of apoptosis	3.05E-02	FN1, PIK3R1, SFRP2	3

Category	Subcategory	Function	Function Annotation	*p*-value	Genes	# Genes
Cellular Growth and Proliferation	Cell Death	cell viability	cell viability	4.67E-02	FN1, PIK3R1, SLC19A1	3
Cellular Growth and Proliferation		stimulation	stimulation of microglia	9.39E-03	FN1	1
Cellular Growth and Proliferation		colony formation	colony formation of glioma cells	2.33E-02	SFRP2	1
Cellular Growth and Proliferation		proliferation	proliferation of neuroglia	2.63E-02	CLDN11, TRPC3, TSPO	3
Cellular Growth and Proliferation		colony formation	colony formation of cells	3.19E-02	CADM1, LUM, PIK3R1, SFRP2	4
Cellular Growth and Proliferation		growth	growth of carcinoma cell lines	4.14E-02	NOV, PIK3R1	2
Endocrine System Development and Disorders	Endocrine System Development and Function	synthesis	synthesis of pregnenolone	3.70E-02	TSPO	1
Endocrine System Development and Disorders	Endocrine System Disorders	diabetic neuropathy	diabetic neuropathy	4.67E-03	PDE5A, TSPO	2
Endocrine System Development and Disorders	Endocrine System Disorders	gestational diabetes mellitus	gestational diabetes mellitus	1.41E-02	PIK3R1	1
Endocrine System Development and Disorders	Endocrine System Disorders	insulin resistance	insulin resistance	2.08E-02	PDE5A, PIK3R1, TSPO	3
Endocrine System Development and Disorders	Endocrine System Disorders	experimentally-induced diabetes	experimentally-induced diabetes	2.63E-02	FN1, HLA-C	2
Endocrine System Development and Disorders	Endocrine System Disorders	insulin tolerance	insulin tolerance	3.25E-02	PIK3R1	1
Endocrine System Development and Disorders	Endocrine System Disorders	insulin-dependent diabetes mellitus	insulin-dependent diabetes mellitus	4.47E-02	ALX4, ATP10A, CADM1, FGGY, HLA-C, ME3, TSPO	7
Endocrine System Development and Disorders	Endocrine System Disorders	metabolic syndrome X	metabolic syndrome X	4.69E-02	PDE5A, TSPO	2
Protein Synthesis and Trafficking	Protein Synthesis	localization	localization of protein fragment	4.71E-03	HLA-C	1
Protein Synthesis and Trafficking	Protein Synthesis	localization	localization of protein	1.28E-02	HLA-C, PIK3R1, SLC9A2	3
Protein Synthesis and Trafficking	Protein Trafficking	accumulation	accumulation of protein fragment	4.71E-03	FN1	1
Protein Synthesis and Trafficking	Protein Trafficking	localization	localization of protein fragment	4.71E-03	HLA-C	1
Protein Synthesis and Trafficking	Protein Trafficking	reorganization	reorganization of F-actin	9.39E-03	FN1	1

Category	Subcategory	Function	Function Annotation	*p*-value	Genes	# Genes
Protein Synthesis and Trafficking	Protein Trafficking	localization	localization of protein	1.28E-02	HLA-C, PIK3R1, SLC9A2	3
Gene Expression		activation	activation of ESE box motif	4.71E-03	HES6	1
Gene Expression		activation	activation of FGF-inducible response element	1.87E-02	FN1	1
Gene Expression		transactivation	transactivation of p53 response element	3.25E-02	PIK3R1	1
Amino Acid Metabolism		influx	influx of methotrexate	4.71E-03	SLC19A1	1
Amino Acid Metabolism		uptake	uptake of methotrexate	4.71E-03	SLC19A1	1
Amino Acid Metabolism		cleavage	cleavage of amino acids	3.25E-02	CPM	1
Amino Acid Metabolism		transport	transport of folic acid	3.25E-02	SLC19A1	1
Amino Acid Metabolism		transport	transport of methotrexate	3.25E-02	SLC19A1	1
Embryonic Development		G0/G1 phase transition	arrest in G0/G1 phase transition of embryonic stem cells	4.71E-03	PIK3R1	1
Embryonic Development		development	development of organ	6.36E-03	ALX4, CADM1, COL3A1, DSP, FN1, HS6ST2, MGP, PGF, SFRP2, SLC19A1, ZIC2	11
Embryonic Development		morphology	morphology of visceral endoderm	1.41E-02	SERPINH1	1
Embryonic Development		cell spreading	cell spreading of embryonic cell lines	1.87E-02	FN1, VIM	2
Embryonic Development		apoptosis	apoptosis of embryonic cells	2.03E-02	ALX4, PIK3R1	2
Embryonic Development		branching morphogenesis	branching morphogenesis	2.28E-02	FN1, MGP, PGF	3
Embryonic Development		segmentation	segmentation of somites	2.33E-02	SFRP2	1
Embryonic Development		development	development of neural tube	2.37E-02	FN1, SFRP2	2
Embryonic Development		patterning	patterning of rostrocaudal axis	3.10E-02	ALX4, SFRP2	2
Embryonic Development		developmental process	developmental process of embryonic stem cells	3.40E-02	PIK3R1, SFRP2	2
Nucleic Acid Metabolism		accumulation	accumulation of thiamine	4.71E-03	SLC19A1	1
Nucleic Acid Metabolism		uptake	uptake of thiamine	4.71E-03	SLC19A1	1
Nucleic Acid Metabolism		incorporation	incorporation of adenine	1.41E-02	SLC19A1	1
Nucleic Acid Metabolism		catabolism	catabolism of cyclic GMP	1.87E-02	PDE5A	1

Category	Subcategory	Function	Function Annotation	*p*-value	Genes	# Genes
Nucleic Acid Metabolism		hydrolysis	hydrolysis of cyclic GMP	1.87E-02	PDE5A	1
Nucleic Acid Metabolism		incorporation	incorporation of nucleotide	3.70E-02	SLC19A1	1
Carbohydrate Metabolism		release	release of proteoglycan	9.39E-03	FN1	1
Carbohydrate Metabolism		accumulation	accumulation of phosphatidylinositol-3-phosphate	1.87E-02	PIK3R1	1
Carbohydrate Metabolism		binding	binding of phosphatidylinositol 4,5-diphosphate	1.87E-02	FN1	1
Carbohydrate Metabolism		glycolysis	glycolysis of D-glucose	3.70E-02	PIK3R1	1
Cancer	Tumor Morphology	adhesion	adhesion of glioma cells	9.39E-03	FN1	1
Cancer	Tumor Morphology	colony formation	colony formation of glioma cells	2.33E-02	SFRP2	1
Cancer	Tumor Morphology	transformation	transformation of tumor cells	2.79E-02	SFRP2	1
Cancer	Tumor Morphology	invasion	invasion of tumor cells	3.61E-02	FN1, NOV	2
Cancer		metastasis	metastasis of carcinoma cell lines	2.79E-02	FN1	1
Cancer		transformation	transformation of tumor cells	2.79E-02	SFRP2	1
Cancer		carcinoma	carcinoma	3.15E-02	ALX4, C2ORF40, CALB2, CLDN11, COL3A1, FN1, MGP, MXRA8, PCSK1, PDE5A, PGF, PIK3R1, PTGDS, SFRP2, SLC19A1, TSPO, VIM, ZIC2	18
Cancer		metastasis	metastasis of carcinoma	4.61E-02	PIK3R1, VIM	2
Cellular Function and Maintenance		homeostasis	homeostasis of neurons	1.41E-02	FGGY	1
DNA Replication, Recombination, and Repair		catabolism	catabolism of cyclic GMP	1.87E-02	PDE5A	1
DNA Replication, Recombination, and Repair		hydrolysis	hydrolysis of cyclic GMP	1.87E-02	PDE5A	1
Organismal Survival		lifespan	lifespan of organism	3.01E-02	COL3A1, NPC2	2

SI Table 3.4. Detailed list of potential regulatory molecules and their interactions with genes that were disregulated by exposure to 890 (LD) and 38,000 (HD) ng/g perfluorohexane sulfonate. Fold change (FC) and p-values from microarray are also reported.

Molecule	Entrez Name	Interacting genes	Entrez Gene Name	Interaction type	LD		HD	
					p-value	FC	*p*-value	FC
MYC	v-myc myelocytomatosis viral oncogene homolog (avian)	TSPO	translocator protein (18kDa)	DIRECT			3.33E-04	-2.30
		PDS5A	PDS5, regulator of cohesion maintenance, homolog A (S. cerevisiae)	DIRECT			1.33E-04	-1.76
		DSP	desmoplakin	DIRECT			5.33E-04	-1.66
		FN1	fibronectin 1	DIRECT			4.67E-04	-1.57
		MSN	moesin	DIRECT			0.00E+00	-1.57
		PTBP1	polypyrimidine tract binding protein 1	DIRECT			5.67E-04	-1.56
		ZIC2	Zic family member 2	indirect			1.00E-04	-1.84
		WNT5A	wingless-type MMTV integration site family, member 5A	indirect	7.00E-04	-1.73		
SRC	v-src sarcoma viral oncogene homolog (avian)	SLC9A2	solute carrier family 9 (sodium/hydrogen exchanger), member 2	DIRECT			4.00E-04	-2.58
		VIM	vimentin	DIRECT			6.67E-04	-1.81
		TRPC3	transient receptor potential cation channel, subfamily C, member 3	DIRECT			7.00E-04	-1.72
		PTBP1	polypyrimidine tract binding protein 1	DIRECT			5.67E-04	-1.56
		PIK3R1	phosphoinositide-3-kinase, regulatory subunit 1 (alpha)	DIRECT			8.67E-04	1.67
		DSP	desmoplakin	indirect			5.33E-04	-1.66
		FN1	fibronectin 1	indirect			4.67E-04	-1.57
HIF1A	hypoxia inducible factor 1, alpha subunit	HES6	hairy and enhancer of split 6 (Drosophila)	DIRECT			1.00E-04	-1.97
		GCHFR	GTP cyclohydrolase I feedback regulator	DIRECT			1.00E-04	-1.78
		SERPINH1	serpin peptidase inhibitor, clade H, member 1	DIRECT			2.67E-04	-1.74
		PGF	placental growth factor	DIRECT			7.67E-04	-1.53
		VIM	vimentin	indirect			6.67E-04	-1.81
		FN1	fibronectin 1	indirect			4.67E-04	-1.57

Molecule	Entrez Name	Interacting genes	Entrez Gene Name	Interaction type	LD		HD	
					p-value	FC	*p*-value	FC
HNF4A	hepatocyte nuclear factor 4, alpha	PTGDS	prostaglandin D2 synthase 21kDa (brain)	DIRECT			0.00E+00	-2.24
		HES6	hairy and enhancer of split 6 (Drosophila)	DIRECT			1.00E-04	-1.97
		GCHFR	GTP cyclohydrolase I feedback regulator	DIRECT			1.00E-04	-1.78
		ATP10A	ATPase, class V, type 10A	DIRECT	2.33E-04	-1.51	0.00E+00	-1.53
		HLA-C	major histocompatibility complex, class I, C	DIRECT			1.33E-04	1.70
CEBPB	CCAAT/enhancer binding protein (C/EBP), beta	MGP	matrix Gla protein	DIRECT			6.67E-05	-2.99
		VIM	vimentin	DIRECT			6.67E-04	-1.81
		HLA-C	major histocompatibility complex, class I, C	DIRECT			1.33E-04	1.70
		FN1	fibronectin 1	indirect			4.67E-04	-1.57
SP1	Sp1 transcription factor	TSPO	translocator protein (18kDa)	DIRECT			3.33E-04	-2.30
		VIM	vimentin	DIRECT			6.67E-04	-1.81
		FN1	fibronectin 1	DIRECT			4.67E-04	-1.57
		SLC19A1	solute carrier family 19 (folate transporter), member 1	DIRECT			1.33E-04	-1.50
ITGB1	integrin, beta 1	CLDN11	claudin 11	DIRECT			0.00E+00	-3.18
		FN1	fibronectin 1	DIRECT			4.67E-04	-1.57
		PIK3R1	phosphoinositide-3-kinase, regulatory subunit 1 (alpha)	DIRECT			8.67E-04	1.67
		NOV	nephroblastoma overexpressed gene	indirect			0.00E+00	-5.22
THBS1	thrombospondin 1	SFRP2	secreted frizzled-related protein 2	DIRECT			0.00E+00	-2.84
		COL3A1	collagen, type III, alpha 1	DIRECT			3.33E-05	-1.98
		FN1	fibronectin 1	DIRECT			4.67E-04	-1.57
		MSN	moesin	DIRECT			0.00E+00	-1.57